Summary of Cornerstone 2D NMR Experiments

Name:	Correlation by:
EXSY (NOESY)	^{1}H-^{1}H exchange
COSY (DQF-*COSY*)	^{1}H-^{1}H Scalar Couplings (directly coupled spins only)
TOCSY	^{1}H-^{1}H Scalar Couplings (whole spin system)
HSQC / HMQC	^{1}H-X $^{1}J_{HX}$ Scalar couplings (X = ^{13}C, ^{13}N, ^{13}P, ^{29}Si…)

Summary of Cornerstone 2D NMR Experiments

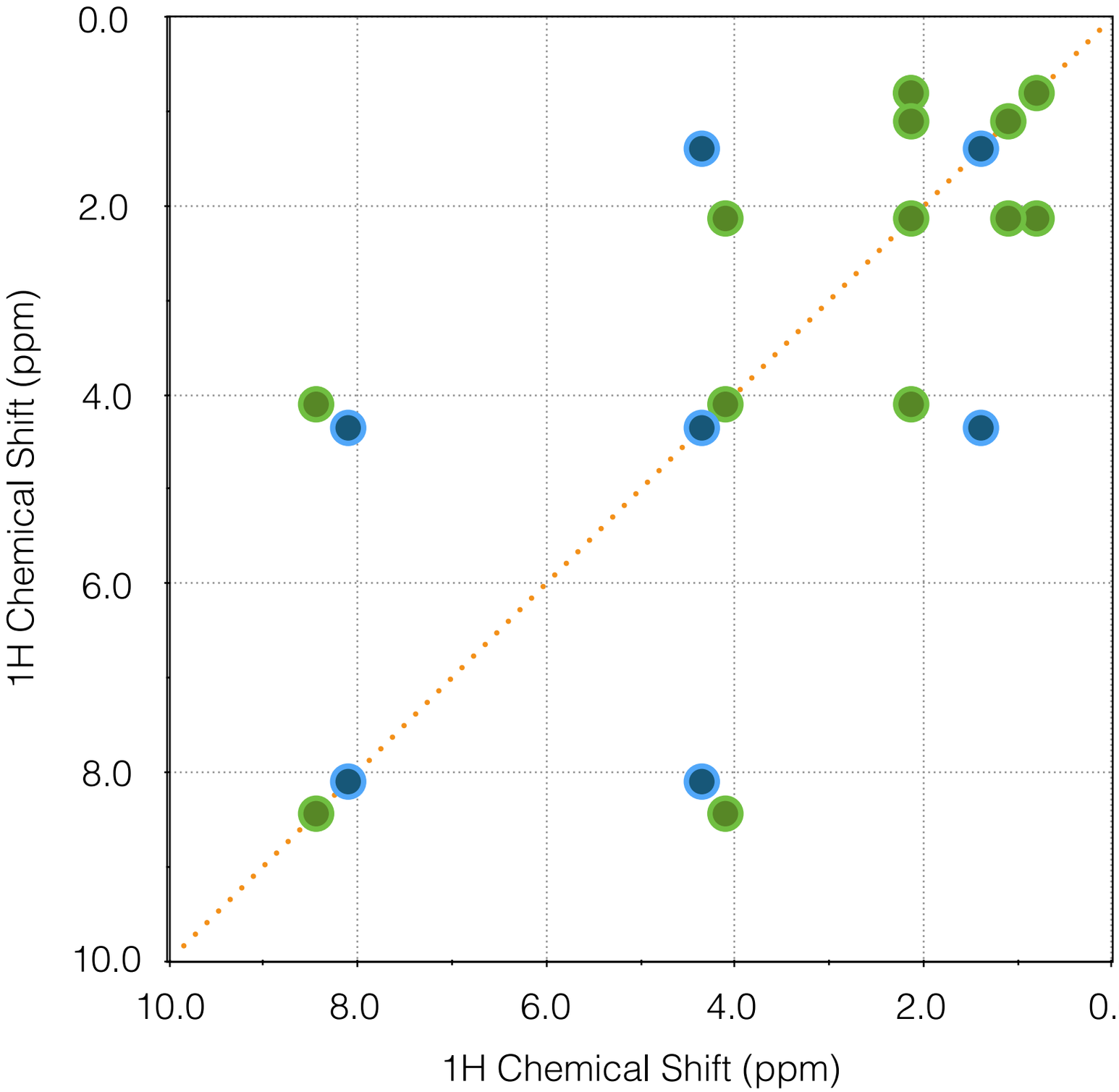

DQF-COSY
(directly J coupled connections)

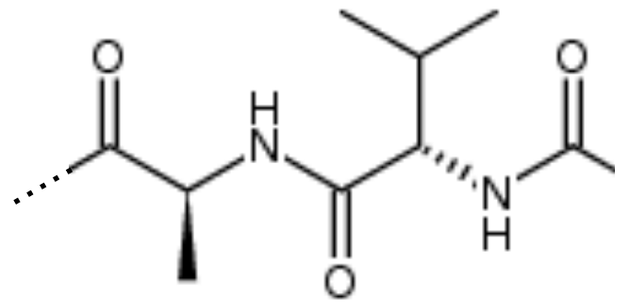

(example of schematic connections expected for a valine-alanine fragment in a protein)

homework: assign the spectrum

Summary of Cornerstone 2D NMR Experiments

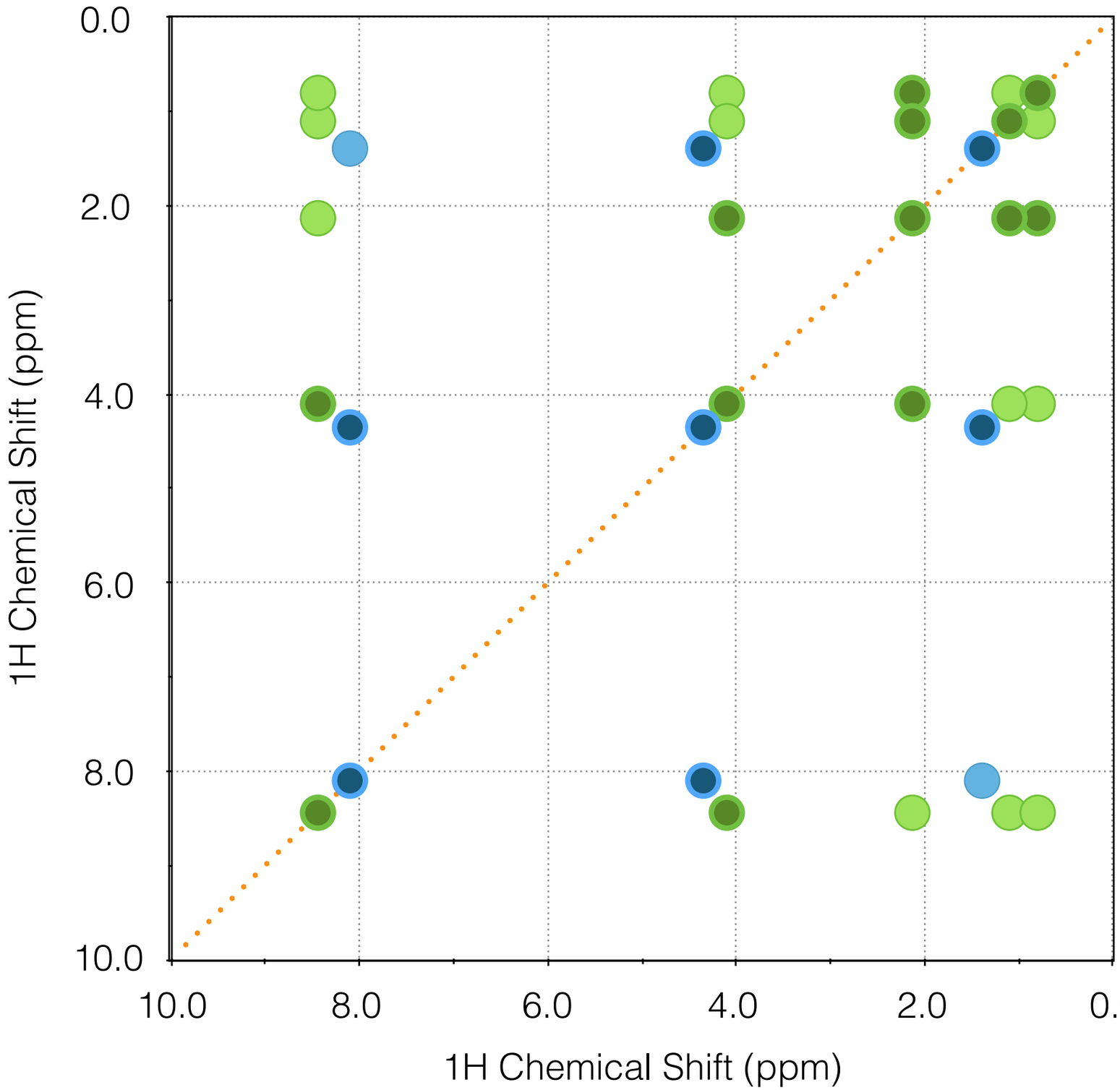

TOCSY
(all connections within a coupled spin system)

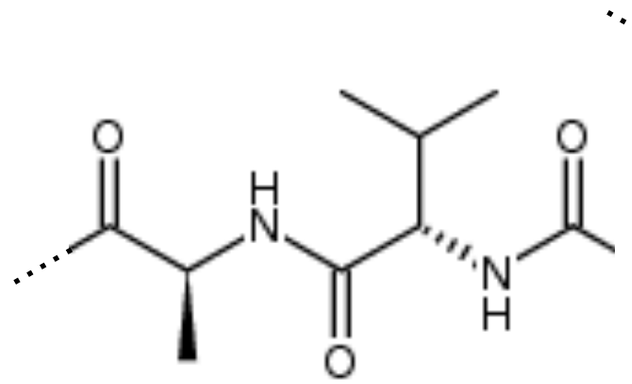

(example of schematic connections expected for a valine-alanine fragment in a protein)

homework: assign the spectrum

The Tip of the Iceberg….

TABLE V
TWO-, THREE-, AND FOUR-DIMENSIONAL NMR EXPERIMENTS

Experiment class[a] (X = C or N)	Experiment[b]	Ref.[c]
(t_1, t_2) = (H, H)	COSY	(1)
	RELAY	(2)
	HOHAHA-TOCSY	(3)
	NOESY	(4)
	ROESY	(5)
	DEPT-HMQC	(23)
	DEPT-HMQC filtered TOCSY	(23)
(t_1, t_2, t_3) = (H, H, H)	HOHAHA-NOESY	(6)
(t_1, t_2) = (X, H)	HMQC	(7)
	HSQC	(8)
	CT-HSQC	(9)
	HSMQC	(10)
	HMBC	(11)
	HETERO-RELAY	(12)
	HETERO-NOE	(13)
	H-X EXCSY	(14)
(t_1, t_2) = (C, C)	CC-DQC	(15, 16)
	CC-COSY	(16)
	XX-EXCSY	(14)
(t_1, t_2) = (N, C)	CN-MBC	(17)
(t_1, t_2, t_3) = (H, X, H)/(X, H, H)	NOESY-HMQC	(18)
	HOHAHA-HMQC	(19)
	SE-TOCSY-HSQC	(20)
	SE-HSQC-TOCSY	(20)
	SE-NOESY-HMQC	(20)
	SE-NOESY-HSQC	(20)
	HMQC-TOCSY	(21)
	^{15}N-TOCSY-NOESY	(22)
	^{15}N-NOESY-TOCSY	(22)
	DEPT-TOCSY	(23)
	HMQC-COSY (gradient)	(24)
	NOESY-HMQC (gradient)	(25)
(t_1, t_2, t_3) = (H, C, H)	HCCH-COSY	(26)
	CT-HCCH-COSY	(27)
	HCCH-TOCSY	(26)
	HCCH-TOCSY (gradient)	(28)
	H(CA)CO-TOCSY	(29)
	H(CA)CO-COSY	(29)
	(HCA)CO-CBHB	(29)
	HA[CAN]HN	(30)

TABLE V (*continued*)

Experiment class[a] (X = C or N)	Experiment[b]	Ref.[c]
(t_1, t_2, t_3) = (C, C, H)	HCACO	(31)
	CT-HCACO	(32)
	C TOCSY-REVINEPT	(33)
	H(N)CACO	(34)
	^{13}C–^{13}C correlations	(35)
	CBCACOHA (gradient)	(36)
	CBCACOHA-TOCSY	(37)
(t_1, t_2, t_3) = (N, C, H)	HNCO	(31)
	CT-HNCO	(38)
	HNCA	(31, 39)
	CT-HNCA	(38)
	HN(CO)CA	(40, 41)
	CT-HN(CO)CA	(38)
	CT-HN(CA)CO	(42)
	HNCO (gradient)	(43)
(t_1, t_2, t_3) = (C, N, H)	HCA(CO)N	(31)
	CT-HCA(CO)N	(32, 44)
	CBCA(CO)NH	(45)
	HNCACB	(46)
	HC(CO)NH-TOCSY	(47)
	HC(C)NH-TOCSY	(48)
(t_1, t_2, t_3) = (H, N, H)	HA(CA)NNH	(49)
	HN(CA)HA-GLY	(50)
	HBHA(CO)NH	(51)
	H(CCO)NH-TOCSY	(47)
	HN(CA)NNH	(52)
	HA[CAN]HN	(30)
(t_1, t_2, t_3) = (N, N, H)	^{15}N/^{15}N edited ^{1}H–^{1}H NOESY	(53)
	HN(CA)NNH	(52)
(t_1, t_2, t_3) = (N, H, H)	HN(CA)HA	(54)
	HN(COCA)HA	(55)
(t_1, t_2, t_3, t_4) = (C, H, N, H)	^{13}C/^{15}N-edited ^{1}H–^{1}H NOESY	(56)
	HNCAHA	(57)
	HN(CO)CAHA	(57)
(t_1, t_2, t_3, t_4) = (H, C, N, H)	HCANNH	(58)
	HCC(CO)NNH	(59)
(t_1, t_2, t_3, t_4) = (C, H, C, H)	^{13}C/^{13}C-edited ^{1}H–^{1}H NOESY	(60)
	^{13}C/^{13}C ^{1}H–^{1}H NOESY (gradient)	(61)
(t_1, t_2, t_3, t_4) = (C, C, N, H)	HCACON	(62)
(t_1, t_2, t_3, t_4) = (H, C, C, H)	HCCH-TOCSY	(63)
(t_1, t_2, t_3, t_4) = (H, N, N, H)	HN(COCA)NH	(64)

[a] Pulse sequences are organized by the nuclei that are operative in the various acquisition periods. The number of time domains (t_i values) establishes the dimensionality of the

(*continued*)

The Tip of the Iceberg….

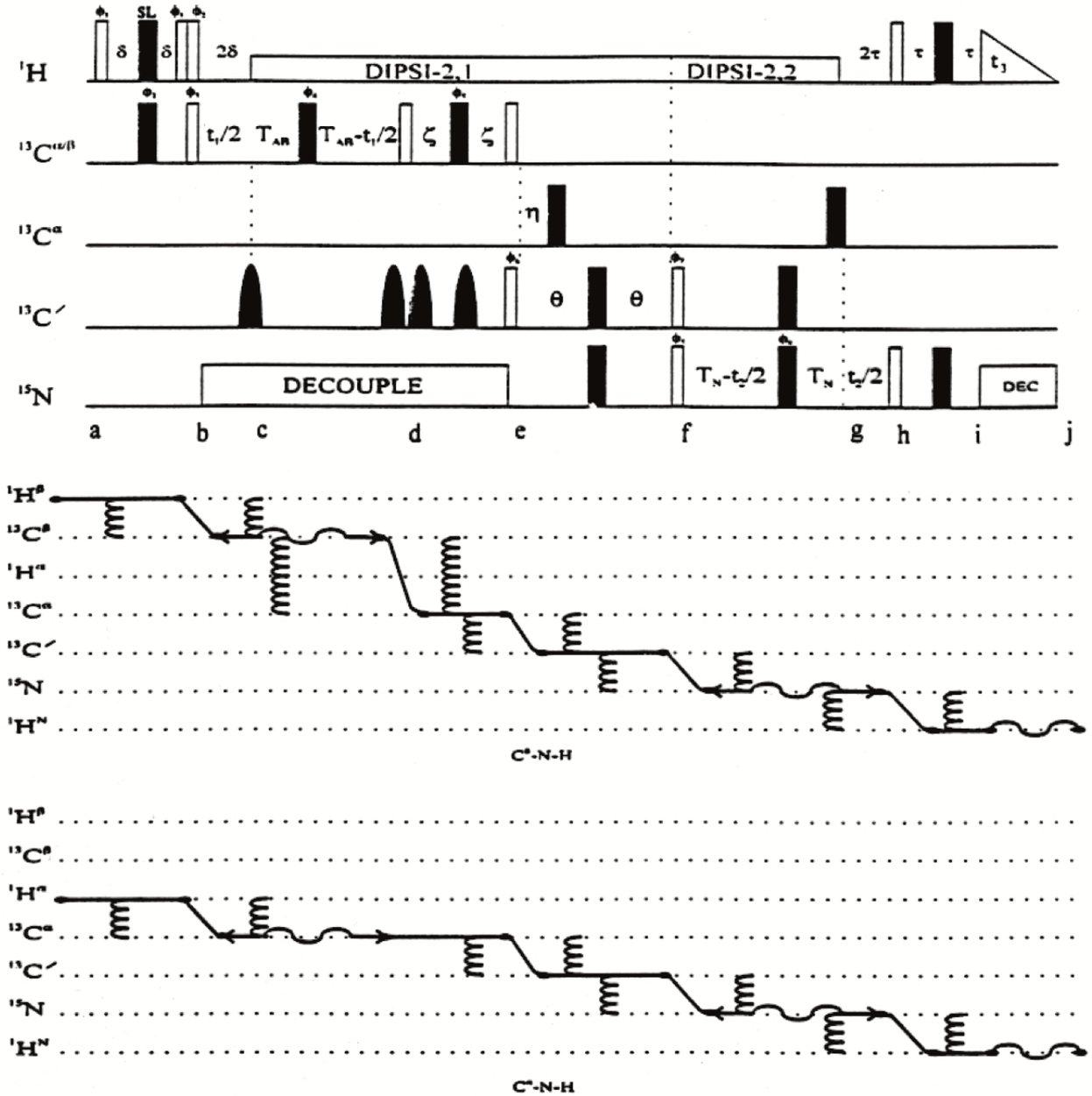

FIG. 14. Pulse sequence and CFN for 3D-CBCA(CO)NH.[11] The pulses and phases have the same convention described in Fig. 12. For values of the delays, consult the original work. The second and third selective (rounded) carbonyl pulses and the phase labeled ϕ_7 serve to remove nonresonant phase distortions (Section III.C). The CFN is best shown as two separate experiments, one originating from $^1H^\beta$ and the second originating from $^1H^\alpha$.

Advanced NMR & Imaging

Week 10: Relaxation & Structure Determination

CH-401

Advanced NMR and imaging

Emsley David Lyndon

Cursus	Sem.	Type
Chimiste	MA2	Opt.

Language	English
Credits	3
Session	Summer
Semester	Spring
Exam	Written
Workload	90h
Weeks	14
Hours	**2 weekly**
Lecture	2 weekly

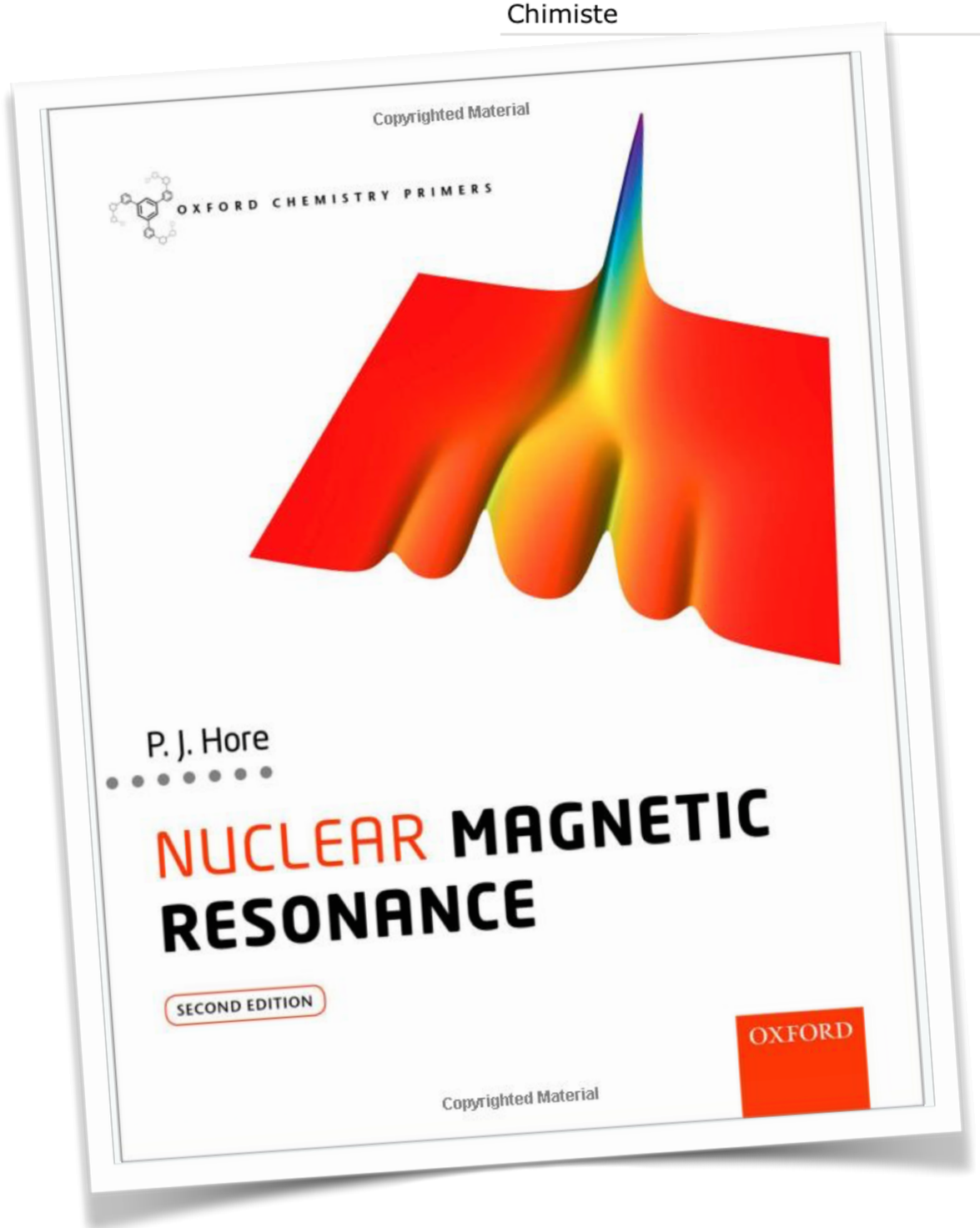

Objectives

- Learn how nuclear magnetism returns to equilibrium.
- Know the approach the describing the process microscopically.
- Relate this to molecular properties.

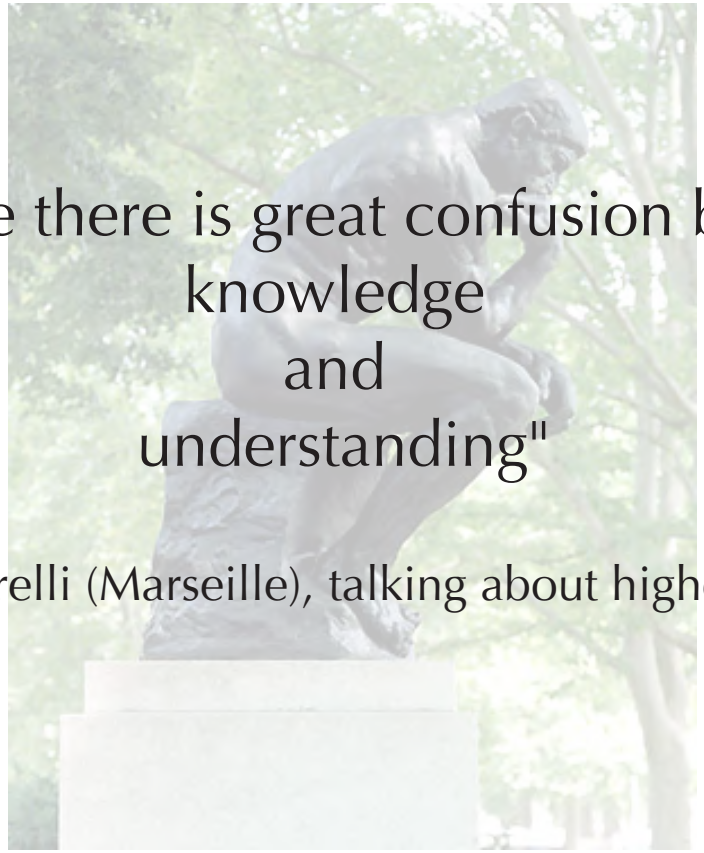

"In France there is great confusion between
knowledge
and
understanding"

Prof. S. Caldarelli (Marseille), talking about higher education.

Nuclear Spin Relaxation

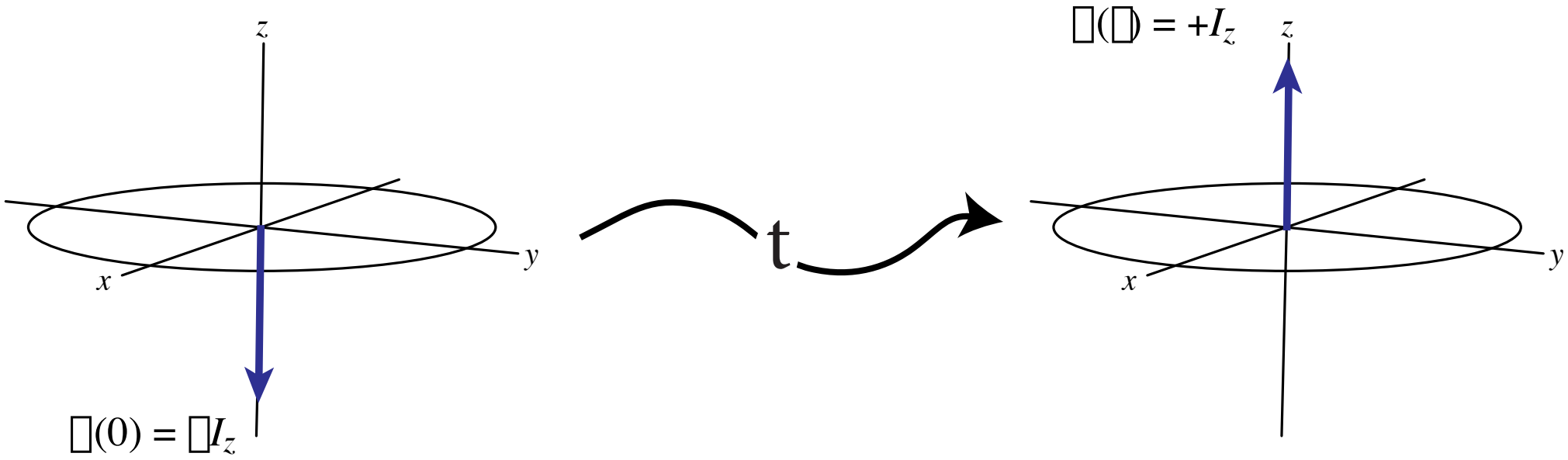

how does the system move from the non equilibrium state back to equilibrium?

Nuclear Spin Relaxation

Relaxation (the return to equilibrium) is induced by fluctuating magnetic fields that induce transitions.

These fields can induce rotations around the *z*-axis, or around the *x,y* axes.

If the fields were coherent (i.e. the same everywhere in the sample) they would induce rotations of the bulk magnetization (e.g. a pulse). Coherent fields are treated using normal density matrix theory.

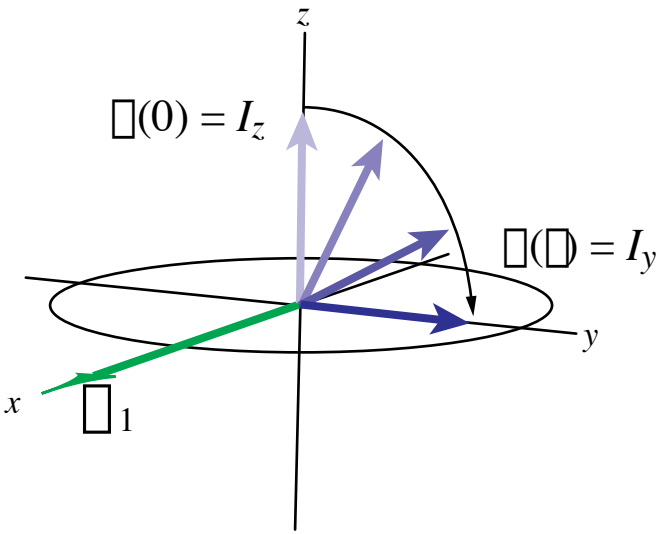

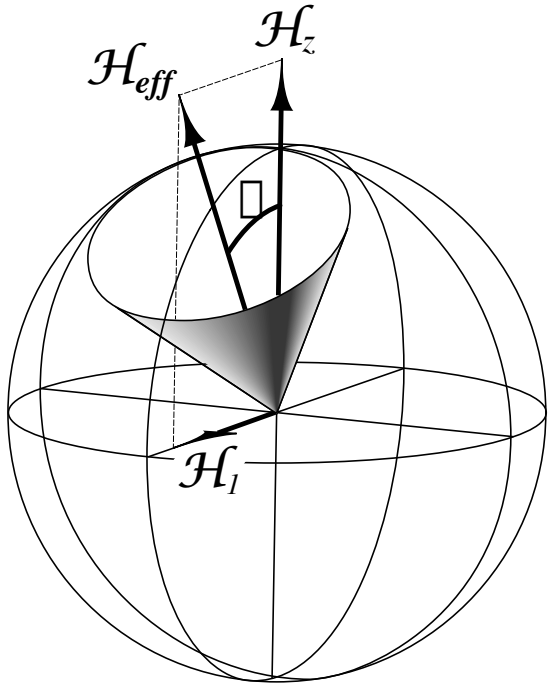

Nuclear Spin Relaxation

If the fields are not coherent (e.g. different parts of the ensemble experience different fields) they will lead to *a loss of coherence*.

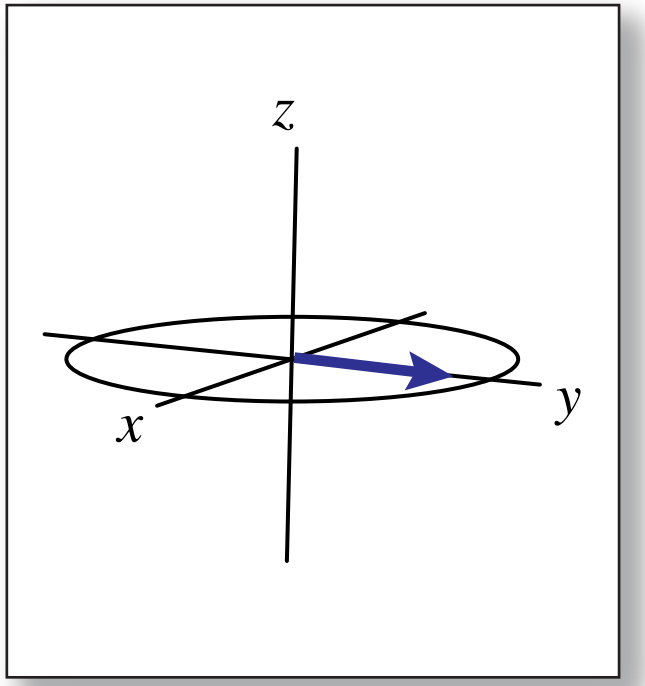

=

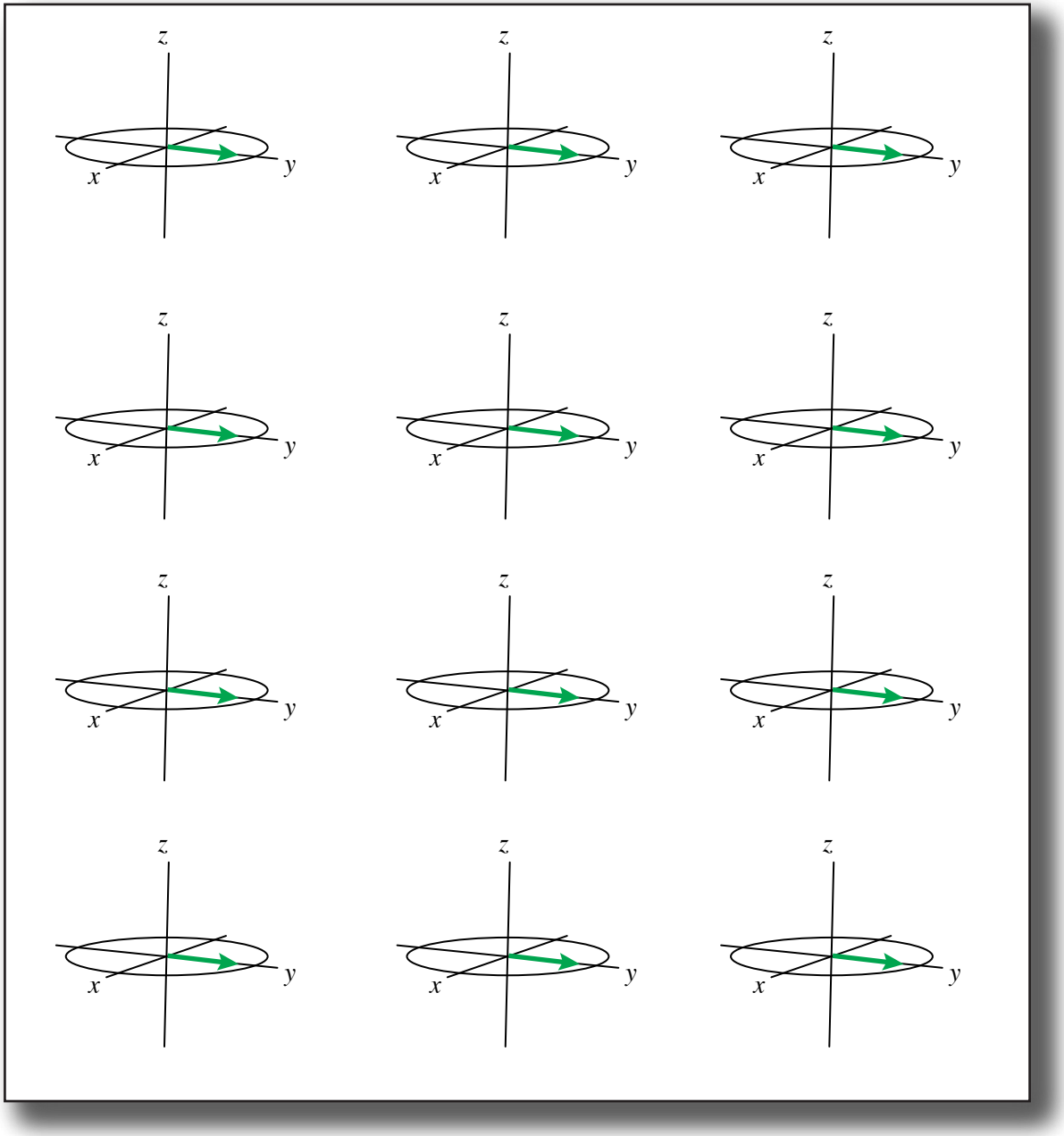

Loss of Coherence

Dephasing in the Ensemble

random uncorrelated
longitudinal fields

□(0) □(t)

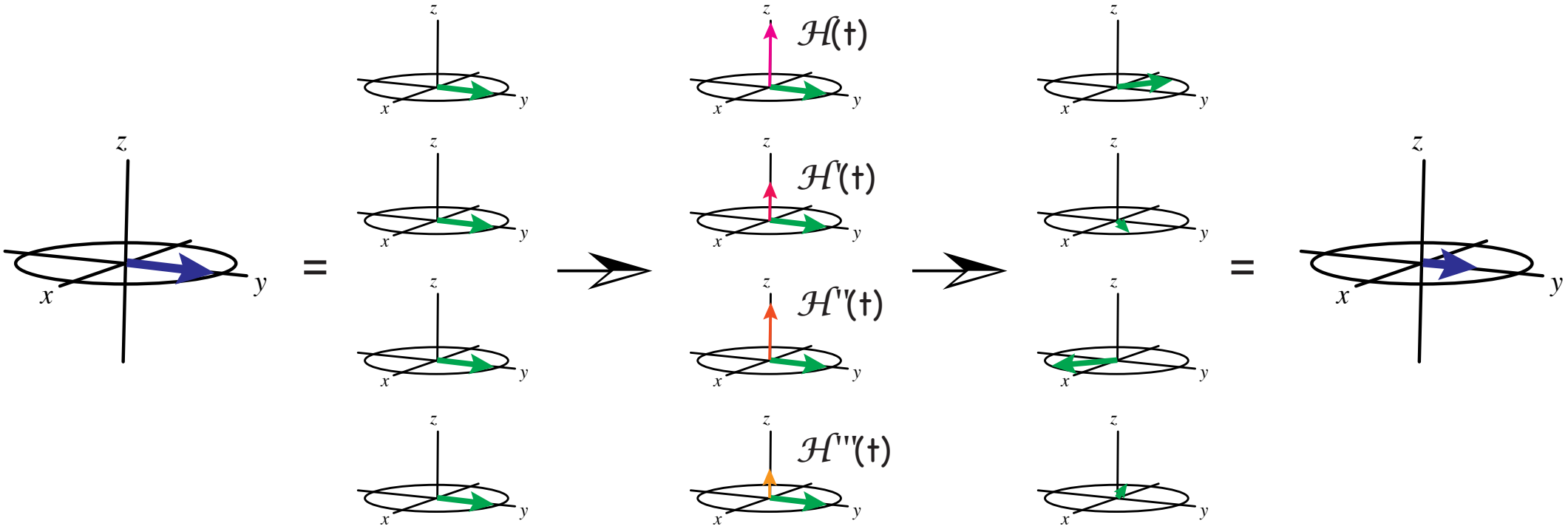

Note that in this picture, each micro-element of the ensemble undergoes a perfectly coherent unitary rotation. Simply because these rotations are different for each element, the macroscopic ensemble loses coherence.
(there is no magic)

Nuclear Spin Relaxation

If the fields are not coherent (e.g. different parts of the ensemble experience different fields) they will lead to *a loss of coherence*.

For example, an incoherent rotation around the *z* axis will lead to dephasing. This is transverse relaxation. It is caused by fields with a modulation frequency around 0. (They do not change the total energy of the system: "spin-spin relaxation")

Incoherent rotations around the *x,y* axis will change the value of the z-component of the magnetization. They are caused by fields with a modulation frequency around the Larmor frequency. (They change the total energy of the system: "spin-lattice relaxation").

How can we describe the effect of incoherent fields on the system?
What generates the incoherent fields?

Quantum Spins in a Classical Lattice:

The Abragam formulation of the Redfield Approach

Consider a spin system with a Hamiltonian:

$$\mathcal{H} = \mathcal{H}_0 + \mathcal{H}_1(t)$$

The equation of motion is, as always:

$$\frac{d\sigma}{dt} = -i\left[\left(\mathcal{H}_0 + \mathcal{H}_1(t)\right),\sigma\right] \qquad (1)$$

However, the task of calculating the evolution of the density matrix when part of the Hamiltonian is random obviously requires a special treatment.

(1) Isolate the effect of the spin-lattice coupling through the use of an interaction representation:

$$Q = \exp\left(-i\mathcal{H}_0 t\right) Q \exp\left(+i\mathcal{H}_0 t\right)$$

which yields for one part of the ensemble:

$$\frac{d\tilde{\sigma}(t)}{dt} = -i\left[\left(\tilde{\mathcal{H}} - \mathcal{H}_0\right),\tilde{\sigma}(t)\right] = -i\left[\tilde{\mathcal{H}}_1(t),\tilde{\sigma}(t)\right]$$

we take the average over all identical molecules in the sample, which is equivalent to a time-average for one molecule, indicated by a bar:

$$\frac{d\tilde{\sigma}(t)}{dt} = -i\overline{\left[\tilde{\mathcal{H}}_1(t),\tilde{\sigma}(t)\right]} \qquad (2)$$

Quantum Spins in a Classical Lattice:

The Abragam formulation of the Redfield Approach

$$\frac{d\rho(t)}{dt} = -i\overline{\left[\tilde{\mathcal{H}}_1(t),\rho(t)\right]} \qquad (2)$$

(2) The evolution of the density matrix produced by a small rapidly varying effective Hamiltonian is slow. Starting from $\rho(0)$ we can calculate its form at time *t* through a second order expansion:

$$\rho(t) = \rho(0) - i\int_0^t \overline{\left[\tilde{\mathcal{H}}_1(t'),\rho(0)\right]}dt' - \int_0^t dt' \int_0^{t'} dt'' \overline{\left[\tilde{\mathcal{H}}_1(t'),\left[\tilde{\mathcal{H}}_1(t''),\rho(0)\right]\right]} \qquad (3)$$

(3) Since the spin-lattice coupling has zero average the first term vanishes. Limiting to 2nd order is valid only if *t* is such that $\rho(t) \approx \rho(0)$.

Also we must replace $\rho(0)$ by $\rho(0) - \rho_{eq}$ to account for the finite temperature of the lattice (system does not relax back to zero polarisation):

$$\rho(t) - \rho(0) = -\int_0^t dt' \int_0^{t'} dt'' \overline{\left[\tilde{\mathcal{H}}_1(t'),\left[\tilde{\mathcal{H}}_1(t''),\rho(0) - \rho_{eq}\right]\right]} \qquad (4)$$

Quantum Spins in a Classical Lattice:

The Abragam formulation of the Redfield Approach

$$\dot{\rho}(t) - \dot{\rho}(0) = -\int_0^t dt' \int_0^{t'} dt'' \overline{\left[\tilde{\mathcal{H}}_1(t), \left[\tilde{\mathcal{H}}_1(t''), \rho(0) - \rho_{eq}\right]\right]} \qquad (4)$$

(4) The perturbing Hamiltonian is a sum of terms each of which is the product of a spin operator by a random function of time. In the interaction representation the various spin operators oscillate at different frequencies. For *simplicity* we assume that there is just one operator for each frequency:

$$\mathcal{H}_1(t) = \sum_\alpha V_\alpha F_\alpha(t)$$

and $\tilde{V}_\alpha(t) = \exp(i\omega_\alpha t) V_\alpha$.

The random functions have zero average, and since they are *stationary random functions*:

$$\overline{F_\alpha(t) F_\beta^*(t')} = G_{\alpha\beta}(|t - t'|)$$

and thus equation (4) becomes

$$\dot{\rho}(t) - \dot{\rho}(0) = -\sum_{\alpha\beta} \left[V_\alpha, \left[V_\beta^\dagger, \rho(0) - \rho_{eq}\right]\right] \int_0^t dt' \int_0^{t'} dt'' G_{\alpha\beta}(|t' - t''|) \exp\left\{i(\omega_\beta t' - \omega_\alpha t'')\right\}. \quad (5)$$

Quantum Spins in a Classical Lattice:

The Abragam formulation of the Redfield Approach

$$\sigma(t)-\sigma(0)=-\int_0^t dt'\int_0^{t'} dt''\,\overline{\left[\tilde{\mathcal{H}}_1(t''),\left[\tilde{\mathcal{H}}_1(t'),\sigma(0)-\sigma_{eq}\right]\right]} \qquad (4)$$

(4) The perturbing Hamiltonian is a sum of terms each of which is the product of a spin operator by a random function of time. In the interaction representation the various spin operators oscillate at different frequencies. For *simplicity* we assume that there is just one operator for each frequency:

spin operators

$$\mathcal{H}_1(t)=\sum_\alpha V_\alpha F_\alpha(t)$$

(random) time dependence of the interaction

and $\tilde{V}_\alpha(t)=\exp(i\omega_\alpha t)V_\alpha$.

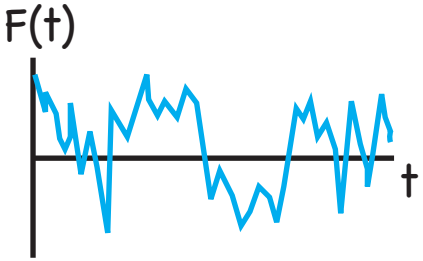

The random functions have zero average, and since they are *stationary random functions*:

$$\overline{F_\alpha(t)F_\beta^*(t')}=G_{\alpha\beta}(t-t')$$

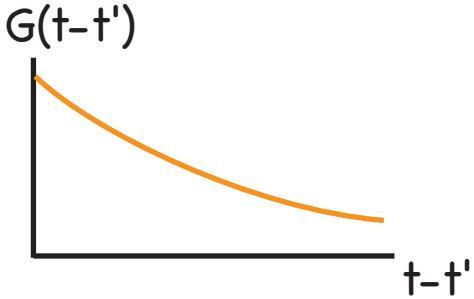

and thus equation (4) becomes

$$\sigma(t)-\sigma(0)=-\sum_{\alpha\beta}\left[V_\alpha,\left[V_\beta^\dagger,\sigma(0)-\sigma_{eq}\right]\right]\int_0^t dt'\int_0^{t'} dt''\,G_{\alpha\beta}(t'-t'')\exp\{i(\omega_\beta t''-\omega_\alpha t')\}. \qquad (5)$$

INFORMATION ONLY

Quantum Spins in a Classical Lattice:

The Abragam formulation of the Redfield Approach

$$\dot{\rho}(t) - \dot{\rho}(0) = -\sum_{\alpha\beta}\left[V_\alpha,\left[V_\beta^\dagger,\rho(0) - \rho_{eq}\right]\right]\int_0^t dt'\int_0^{t'} dt''\, G_{\alpha\beta}(t'-t'')\exp\left\{i\left(\omega_\alpha t' - \omega_\beta t''\right)\right\}. \quad (5)$$

(5) We now make a *secular approximation* that the contribution to the evolution of $\rho(0)$ of terms with $\omega_a \neq \omega_\beta$ $(\alpha \neq \beta)$ can be neglected. We also introduce a change of variables $\tau = t' - t''$ and we obtain for the double integral:

$$\int_0^t dt' \int_0^{t'} dt'' \ldots = \int_0^t (t-\tau)\, G_{\alpha\beta}(\tau)\exp\{i\omega_\beta\tau\}\, d\tau$$

We now make a ***physical approximation*** that τ_c, the decay time of the autocorrelation function $G_{\alpha\beta}(\tau)$ is much shorter than the timescale of evolution of ρ. Thus we can choose a time $t >> \tau_c$ and still short enough for the change in ρ to be small. We have then

$$\int_0^t dt' \int_0^{t'} dt'' \ldots \approx t \int_0^t G_{\alpha\beta}(\tau)\exp\{i\omega_\beta\tau\}\, d\tau$$

or, defining a ***spectral density function,***

$$\int_0^t dt' \int_0^{t'} dt'' \ldots \approx t J_{\alpha\beta}(\omega).$$

Since $\rho(t) - \rho(0)$ is small, we have approximately $\frac{\rho(t) - \rho(0)}{t} \approx \frac{d\rho}{dt}$ and equation (5) becomes

$$\frac{d\rho}{dt} = -\sum_{\alpha\beta}\left[V_\alpha,\left[V_\beta^\dagger,(\rho - \rho_{eq})\right]\right]J_\alpha(\omega_\beta) \quad (6)$$

THIS IS THE REDFIELD-ABRAGAM MASTER EQUATION FOR THE EVOLUTION OF THE DENSITY MATRIX UNDER THE EFFECT OF A RANDOM PERTURBATION.

It is valid on a coarse grained time scale, that is over time intervals several times larger than τ_c.

Quantum Spins in a Classical Lattice:

The Abragam formulation of the Redfield Approach

$$\dot{\rho}(t) - i\omega\rho(0) = -\sum_{\alpha\beta}\left[V_\alpha,\left[V_\beta^\dagger,\rho(0) - \rho_{eq}\right]\right]\int_0^t dt'\int_0^{t'} dt''\, G_{\alpha\beta}(t'-t'')\exp\left\{i\left(\omega_\alpha t' - \omega_\beta t''\right)\right\}. \quad (5)$$

(5) We now make a *secular approximation* that the contribution to the evolution of $\rho(0)$ of terms with $\omega_\alpha \neq \omega_\beta$ $(\alpha \neq \beta)$ can be neglected. We also introduce a change of variables $\tau = t' - t''$ and we obtain for the double integral:

$$\int_0^t dt' \int_0^{t'} dt'' \ldots = \int_0^t (t - \tau) G_{\alpha\beta}(\tau)\exp\{i\omega_\alpha\tau\} d\tau$$

We now make a ***physical approximation*** that τ_c, the decay time of the autocorrelation function $G_{\alpha\beta}(\tau)$ is much shorter than the timescale of evolution of ρ. Thus we can choose a time $t >> \tau_c$ and still short enough for the change in ρ to be small. We have then

$$\int_0^t dt' \int_0^{t'} dt'' \ldots \approx t \int_0^t G_{\alpha\beta}(\tau)\exp\{i\omega_\alpha\tau\} d\tau$$

or, defining a ***spectral density function,***

$$\int_0^t dt' \int_0^{t'} dt'' \ldots \approx t J_{\alpha\beta}(\omega).$$

Since $\dot{\rho}(t) - i\omega\rho(0)$ is small, we have approximately $\frac{\rho(t) - \rho(0)}{t} \approx \frac{d\rho}{dt}$ and equation (5) becomes

$$\frac{d\rho}{dt} = -\sum_{\alpha\beta}\left[V_\alpha,\left[V_\beta^\dagger,(\rho - \rho_{eq})\right]\right]J_\alpha(\omega_\alpha) \quad (6)$$

the double commutator

the (auto) correlation function

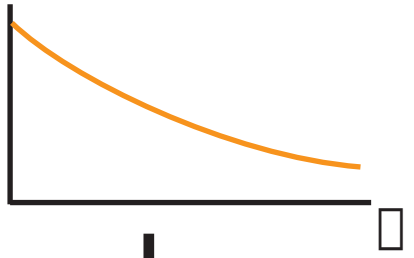

FT

the spectral density function

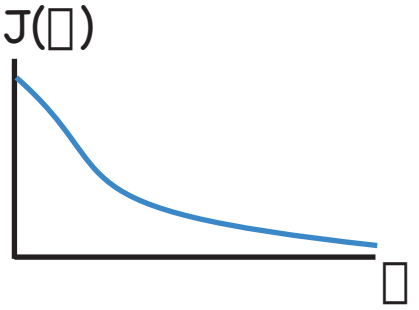

THIS IS THE REDFIELD-ABRAGAM MASTER EQUATION FOR THE EVOLUTION OF THE DENSITY MATRIX UNDER THE EFFECT OF A RANDOM PERTURBATION.

It is valid on a coarse grained time scale, that is over time intervals several times larger than τ_c.

INFORMATION ONLY

Quantum Spins in a Classical Lattice:

The Abragam formulation of the Redfield Approach

$$\frac{d\rho}{dt} = -\int_0^\infty \left[V_I(t),\left[V_I^\dagger(t-\tau),\rho(t)-\rho_{eq}\right]\right] J_I(\omega_I)\,d\tau$$

the double commutator:
the dynamics of the density matrix induced by the fluctuations depend on the operator form of the perturbing Hamiltonian

the (auto) correlation function

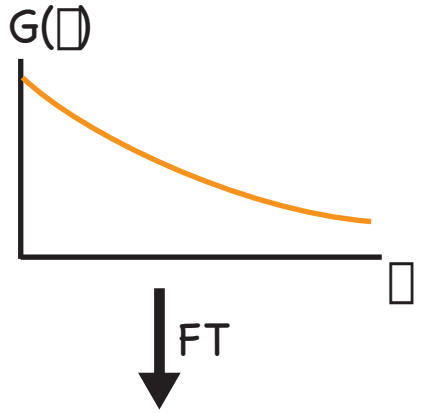

FT

the spectral density function

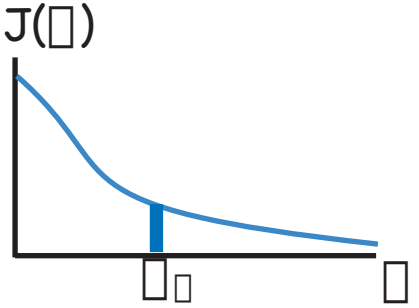

the value of $J_I(\omega_I)$ gives the size of the field generated by the random fluctuations at the relevant frequency (e.g. 0, ω_0, $2\omega_0$)

Quantum Spins in a Classical Lattice:

The Abragam formulation of the Redfield Approach

The evolution in the interaction representation of a physical variable Q is given by

$$\frac{d}{dt}\langle Q\rangle = -\sum_{\alpha} J_{\alpha}(\omega_{\alpha})\left\{\left\langle\left[\left[Q,V_{\alpha}\right],V_{\alpha}^{\dagger}\right]\right\rangle - \left\langle\left[\left[Q,V_{\alpha}\right],V_{\alpha}^{\dagger}\right]\right\rangle_{eq}\right\} \tag{7}$$

EXAMPLE: LONGITUDINAL RELAXATION OF IDENTICAL SPINS

$$\tilde{\mathcal{H}} = \omega_0 I_z$$

The spin-lattice Hamiltonian is of the form

$$\mathcal{H}_1(t) = \sum_m V_m F_m(t)$$

where we have $\left[I_z,V_m\right] = mV_m$ so that $\tilde{V}_m(t) = \exp(im\omega_0 t)V_m$. Equation (7) applied to $Q = I_z$ yields

$$\frac{d}{dt}\langle I_z\rangle = -\sum_m J_m(m\omega_0)\left\{\left\langle\left[\left[I_z,V_{\alpha}\right],V_{\alpha}^{\dagger}\right]\right\rangle - \left\langle\left[\left[I_z,V_{\alpha}\right],V_{\alpha}^{\dagger}\right]\right\rangle_{eq}\right\}.$$

We can evaluate the trace and obtain

$$\frac{d}{dt}\langle I_z\rangle = -\frac{1}{T_1}\left(\langle I_z\rangle - \langle I_z\rangle_{eq}\right),$$

with

$$\frac{1}{T_1} = \sum_m m^2 \frac{Tr\left(V_m V_m^{\dagger}\right)}{Tr\left(I_z^2\right)} J_m(m\omega_0). \tag{8}$$

Quantum Spins in a Classical Lattice:

The Abragam formulation of the Redfield Approach

$$\frac{1}{T_1} = \sum_m m^2 \frac{Tr\left(V_m V_m^{\dagger}\right)}{Tr\left(I_z^2\right)} J_m\left(m\omega_0\right). \tag{8}$$

we often find that correlation functions are exponential,

$$\overline{F_m(t)F_m^{*}(t+\tau)} = \left|\overline{F_m^2}\right| \exp\left(-|\tau|/\tau_c\right)$$

so that

$$J_m(\omega) = \left|\overline{F_m^2}\right| \int_0^{\infty} \exp(-\tau/\tau_c)\exp(i\omega\tau)d\tau$$

$$J_m(\omega) = \left|\overline{F_m^2}\right| \left[\frac{\tau_c}{1+\omega^2\tau_c^2} + i\frac{\omega\tau_c^2}{1+\omega^2\tau_c^2}\right] \tag{9}$$

which is complex. The imaginary part is compensated by the term $J_{-m}(\omega)$, so we retain only the real part, ensuring that T_1 is real, as befits a longitudinal relaxation rate.

The NMR Hamiltonian: The Key to the Spectrum

Reminder:

$$\rho(t) = \exp(-i\mathcal{H}t)\rho(0)\exp(+i\mathcal{H}t).$$

$$\mathcal{H} = \mathcal{H}_z + \mathcal{H}_Q + \mathcal{H}_D + \mathcal{H}_{cs} + \mathcal{H}_J$$

Zeeman Interaction
(~100 MHz)

Quadrupolar Interaction
(0-100 MHz)

Dipolar Interaction
(0-20 kHz)

Chemical Shift
(0-2000 ppm)

Scalar Coupling
(0-200 Hz)

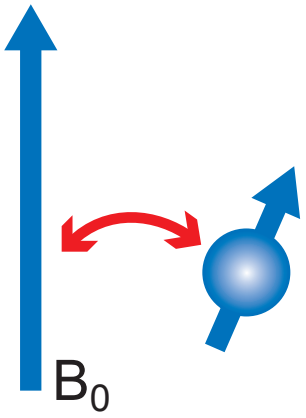

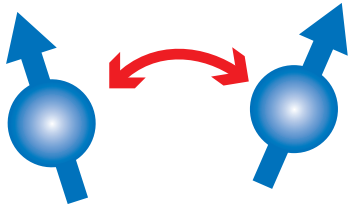

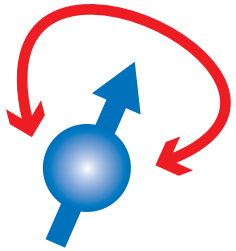

NMR interactions are anisotropic

	s ($\ell = 0$)	p ($\ell = 1$)			d ($\ell = 2$)					f ($\ell = 3$)						
	$m = 0$	$m = 0$	$m = \pm 1$		$m = 0$	$m = \pm 1$		$m = \pm 2$		$m = 0$	$m = \pm 1$		$m = \pm 2$		$m = \pm 3$	
	s	p_z	p_x	p_y	d_{z^2}	d_{xz}	d_{yz}	d_{xy}	$d_{x^2-y^2}$	f_{z^3}	f_{xz^2}	f_{yz^2}	f_{xyz}	$f_{z(x^2-y^2)}$	$f_{x(x^2-3y^2)}$	$f_{y(3x^2-y^2)}$
$n = 1$																
$n = 2$	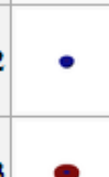		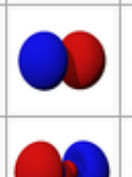	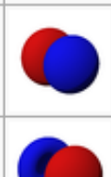												
$n = 3$		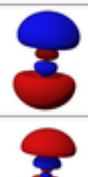	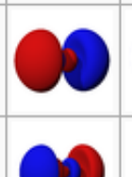	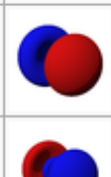	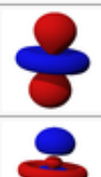	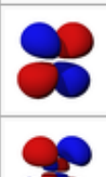		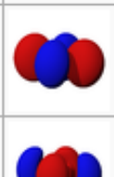	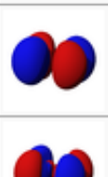							
$n = 4$		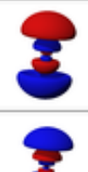	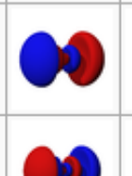	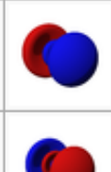	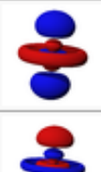	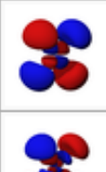	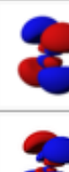	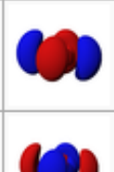	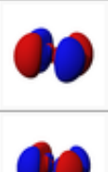	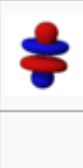	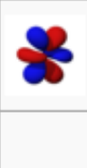	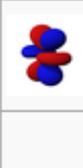	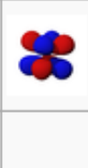	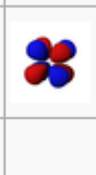	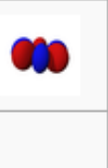	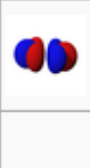
$n = 5$			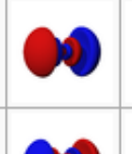	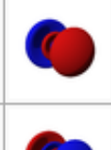		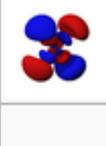		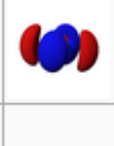	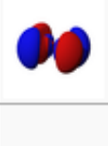	...	...	...	...	...	...	...
$n = 6$					...	...	...	...	...	...	...	...	...	...	...	...
$n = 7$		...	...	...	...	...	...	...	...	...	...	...	...	...	...	...

The chemical shift can be thought of as the shielding of the nucleus from the external magnetic field by the electrons.

The magnetic field is a vector quantity (the magnetic field has a well defined direction). The electronic distribution around the nucleus is highly ***anisotropic***.

Therefore the chemical shift must depend on the orientation of the molecule with respect to the magnetic field.

NMR interactions are anisotropic

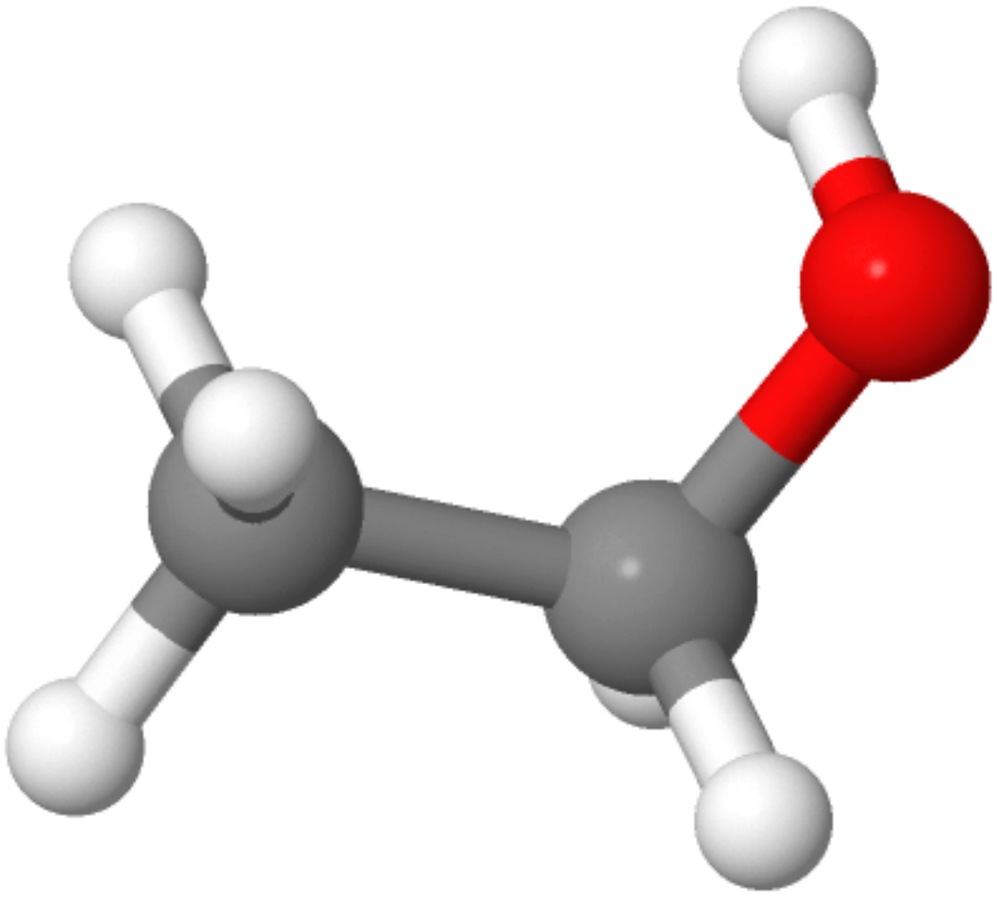

Consider the chemical shift of the CH_2 carbon resonance in ethanol

NMR interactions are anisotropic

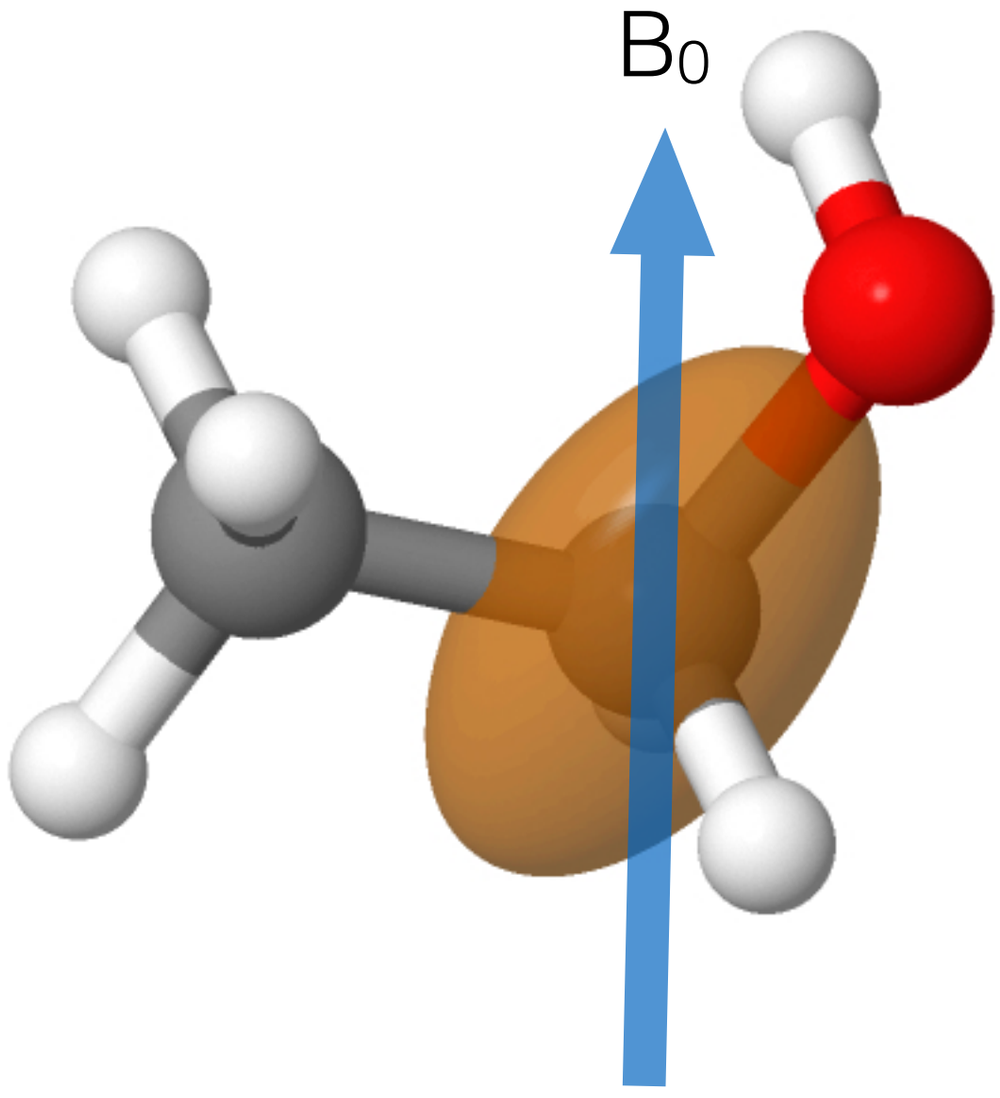

Here we show the chemical shift tensor as an ellipsoid superimposed on the molecular structure.

The shift tensor is fixed in the molecular frame.

Reminder: Shielding (σ) is related to chemical shift (δ) by:
$\delta \propto (1 - \sigma)$

The chemical shift is anisotropic. It is not described by a single number, but by a second rank spatial tensor, defined by the three principal values of the tensor and the angles that define the orientation of the principle values in the molecular reference frame.

NMR interactions are anisotropic

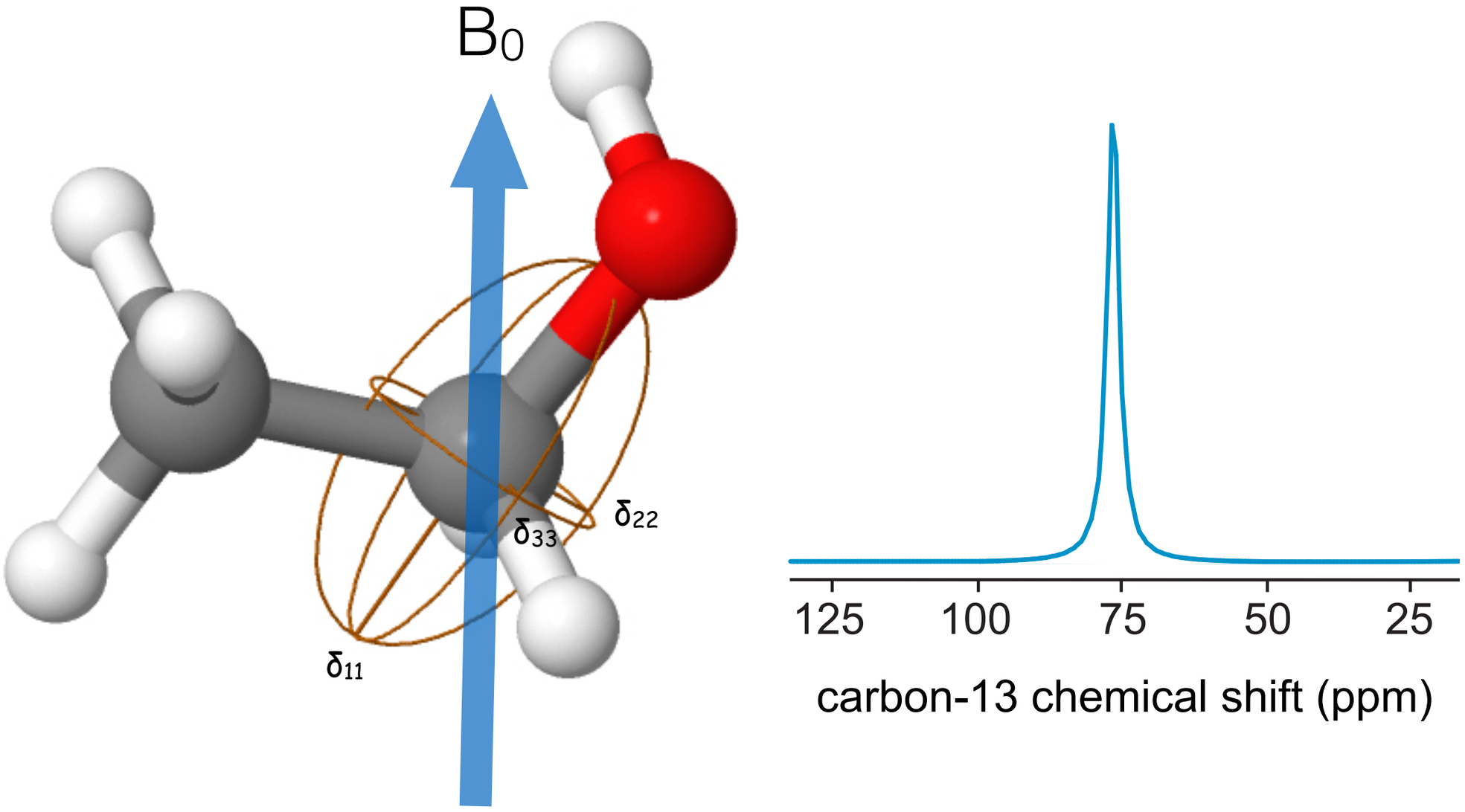

δ_{11} = 104 ppm ; δ_{22} = 44 ppm ; δ_{33} = 25 ppm (by convention $\delta_{11} > \delta_{22} > \delta_{33}$)

The chemical shift is anisotropic. Therefore the chemical shift must depend on the orientation of the molecule with respect to the magnetic field. The chemical shift is given by the magnitude of the tensor component that is parallel to the magnetic field for a given orientation.

NMR interactions are anisotropic

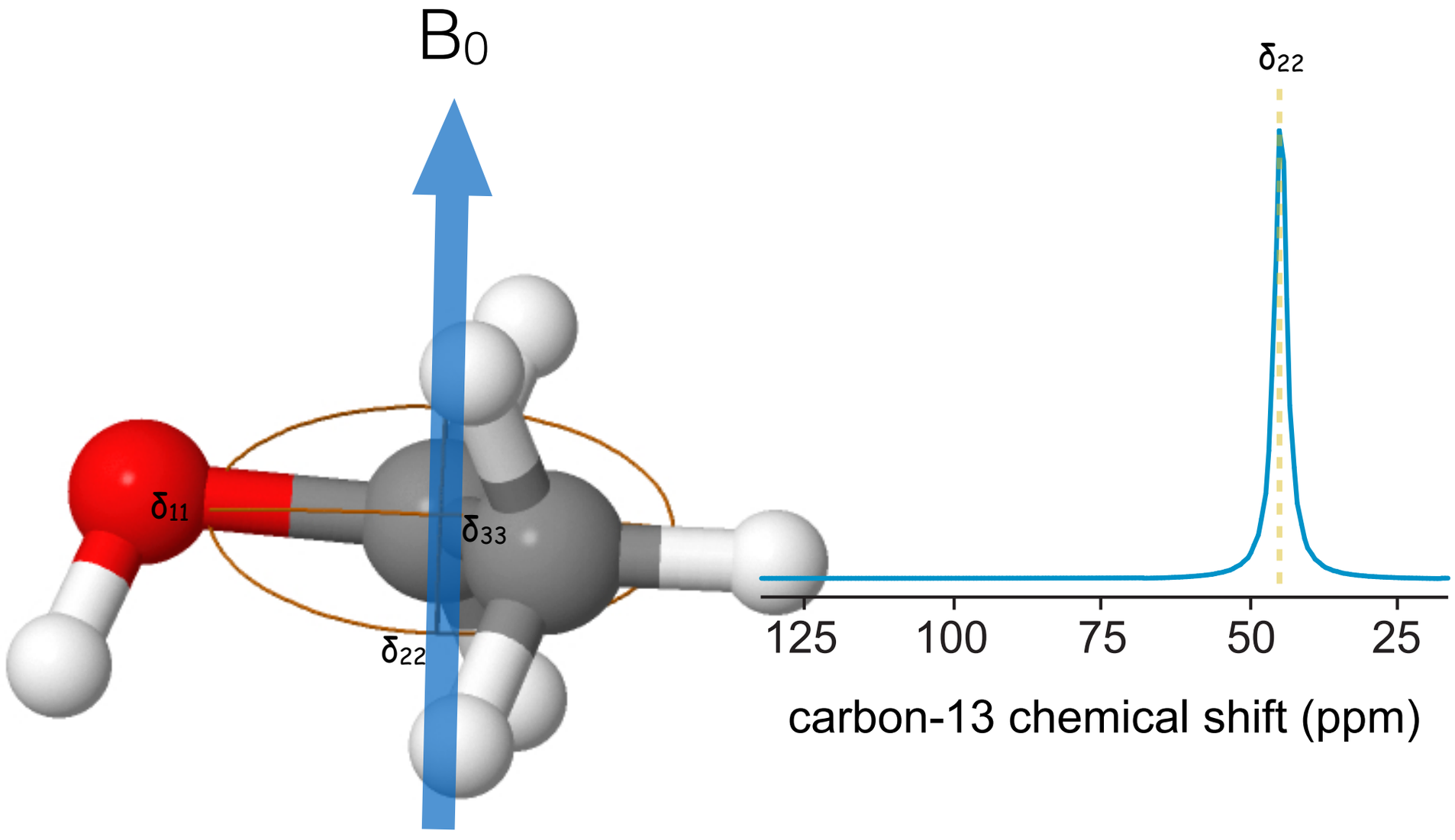

δ_{11} = 104 ppm ; δ_{22} = 44 ppm ; δ_{33} = 25 ppm (by convention $\delta_{11} > \delta_{22} > \delta_{33}$)

The chemical shift is anisotropic. It is not described by a single number, but by a second rank spatial tensor, defined by the three principal values of the tensor and the angles that define the orientation of the principle values in the molecular reference frame.

NMR interactions are anisotropic

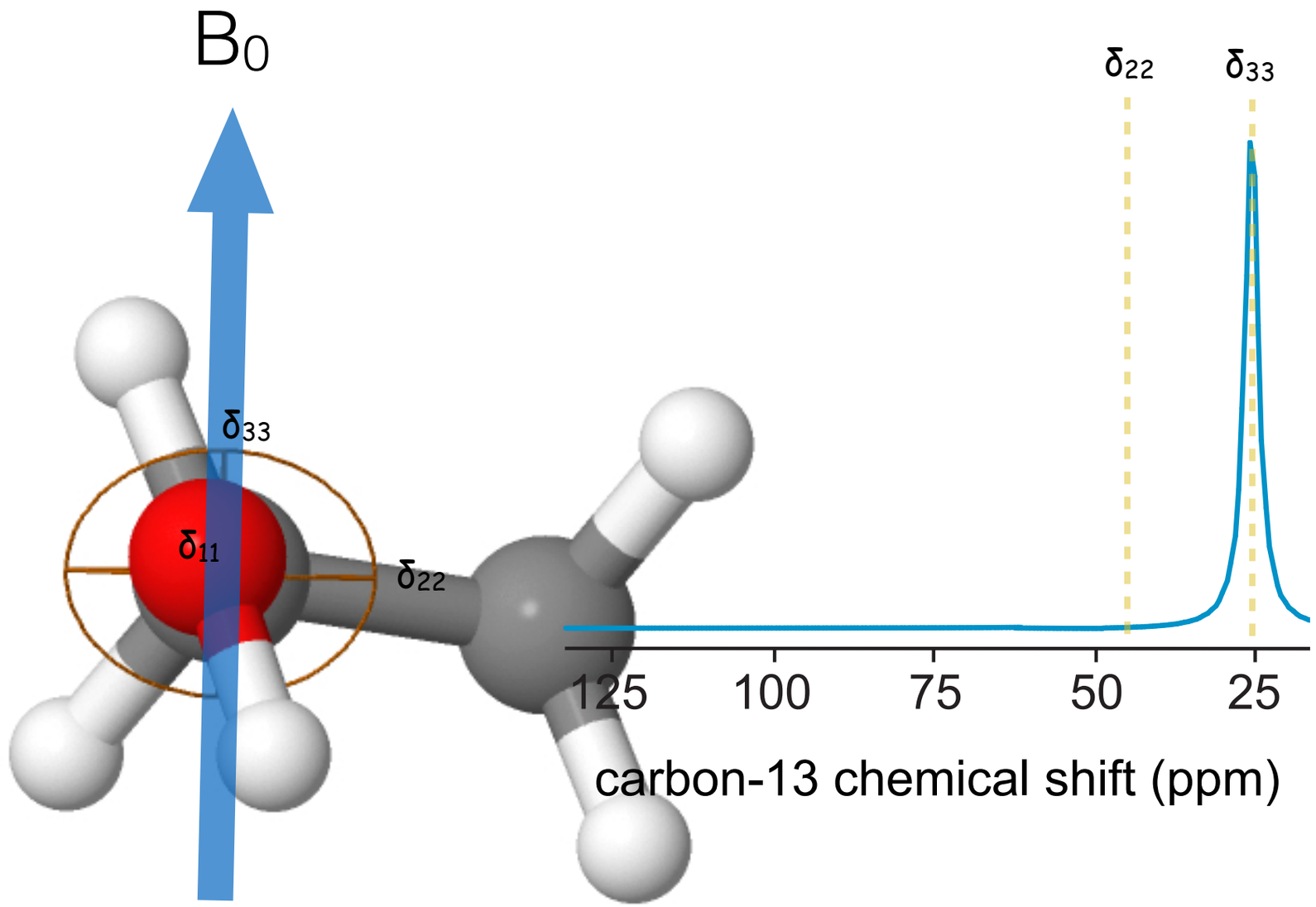

δ_{11} = 104 ppm ; δ_{22} = 44 ppm ; δ_{33} = 25 ppm (by convention $\delta_{11} > \delta_{22} > \delta_{33}$)

The chemical shift is anisotropic. It is not described by a single number, but by a second rank spatial tensor, defined by the three principal values of the tensor and the angles that define the orientation of the principle values in the molecular reference frame.

NMR interactions are anisotropic

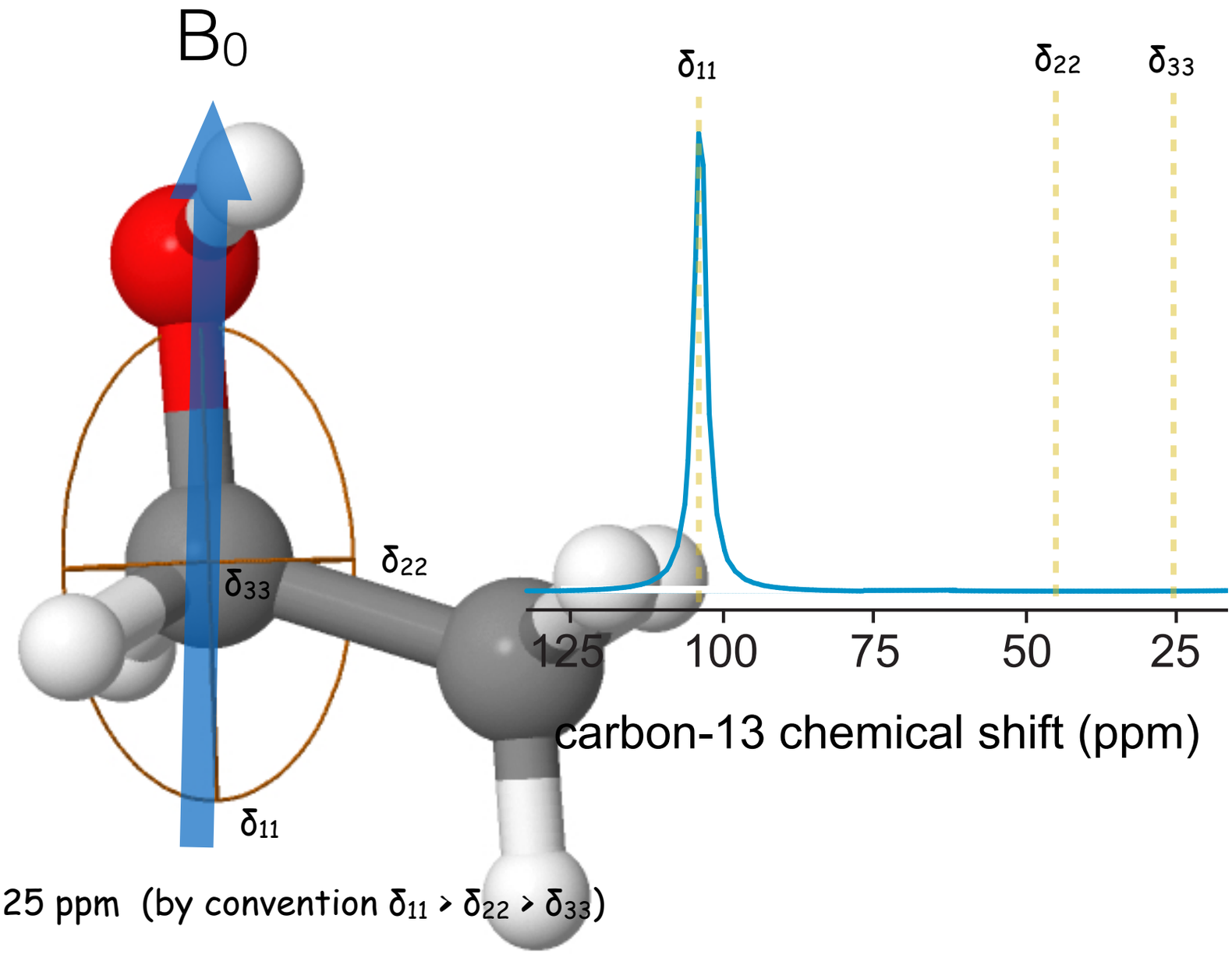

δ_{11} = 104 ppm ; δ_{22} = 44 ppm ; δ_{33} = 25 ppm (by convention $\delta_{11} > \delta_{22} > \delta_{33}$)

The chemical shift is anisotropic. It is not described by a single number, but by a second rank spatial tensor, defined by the three principal values of the tensor and the angles that define the orientation of the principle values in the molecular reference frame.

NMR interactions are anisotropic

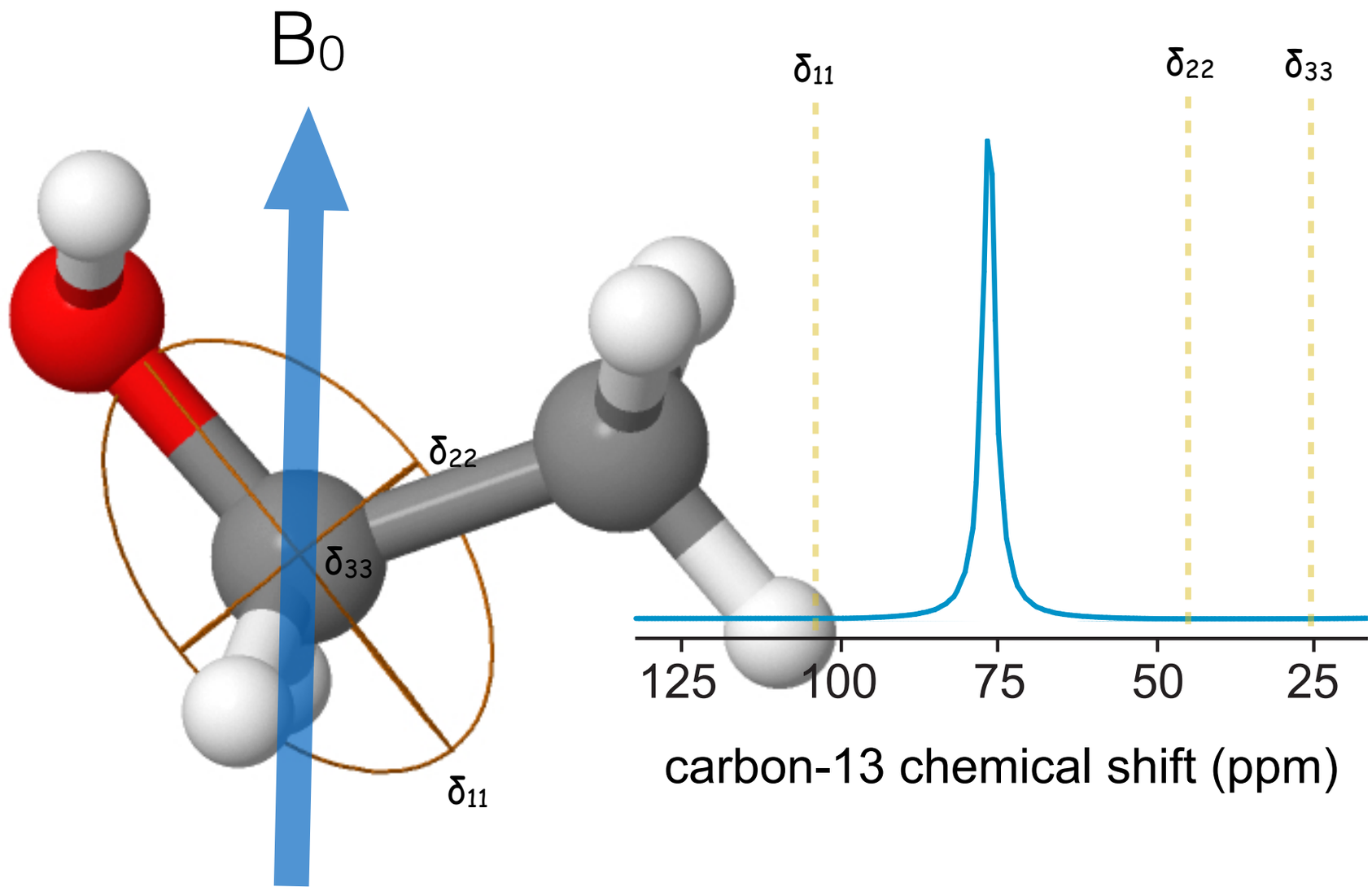

δ_{11} = 104 ppm ; δ_{22} = 44 ppm ; δ_{33} = 25 ppm (by convention $\delta_{11} > \delta_{22} > \delta_{33}$)

The chemical shift is anisotropic. It is not described by a single number, but by a second rank spatial tensor, defined by the three principal values of the tensor and the angles that define the orientation of the principle values in the molecular reference frame.

NMR interactions are anisotropic

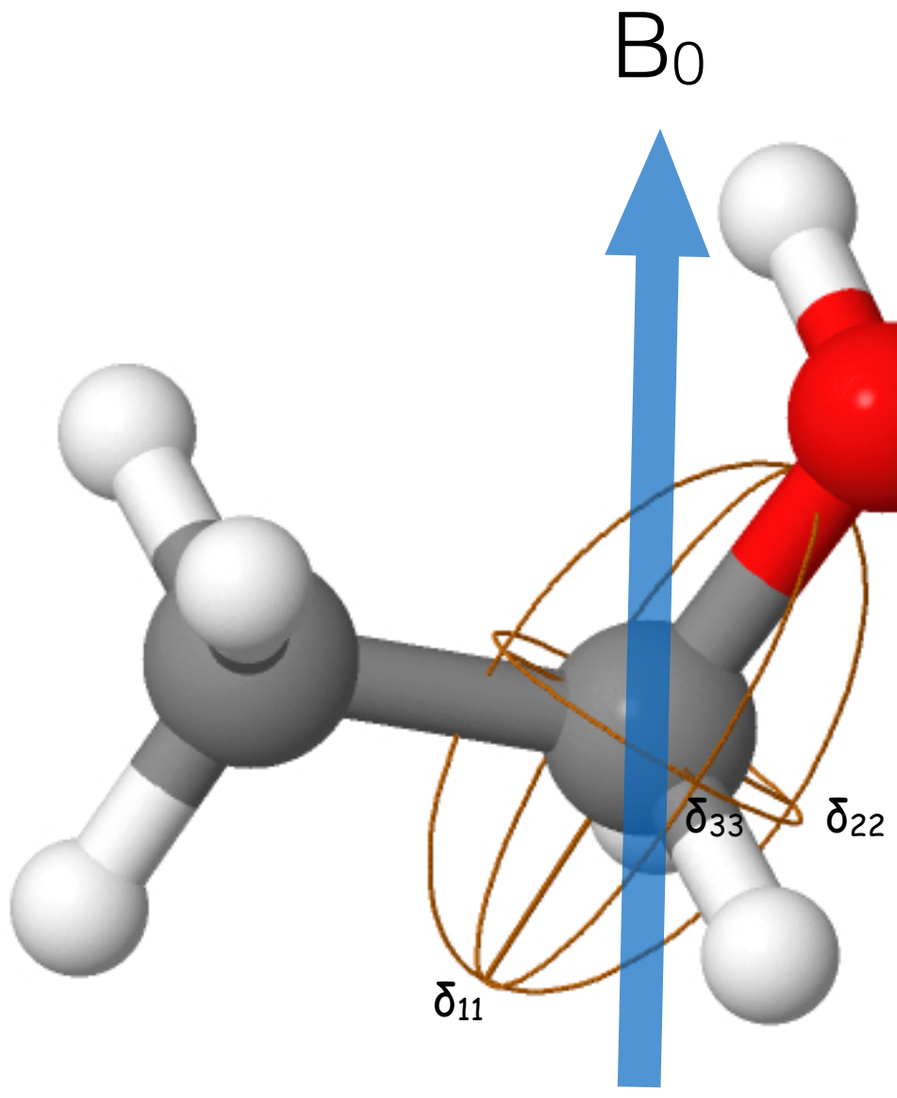

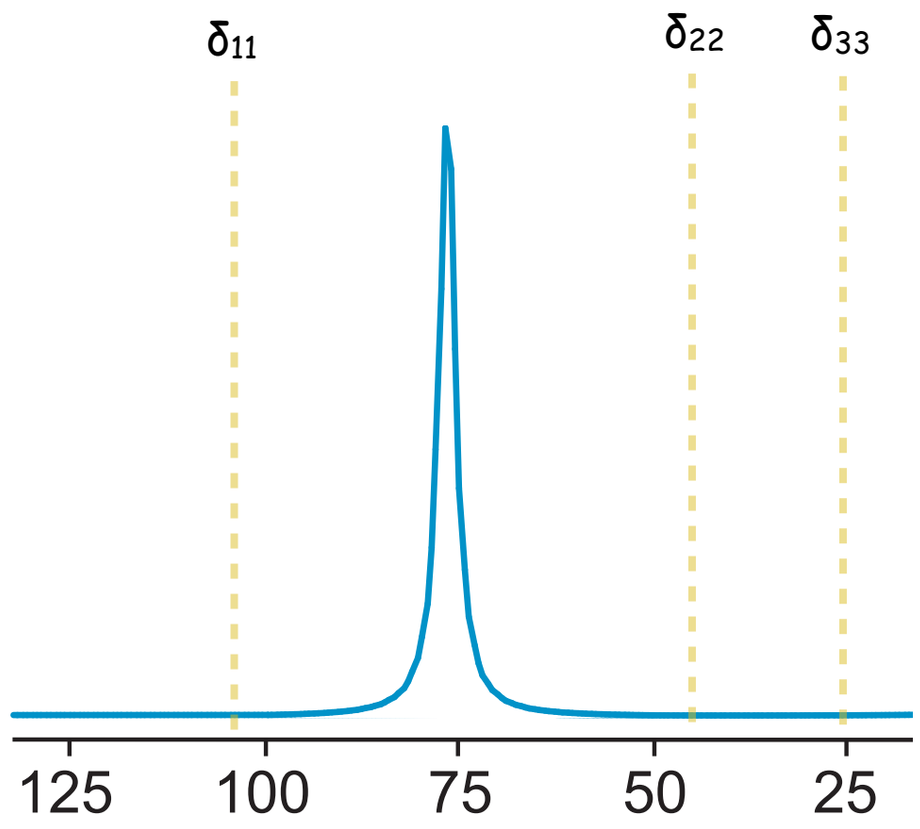

δ_{11} = 104 ppm ; δ_{22} = 44 ppm ; δ_{33} = 25 ppm (by convention $\delta_{11} > \delta_{22} > \delta_{33}$)

The chemical shift is anisotropic. It is not described by a single number, but by a second rank spatial tensor, defined by the three principal values of the tensor and the angles that define the orientation of the principle values in the molecular reference frame.

NMR interactions are anisotropic

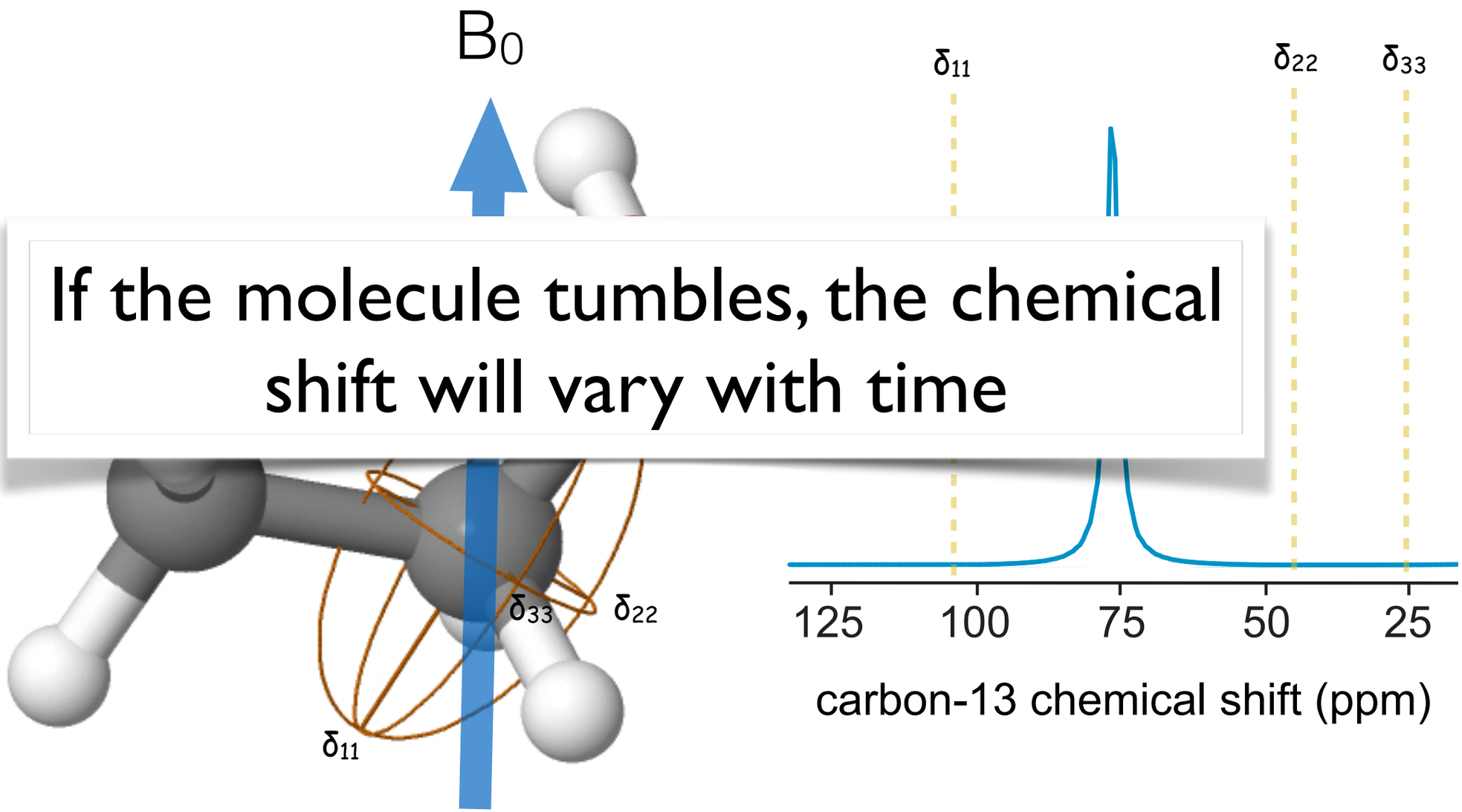

If the molecule tumbles, the chemical shift will vary with time

δ_{11} = 104 ppm ; δ_{22} = 44 ppm ; δ_{33} = 25 ppm (by convention $\delta_{11} > \delta_{22} > \delta_{33}$)

The chemical shift is anisotropic. It is not described by a single number, but by a second rank spatial tensor, defined by the three principal values of the tensor and the angles that define the orientation of the principle values in the molecular reference frame.

The Dipolar Interaction

The classical interaction energy E between two magnetic moments μ_1 and μ_2 is

$$E = \left(\frac{\mu_1 . \mu_2}{r^3} - \frac{3(\mu_1 . \boldsymbol{r})(\mu_2 . \boldsymbol{r})}{r^5} \right) \frac{\mu_0}{4\pi}$$

and the corresponding spin Hamiltonian is therefore

$$\mathcal{H}_D = \frac{\mu_0 \hbar^2 \gamma_1 \gamma_2}{4\pi r_{12}^3} \left(I_1 . I_2 - \frac{3(I_1 . r_{12})(I_2 . r_{12})}{r_{12}^2} \right)$$

We will now do something strange, because we know that subsequently the dipolar interaction, like the chemical shift, will be truncated by $\mathcal{H}_0$. We expand $\mathcal{H}_D$ into a series of *orientationally dependent* terms, called the dipolar alphabet:

$$\mathcal{H}_D = \frac{\mu_0 \hbar^2 \gamma_1 \gamma_2}{4\pi r^3} (A + B + C + D + E + F)$$

where

$$A = I_{1z} I_{2z} (1 - 3\cos^2\theta)$$

$$B = -\tfrac{1}{4} \left(I_1^+ I_2^- + I_1^- I_2^+ \right) (1 - 3\cos^2\theta)$$

$$C = -\tfrac{3}{2} \left(I_1^+ I_{2z} + I_{1z} I_2^+ \right) \sin\theta \cos\theta \exp(-i\phi)$$

$$D = -\tfrac{3}{2} \left(I_1^- I_{2z} + I_{1z} I_2^- \right) \sin\theta \cos\theta \exp(+i\phi)$$

$$E = -\tfrac{3}{4} I_1^+ I_2^+ \sin^2\theta \exp(-2i\phi)$$

$$F = -\tfrac{3}{4} I_1^- I_2^- \sin^2\theta \exp(+2i\phi)$$

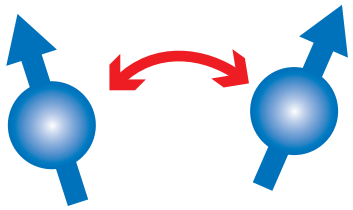

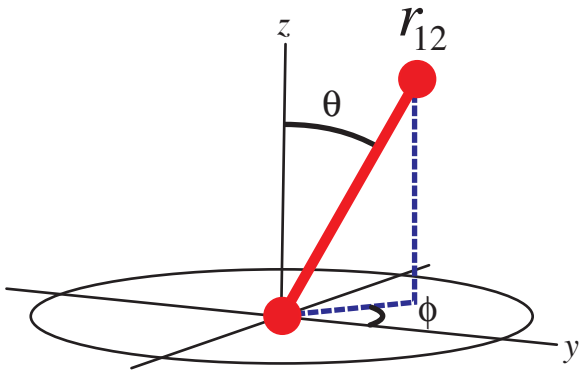

Quantum Spins in a Classical Lattice:

The Abragam formulation of the Redfield Approach

We have described the longitudinal relaxation rate in the presence of some arbitrary fluctuating fields. We immediately see that it is dependent on the correlation time of the fluctuation (i.e. molecular tumbling rate). To see this in detail we must specify the interactions. It will come as no surprise that the fluctuating interaction is usually the dipolar interaction.

$$\mathcal{H}_D = \sum_m T_{2m} R_{2m}$$

Thus, with $V_m = \frac{\gamma^2 h}{r^3} T_{2m}$ and $F_m = R_{2m}$, we obtain with equation (8)

$$\frac{1}{T_1} = \left[\frac{\gamma^2 h}{r^3}\right]^2 \frac{1}{8} 2\tau_c \left(J_1(\omega_0) + 4J_2(2\omega_0)\right)$$

Rotational Brownian motion leads to exponential correlation functions,

$$\overline{|R_{2m}^2|} \exp(-|\tau|/\tau_c) = \frac{6}{5}\exp(-|\tau|/\tau_c)$$

so according to equation (9)we find that the relaxation rate is

$$\frac{1}{T_1} = \frac{3}{10}\left[\frac{\gamma^4 h^2}{r^6}\right]^2 \tau_c \left[\frac{1}{1+\omega_0^2\tau_c^2} + \frac{4}{1+4\omega_0^2\tau_c^2}\right]$$

It depends on internuclear distance and the *details* of molecular motion.

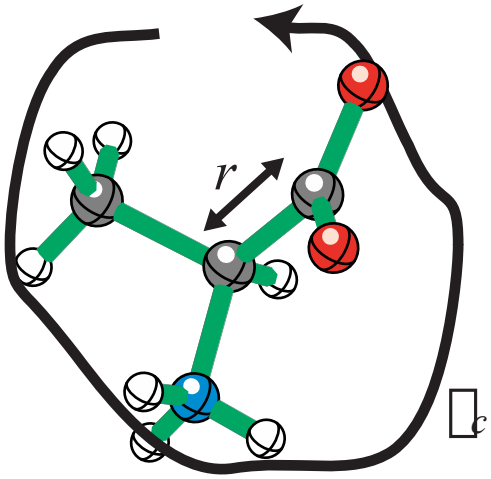

Relaxation in a Nutshell

$$\frac{1}{T_1} = \frac{3}{10}\left(\frac{\gamma^4 h^2}{r^6}\right)\tau_c\left\{\frac{1}{1+\omega_0^2\tau_c^2} + \frac{4}{1+4\omega_0^2\tau_c^2}\right\}$$

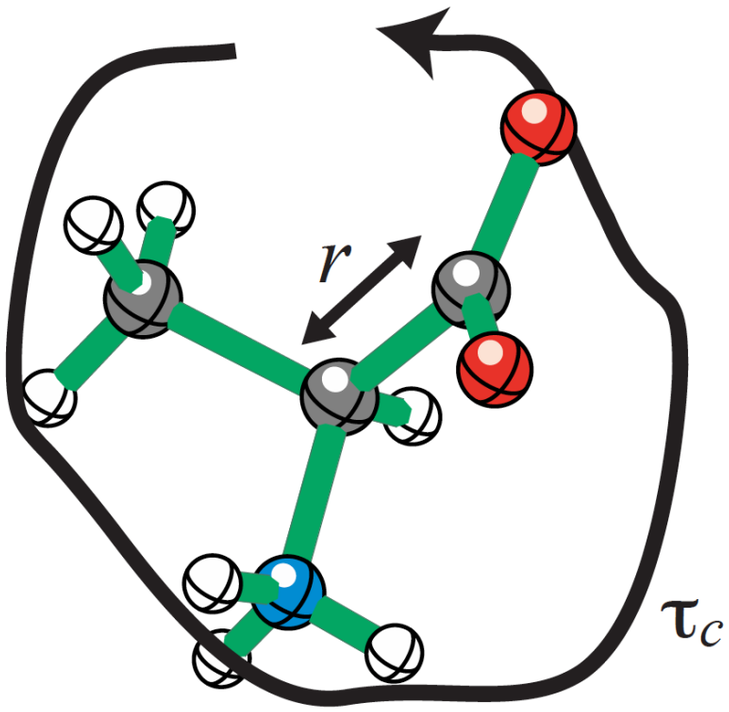

- Using second order perturbation theory, ***Longitudinal & Transverse relaxation rates can be related exactly to internuclear distances and molecular dynamics***

- The example here is T_1 relaxation by the dipolar coupling between two identical spins undergoing rotational Brownian motion

Quantum Spins in a Classical Lattice:

The Abragam formulation of the Redfield Approach

SUMMARY OF THE FORMALISM

What we have outlined is **Redfield theory**, which was first cast in operator form by Abragam.

The **Redfield Apporximations** that we made in the derivation are:

(a) It is possible to neglect the correlation between $\tilde{\mathcal{H}}_1(t)$ and $\rho(0)$. This allows the averaging over the ensemble $-i\left[\overline{\tilde{\mathcal{H}}_1(t),\rho(0)}\right]$

(b) It is possible to replace $\rho(0)$ by $\rho(t)$ on the r.h.s.

(c) It is possible to extend the upper limit of the integral to infinity.

(d) It is possible to neglect all higher order terms in the expansion.

All these approximations are valid if $\sqrt{\overline{\left|\mathcal{H}_1\right|^2}}\tau_c^2$ is a very small number.

Thus it is valid for short correlation times (i.e. rapid molecular motions)

Cross Relaxation Between Unlike Spins

The Abragam formulation of the Redfield Approach

EXAMPLE 2: DIPOLAR RELAXATION OF TWO UNLIKE SPINS

$$\mathcal{H}_0 = \omega_I I_z + \omega_S S_z$$

If there is a large difference in Larmor frequencies, the definition of the V_{ω} leads to a splitting up of the terms in the dipolar Hamiltonian

$$T_{20} = A + B + B[$$

$$T_{2,\pm 1} = C^I_{\pm 1} + C^S_{\pm 1}$$

and in the interaction representation (a doubly rotating frame)

$$\tilde{A}(t) = \tfrac{2}{\sqrt{6}} I_z S_z$$
$$\tilde{B}(t) = \omega \tfrac{1}{2\sqrt{6}} I_+ S_{\omega} \exp\{i(\omega_I \omega \omega_S)t\}$$
$$\tilde{B}^{\dagger}(t) = \omega \tfrac{1}{2\sqrt{6}} I_{\omega} S_+ \exp\{\omega i(\omega_I \omega \omega_S)t\}$$
$$\tilde{C}^I_{\pm 1}(t) = \omega \tfrac{1}{2} I_{\pm} S_z \exp(\pm i \omega_I t)$$
$$\tilde{C}^S_{\pm 1}(t) = \pm \tfrac{1}{2} I_z S_{\pm} \exp(\pm i \omega_I t)$$

whereas the other terms remain unaltered

$$T_{2,\pm 2} = \omega \tfrac{1}{2} I_{\pm} S_{\pm} \exp\{\pm i(\omega_I + \omega_S)t\}.$$

Cross Relaxation Between Unlike Spins

The Abragam formulation of the Redfield Approach

We must now calculate the evolution of $Q = I_z, S_z, ...etc$. We do not give details but we remark that the double commutator

$$\left[\left[I_z, B\right], B^{\dagger}\right] \propto \left[I_+ S_-, I_- S_+\right].$$

Which through repeated use of $[AB,C] = A[B,C] + [A,C]B$ yields

$$\begin{aligned}
\left[I_+ S_-, I_- S_+\right] &= I_+ \left[S_-, I_- S_+\right] + \left[I_+, I_- S_+\right] S_- \\
&= -2 S_z I_+ I_- + 2 I_z S_+ S_- \\
&= -2 S_z \left(\tfrac{1}{2} + I_z\right) + 2 I_z \left(\tfrac{1}{2} + S_z\right) \\
&= I_z - S_z
\end{aligned}$$

Thus this term yields a contribution proportional to $\left(\langle I_z \rangle - \langle I_z \rangle_{eq}\right) - \left(\langle S_z \rangle - \langle S_z \rangle_{eq}\right)$. The detailed calculation finishes with the **Solomon equations** expressing the **nuclear Overhauser effect**.

$$\frac{d}{dt}\begin{pmatrix} I_z \\ S_z \end{pmatrix} = \begin{pmatrix} \rho_I & \sigma \\ \sigma & \rho_S \end{pmatrix} \begin{pmatrix} \Delta I_z \\ \Delta S_z \end{pmatrix}$$

with

$$\rho_I = \frac{1}{10}\left(\frac{\gamma_I^2 \gamma_S^2 h^2}{r^6}\right) \tau_c \left\{ \frac{3}{1 + \omega_I^2 \tau_c^2} + \frac{1}{1 + \left(\omega_I - \omega_S\right)^2 \tau_c^2} + \frac{6}{1 + \left(\omega_I + \omega_S\right)^2 \tau_c^2} \right\}$$

$$\sigma = \frac{1}{10}\left(\frac{\gamma_I^2 \gamma_S^2 h^2}{r^6}\right) \tau_c \left\{ \frac{1}{1 + \left(\omega_I - \omega_S\right)^2 \tau_c^2} + \frac{6}{1 + \left(\omega_I + \omega_S\right)^2 \tau_c^2} \right\}$$

Cross Relaxation Between Unlike Spins

The Abragam formulation of the Redfield Approach

We must now calculate the evolution of $Q = I_z, S_z, ...etc$. We do not give details but we remark that the double commutator

$$\left[\left[I_z,B\right],B^{\dagger}\right] \mu \left[I_+S_-,I_-S_+\right].$$

Which through repeated use of $[AB,C] = A[B,C] + [A,C]B$ yields

$$\begin{aligned}[I_+S_-,I_-S_+] &= I_+[S_-,I_-S_+] + [I_+,I_-S_+]S_- \\ &= -2S_zI_+I_- + 2I_zS_+S_- \\ &= -2S_z\left(\tfrac{1}{2} + I_z\right) + 2I_z\left(\tfrac{1}{2} + S_z\right) \\ &= I_z - S_z\end{aligned}$$

Thus this term yields a contribution proportional to $\left(\langle I_z\rangle - \langle I_z\rangle_{eq}\right) - \left(\langle S_z\rangle - \langle S_z\rangle_{eq}\right)$. The detailed calculation finishes with the **Solomon equations** expressing the **nuclear Overhauser effect**.

$$\frac{d}{dt}\begin{pmatrix} I_z \\ S_z \end{pmatrix} = \begin{pmatrix} \rho_I & \sigma \\ \sigma & \rho_S \end{pmatrix}\begin{pmatrix} \Delta I_z \\ \Delta S_z \end{pmatrix}$$

This has exactly the same form as the exchange matrix: the nOe will lead to magnetization exchange

with

$$\rho_I = \frac{1}{10}\,\frac{\gamma_I^2\gamma_S^2h^2}{r^6}\,\tau_c\left(\frac{3}{1+\omega_I^2\tau_c^2} + \frac{1}{1+(\omega_I-\omega_S)^2\tau_c^2} + \frac{6}{1+(\omega_I+\omega_S)^2\tau_c^2}\right)$$

$$\sigma = \frac{1}{10}\,\frac{\gamma_I^2\gamma_S^2h^2}{r^6}\,\tau_c\left(\frac{1}{1+(\omega_I-\omega_S)^2\tau_c^2} + \frac{6}{1+(\omega_I+\omega_S)^2\tau_c^2}\right)$$

The magnetization exchange rate is determined by the rotational correlation time of the molecule & the inter-nuclear distance

†

INFORMATION ONLY

Cross Relaxation in a Nutshell

$$\frac{d}{dt}\begin{pmatrix} I_z \\ S_z \end{pmatrix} = \begin{pmatrix} \rho_I & \sigma \\ \sigma & \rho_S \end{pmatrix}\begin{pmatrix} \Delta I_z \\ \Delta S_z \end{pmatrix}$$

with

$$\rho_I = \frac{1}{10}\left(\frac{\gamma_I^2\gamma_S^2h^2}{r^6}\right)\tau_c\left\{\frac{3}{1+\omega_I^2\tau_c^2} + \frac{1}{1+(\omega_I-\omega_S)^2\tau_c^2} + \frac{6}{1+(\omega_I+\omega_S)^2\tau_c^2}\right\}$$

$$\sigma = \frac{1}{10}\left(\frac{\gamma_I^2\gamma_S^2h^2}{r^6}\right)\tau_c\left\{\frac{1}{1+(\omega_I-\omega_S)^2\tau_c^2} + \frac{6}{1+(\omega_I+\omega_S)^2\tau_c^2}\right\}$$

- We predict that dipolar relaxation between different spins will lead to ***magnetisation transfer with a rate that depends on internuclear distances and molecular dynamics***

- This is the nuclear Overhauser effect

Conclusions I

- Motion of nuclear spins is always induced by magnetic fields.
- Those fields can be coherent, or incoherent (random).
- Random fields acting statistically independently on an ensemble will induce a return to equilibrium.
- Longitudinal random fields (i.e. at frequencies close to zero) induce transverse relaxation.
- Transverse (i.e. resonant) random fields induce transverse & longitudinal relaxation.

Conclusions II

- The motion of an ensemble of spins experiencing random fields can be described by a second order perturbation approach that yields the Redfield equation of motion. (Under certain approximations.)

- Fluctuating fields arise primarily (but not only) from anisotropic interactions being modulated by molecular motion.

- Anisotropic interactions include the chemical shift and the dipolar coupling. (The quadrupolar interaction for spin $I > 1/2$; the electron-nuclear hyperfine interaction for paramagnetic samples)).

- Dipolar relaxation is usually the dominant mechanism for spin $I = 1/2$ in diamagnetic liquids.

Structure

https://www.youtube.com/watch?v=iaHHgEoa2c8

Objectives

- Discover how can distances be measured experimentally using the nOe with steady-state or transient experiments.

- Understand how distances can be determined from 2D NOESY spectra.

- Understand the five step protocol for complete protein structure determination.

Cross Relaxation in a Nutshell

$$\frac{d}{dt}\begin{pmatrix} I_z \\ S_z \end{pmatrix} = \begin{pmatrix} \rho_I & \sigma \\ \sigma & \rho_S \end{pmatrix}\begin{pmatrix} \Delta I_z \\ \Delta S_z \end{pmatrix}$$

with

$$\rho_I = \frac{1}{10}\left(\frac{\gamma_I^2\gamma_S^2h^2}{r^6}\right)\tau_c\left\{\frac{3}{1+\omega_I^2\tau_c^2} + \frac{1}{1+(\omega_I-\omega_S)^2\tau_c^2} + \frac{6}{1+(\omega_I+\omega_S)^2\tau_c^2}\right\}$$

$$\sigma = \frac{1}{10}\left(\frac{\gamma_I^2\gamma_S^2h^2}{r^6}\right)\tau_c\left\{\frac{1}{1+(\omega_I-\omega_S)^2\tau_c^2} + \frac{6}{1+(\omega_I+\omega_S)^2\tau_c^2}\right\}$$

- We predict that dipolar relaxation between different spins will lead to ***magnetisation transfer with a rate that depends on internuclear distances and molecular dynamics***

- This is the nuclear Overhauser effect

Dependence of Relaxation on Correlation Times

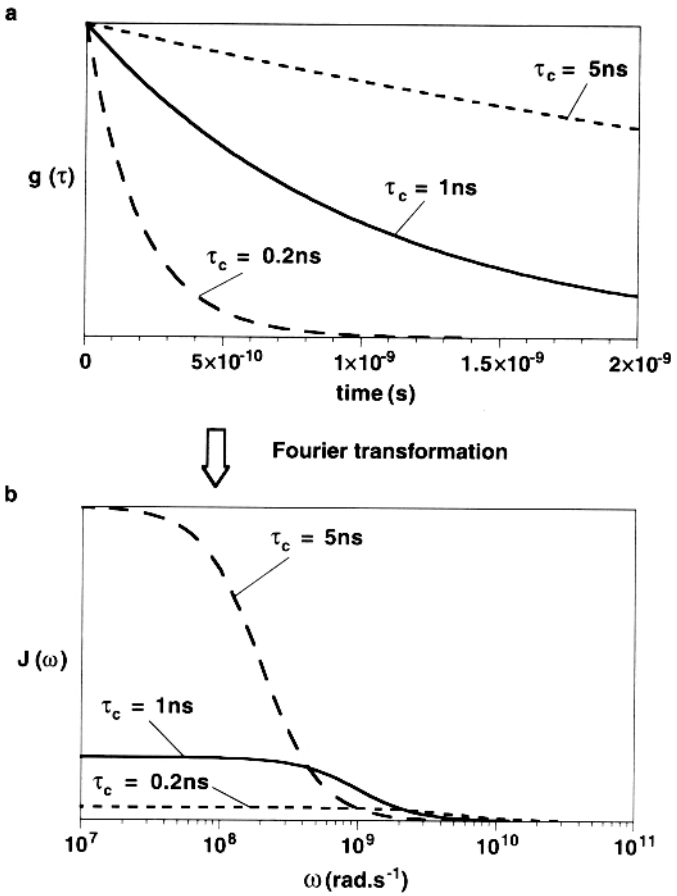

Figure 2.3. Exponentially decaying correlation functions $g(\tau)$ (panel *a*) are converted into Lorentzian spectral density functions $J(\omega)$ (panel *b*) by Fourier transformation. (Note the log scale in panel *b*.) The functions $g(\tau)$ have decay constants of $1/\tau_c$. τ_c values of 0.2 ns, 1 ns and 5 ns have been used to illustrate the behavior expected for short, intermediate, and long values of τ_c respectively. The area under the curve of $J(\omega)$ is the same in all these cases (although it appears otherwise because of the log scale for frequency).

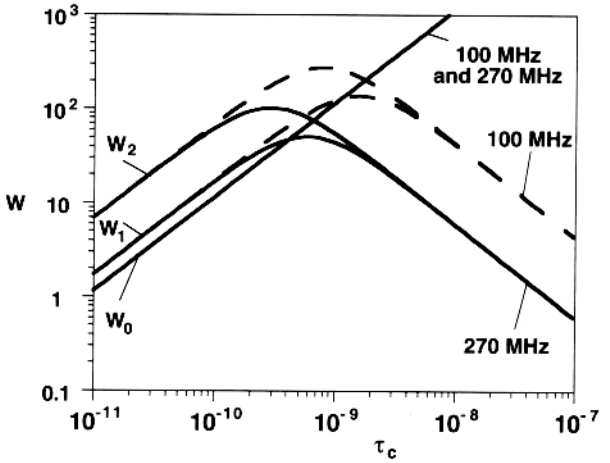

Figure 2.5. Variation of dipolar transition probabilities W_1, W_2, and W_0 with τ_c, shown for spectrometer frequencies of 100 and 270 MHz. Calculated for a pair of protons 1 Å apart. Adapted from ref. 8.

Longitudinal relaxation times go through a minimum at $\omega_0\tau_c \sim 1.1$

Transverse relaxation times decrease with increasing correlation times.

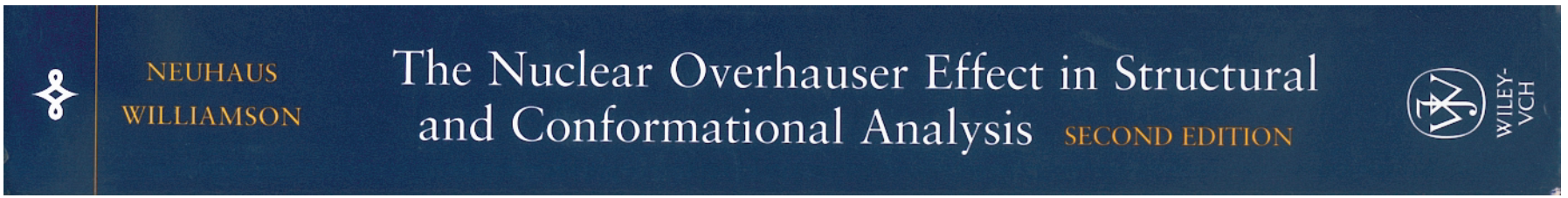

Steady-State nOe

$$\frac{d}{dt}\begin{pmatrix} I_z \\ S_z \end{pmatrix} = \begin{pmatrix} \rho_I & \sigma \\ \sigma & \rho_S \end{pmatrix}\begin{pmatrix} \Delta I_z \\ \Delta S_z \end{pmatrix} \quad \text{with}$$

$$\rho_I = \frac{1}{10}\,\frac{\gamma_I^2\gamma_S^2h^2}{r^6}\,\tau_c\left(\frac{3}{1+\omega_I^2\tau_c^2}+\frac{1}{1+(\omega_I-\omega_S)^2\tau_c^2}+\frac{6}{1+(\omega_I+\omega_S)^2\tau_c^2}\right)$$

$$\sigma = \frac{1}{10}\,\frac{\gamma_I^2\gamma_S^2h^2}{r^6}\,\tau_c\left(\frac{1}{1+(\omega_I-\omega_S)^2\tau_c^2}+\frac{6}{1+(\omega_I+\omega_S)^2\tau_c^2}\right)$$

Consider the case where we continuously irradiate one of the spins (*S*), so as to saturate its transitions. The steady state that results ($dI_z/dt = 0$) is:

$$\left(I_z - I_z^0\right) = \frac{\sigma}{\rho_I}\left(S_z^0\right)$$

From which we can determine the maximum theoretical enhancement for a two-spin system:

$$\eta_{max} = \frac{\gamma_I}{\gamma_S}\frac{\sigma}{\rho_I}$$

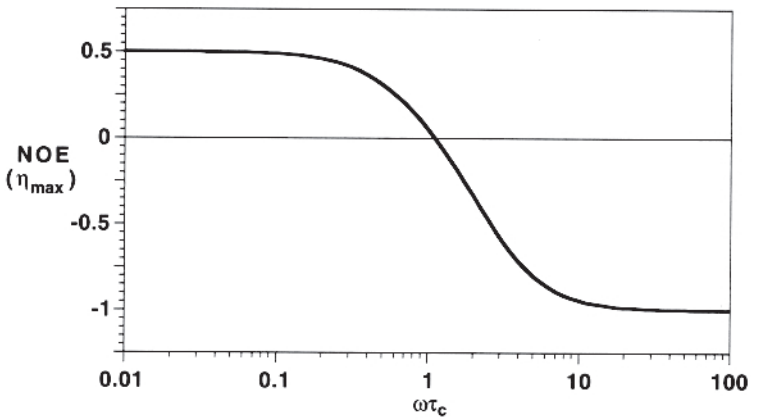

Figure 2.6. Dependence of maximum homonuclear NOE enhancement on $\omega\tau_c$. Note the log scale of $\omega\tau_c$.

Steady-State nOe

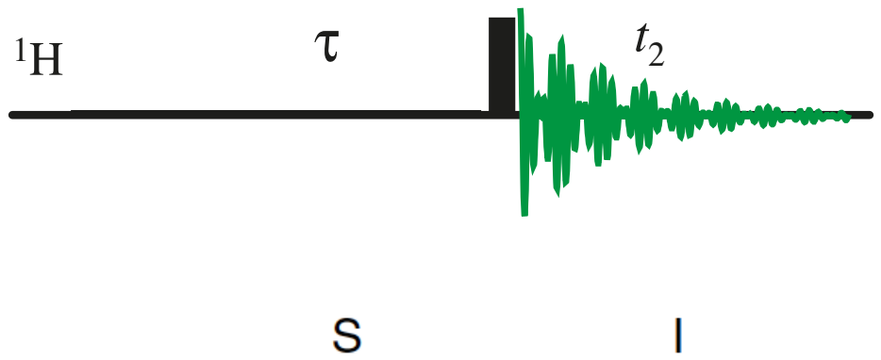

w/wo long low power irradiation at
S spin resonance frequency

Steady-State nOe

with long low power irradiation at
S spin resonance frequency

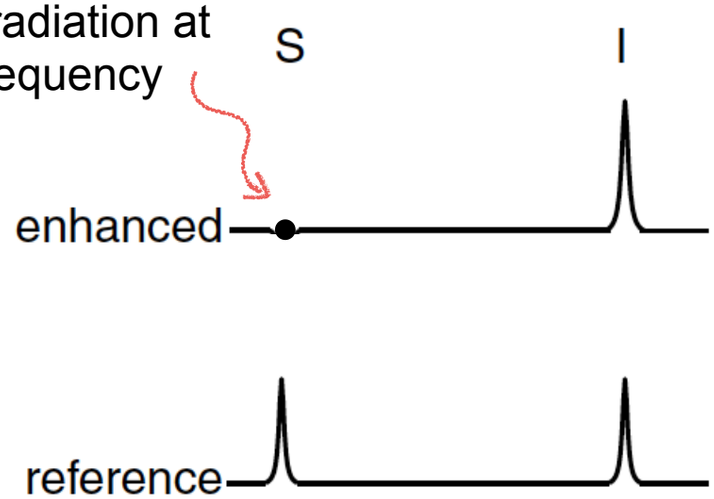

Steady-State nOe

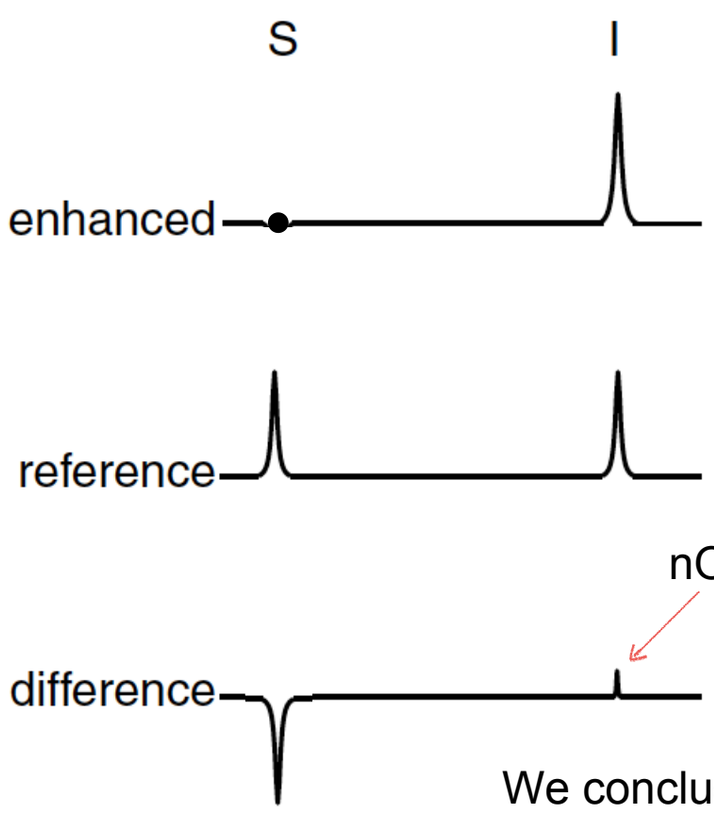

We conclude that S and I are close in space
(typically <5Å)

w/wo long low power irradiation at
S spin resonance frequency

nOe difference experiment on 7-Methoxychrome

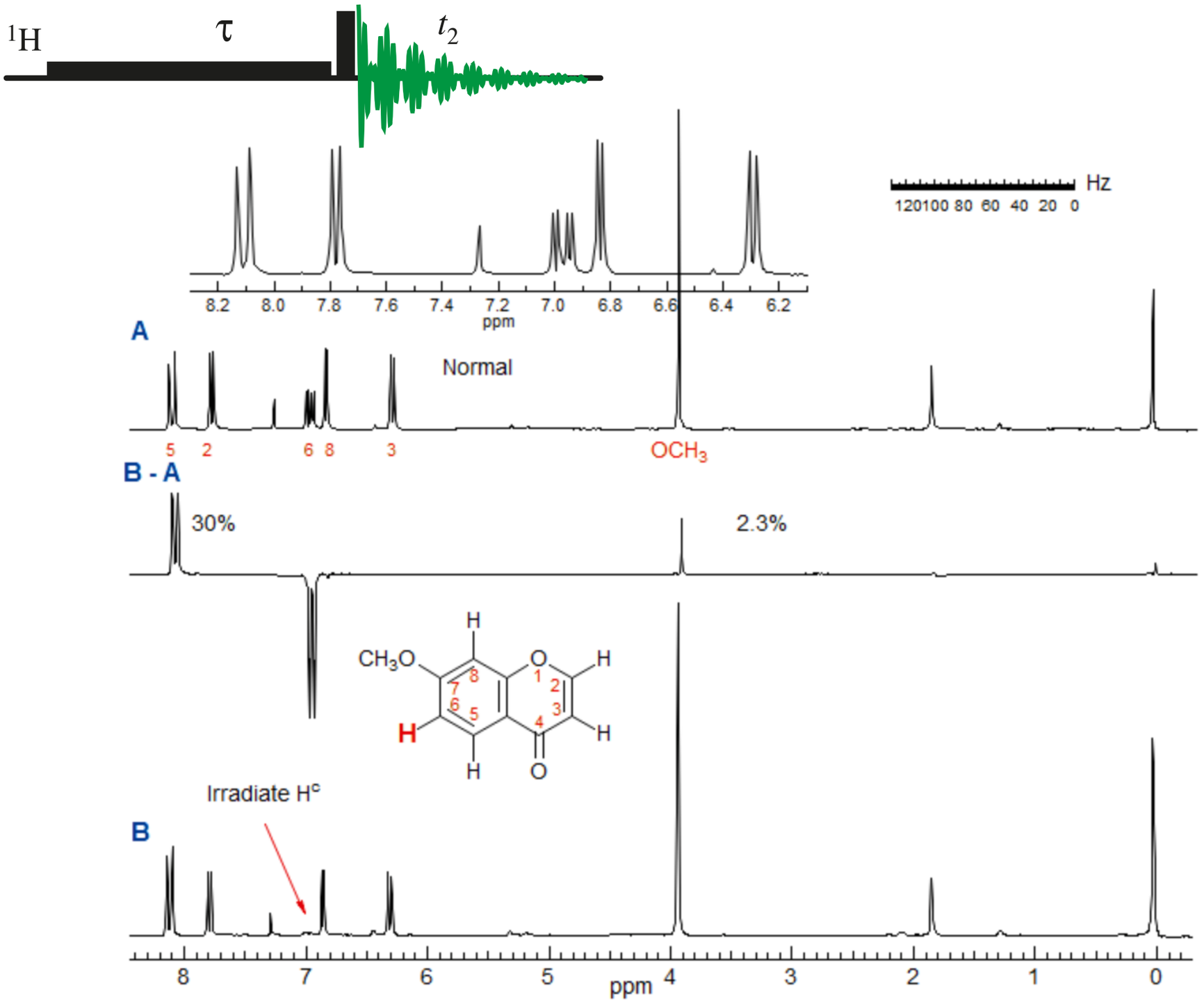

https://www.chem.wisc.edu/areas/reich/nmr/08-tech-02-noe.htm

Examples of the use of nOe difference experiments

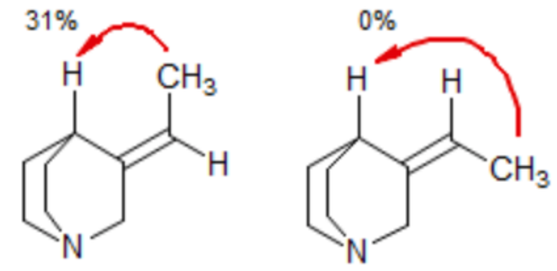

Assignment of E/Z stereochemistry
Tet. Lett. **1967**, 4065

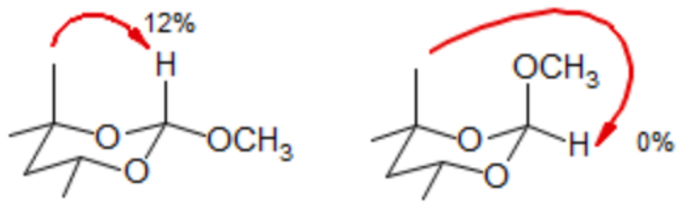

Assignment of stereochemistry

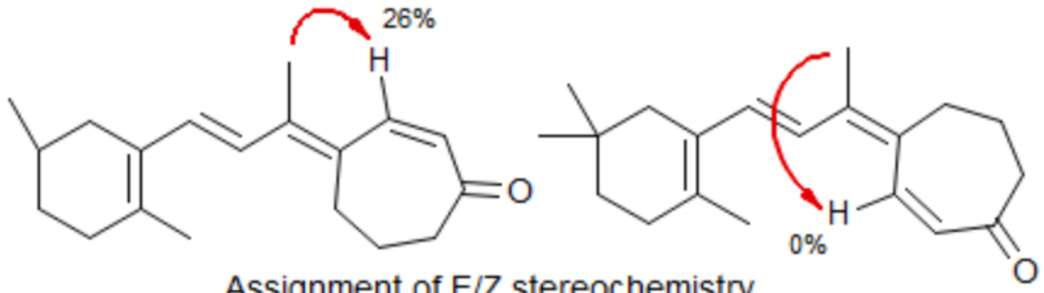

Assignment of E/Z stereochemistry

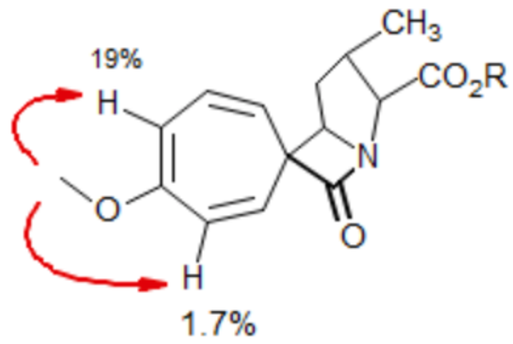

Conformational analysis:
estimated 8:1 ratio of conformers
from rate of NOE buildup
Chem. Comm. **1981**, *22*, 4029

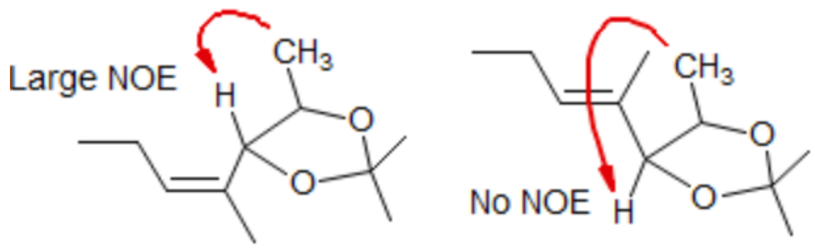

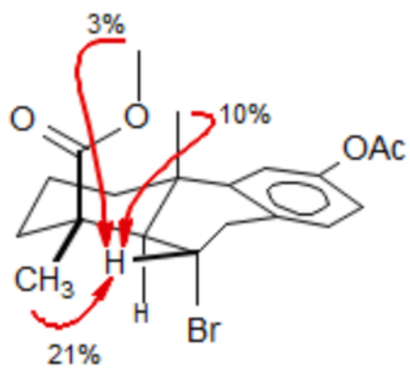

The stereochemistry of the Br was initially misassigned because the 7 Hz coupling was assumed to mean the protons were cis (eq-ax coupling). The NOE experiment demonstrated the stereochemistry shown. *Chem. Comm.* **1968**, 1093

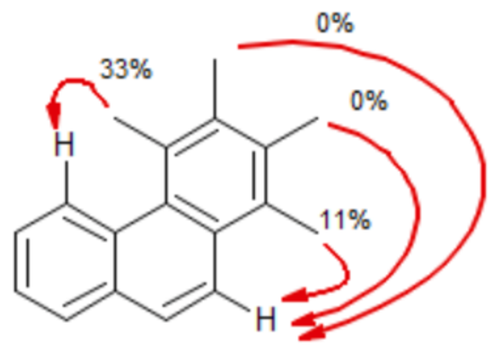

Assignment of Me groups

https://www.chem.wisc.edu/areas/reich/nmr/08-tech-02-noe.htm

Steady-State nOe:
nOe Difference Spectroscopy

long (seconds), very low power continuous irradiation at the exact resonance frequency of one spin

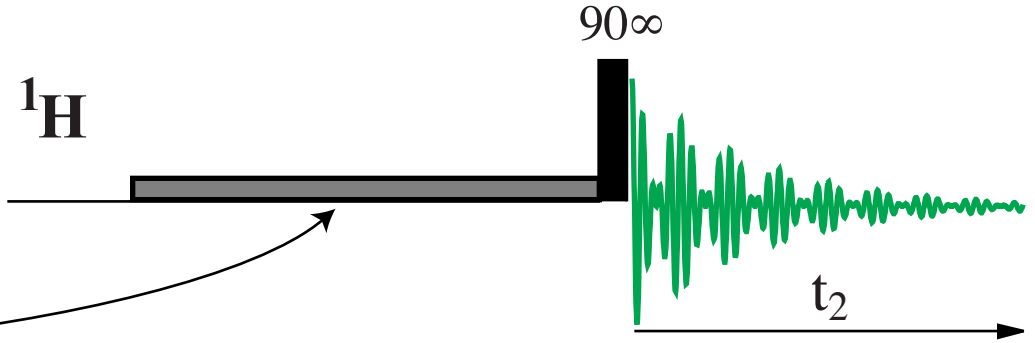

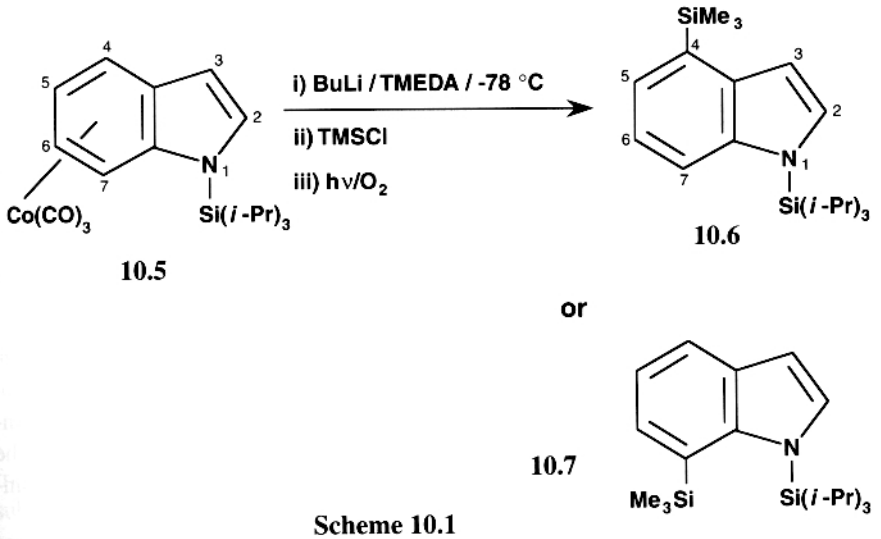

Scheme 10.1

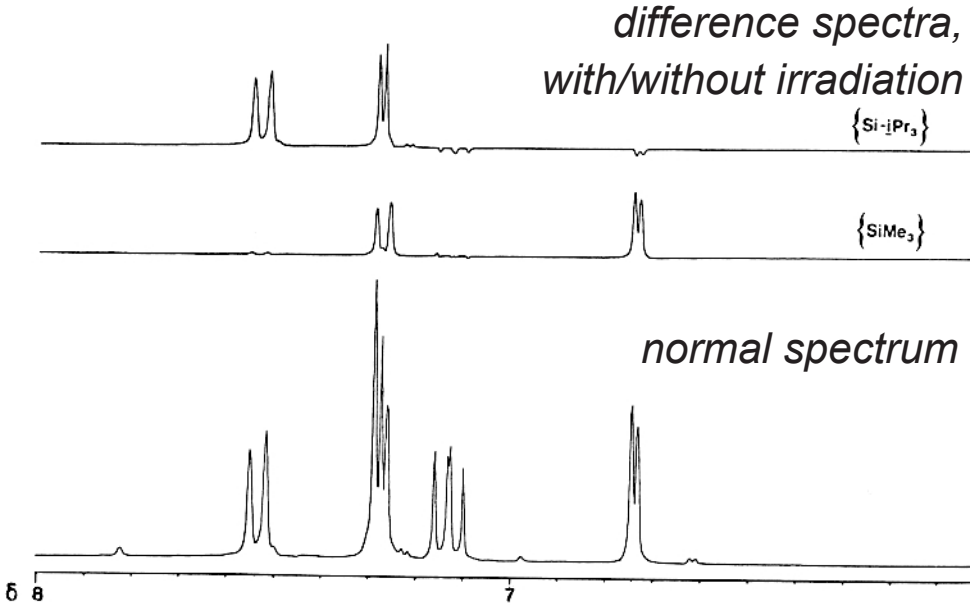

Figure 10.2. NOE difference spectra (aromatic region only) of *N*-triisopropylsilyl-4-trimethylsilylindole **10.6** in $CDCl_3$, recorded at 250 MHz (preirradiation 5 s). These enhancements clearly demonstrate that the TMS group is present at the 4 position of the indole rather than the 7 position. Reproduced with permission from ref. 61.

Steady-State nOe:
nOe Difference Spectroscopy

long (seconds), very low power continuous irradiation at the exact resonance frequency of one spin

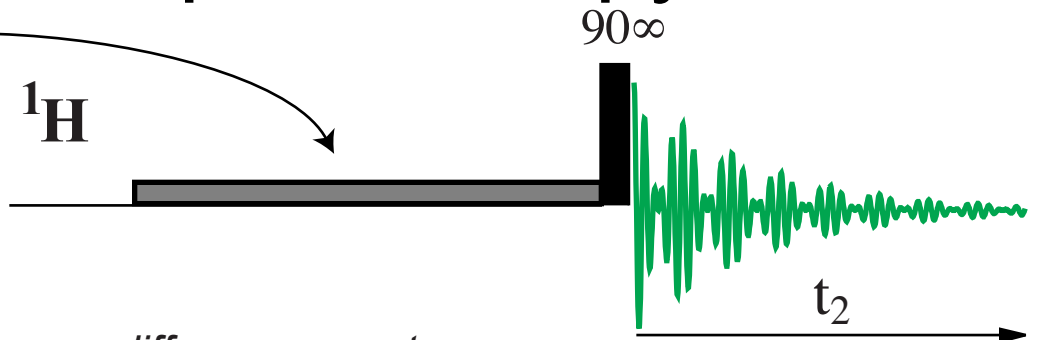

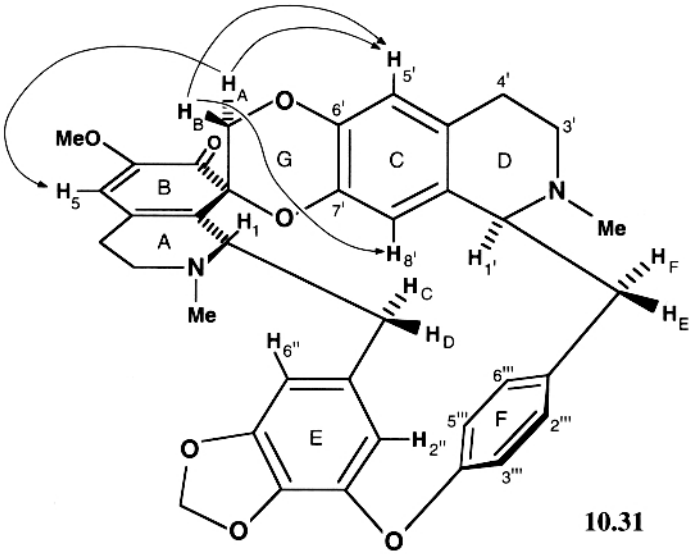

10.31

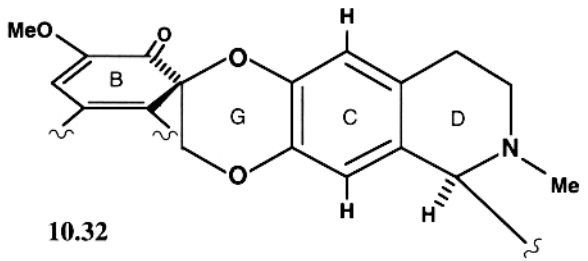

10.32

difference spectra

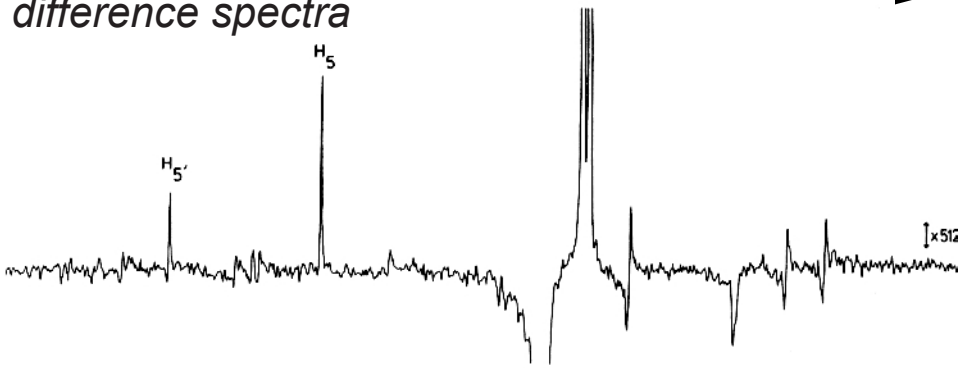

normal spectrum

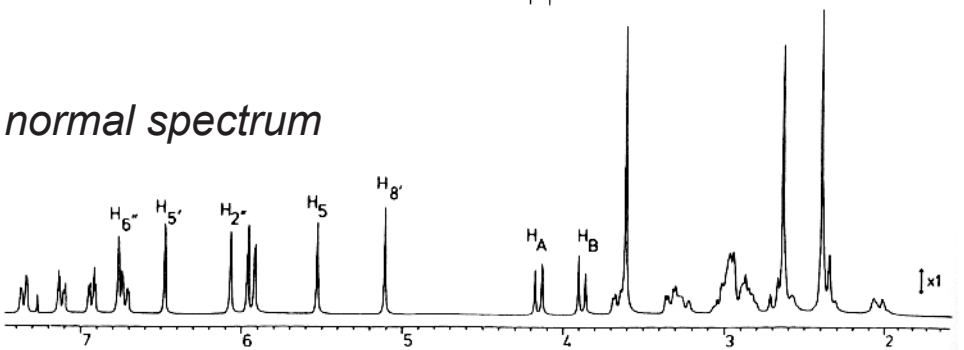

Figure 10.4. NOE difference spectra of repanduline **10.31** (0.26 M in $CDCl_3$) preirradiating H_A; recorded at 250 MHz (preirradiation 5 s). The spectrum results from the combination of a total of 32,000 transients (8,000 with preirradiation of each line of the H_A doublet, and 16,000 controls) acquired over a weekend. The crucial $H_{5'}\{H_A\}$ enhancement of 0.18% shows the correct substitution pattern in ring C to be as in **10.31** rather than **10.32**. See text for further discussion. Reproduced with permission from ref. 24.

Steady-State nOe:
nOe Difference Spectroscopy

long (seconds), very low power continuous irradiation at the exact resonance frequency of one spin

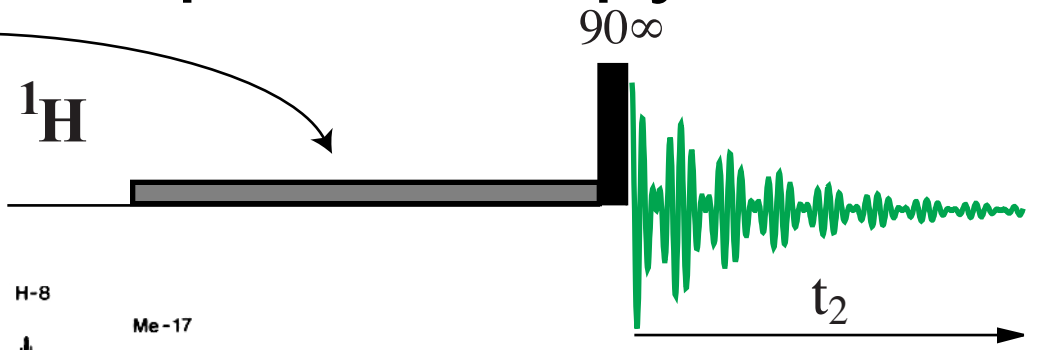

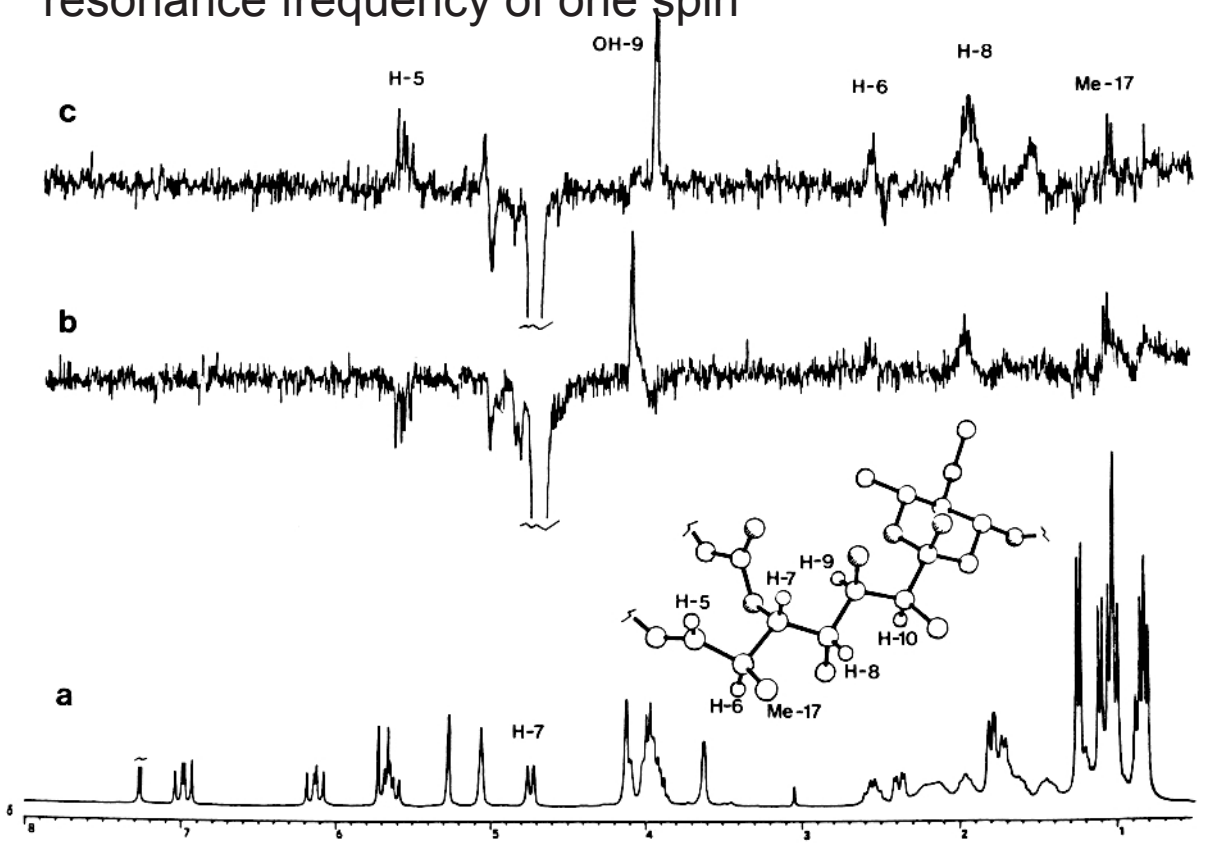

Figure 3.9. NOE difference spectra of the macrocyclic antibiotic elaiophylin (7 mg in 0.5 ml $CDCl_3$) (*b*) at 23°C and (*c*) at 50°C, recorded at 250 MHz. Proton H_7 was the preirradiation target in both cases. The enhancement of H_5 is negative at the lower temperature, because the internuclear vector connecting H_5 and H_7 has a longer correlation time than those corresponding to other enhancements from H_7. See text for further discussion. Reproduced with permission from ref. 6.

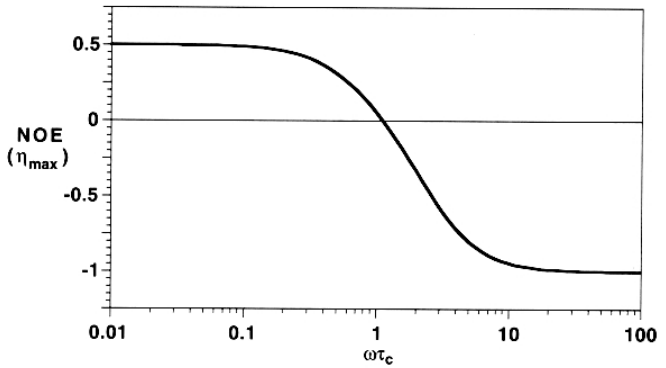

Figure 2.6. Dependence of maximum homonuclear NOE enhancement on $\omega\tau_c$. Note the log scale of $\omega\tau_c$.

Steady-State nOe:
nOe Difference Spectroscopy

long (seconds), very low power continuous irradiation at the exact resonance frequency of one spin

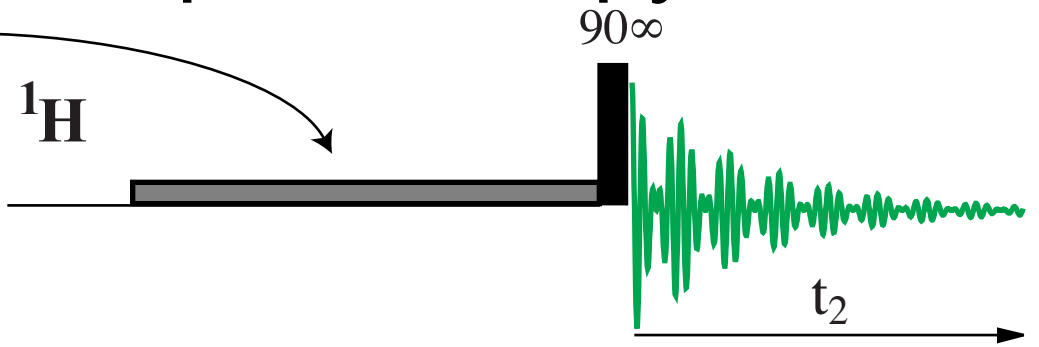

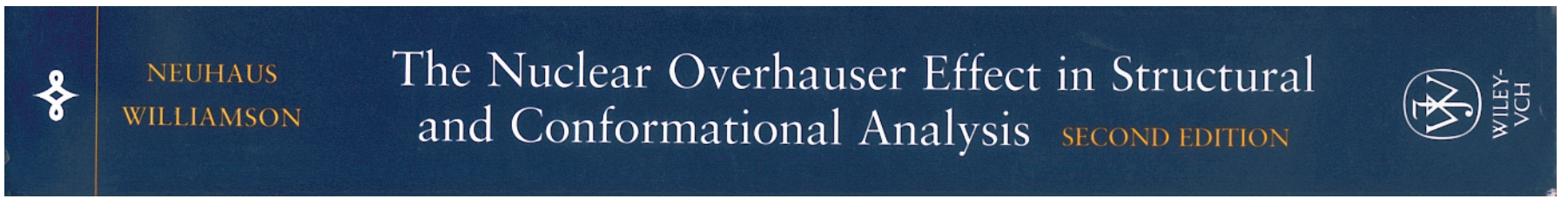

Steady-State vs Transient nOe

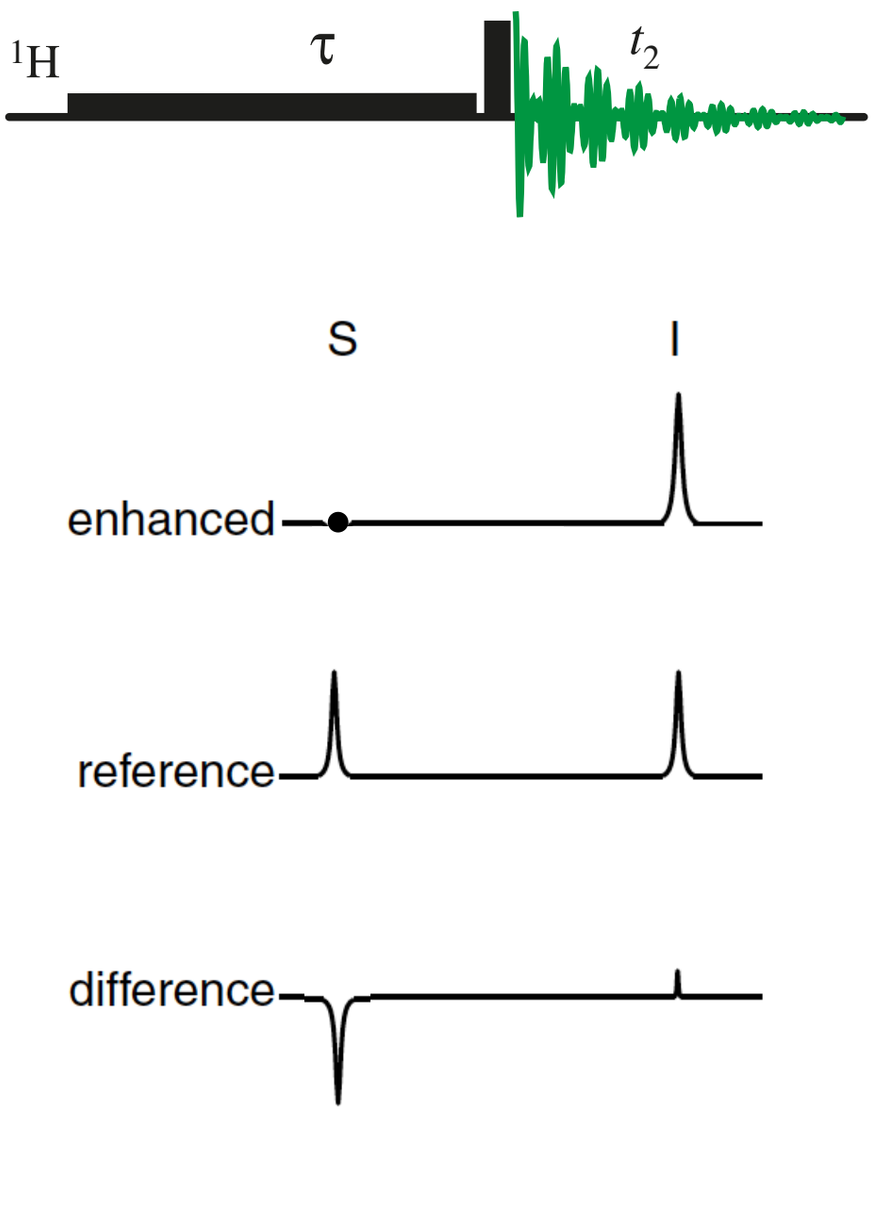

w/wo long low power irradiation at
S spin resonance frequency

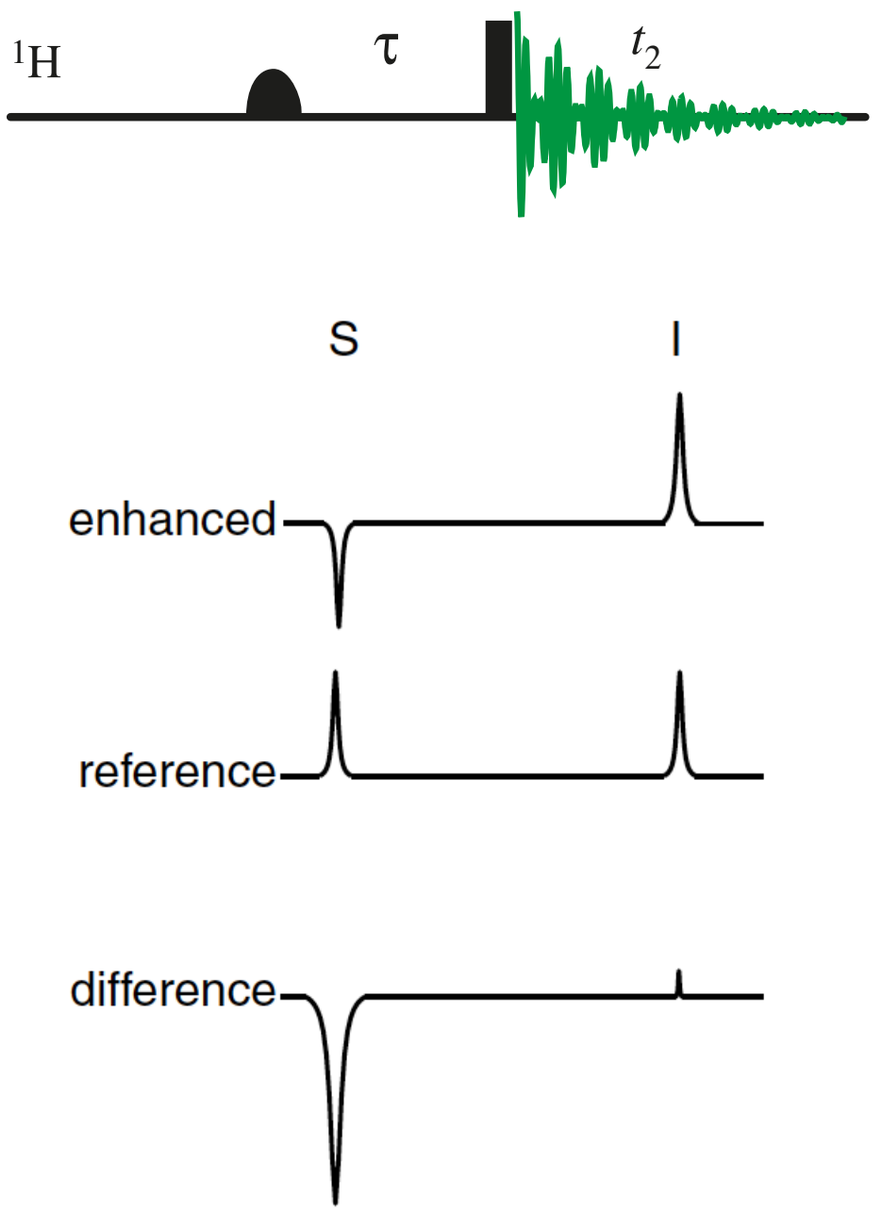

w/wo selective 180° pulse at
S spin resonance frequency

Cornerstone NMR Experiments: NOESY/EXSY

(Determining Exchange and Internuclear Distances)

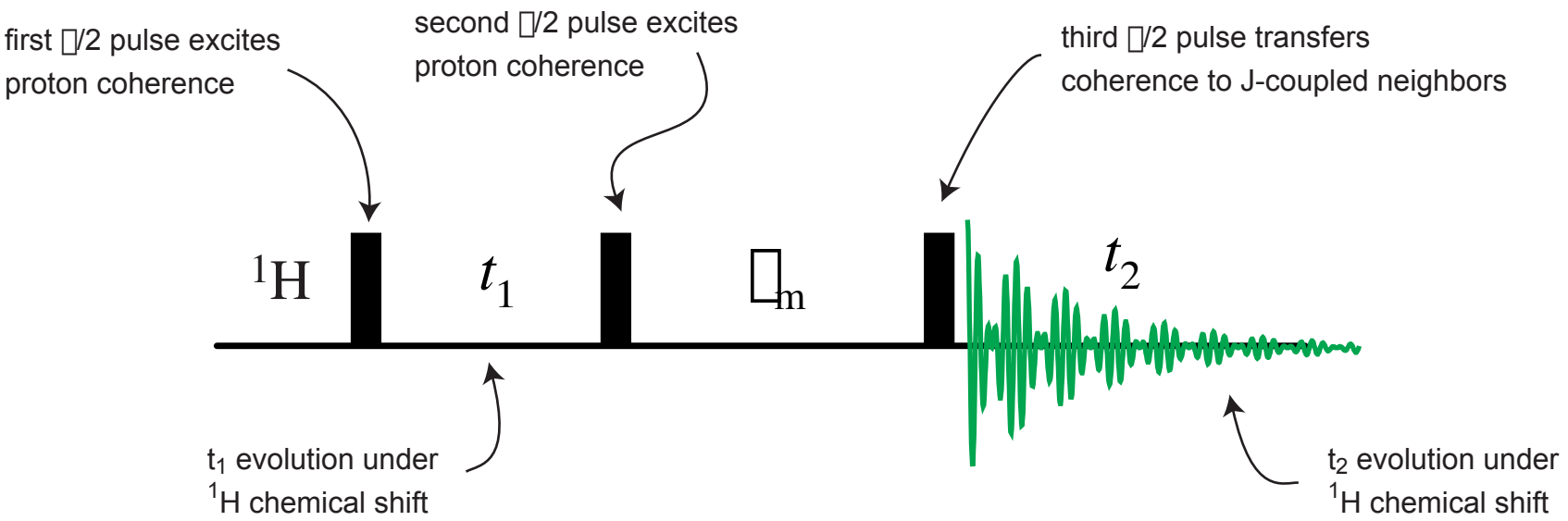

How can we quantify the exchange or relaxation processes going on during the mixing time?
Can we determine internuclear distances from experimental measures of the nuclear Overhauser effect?

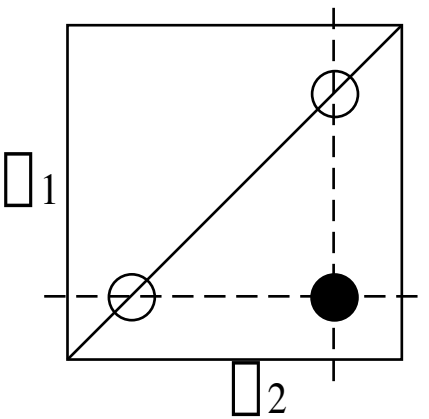

Two-Dimensional Exchange Spectroscopy (EXSY)

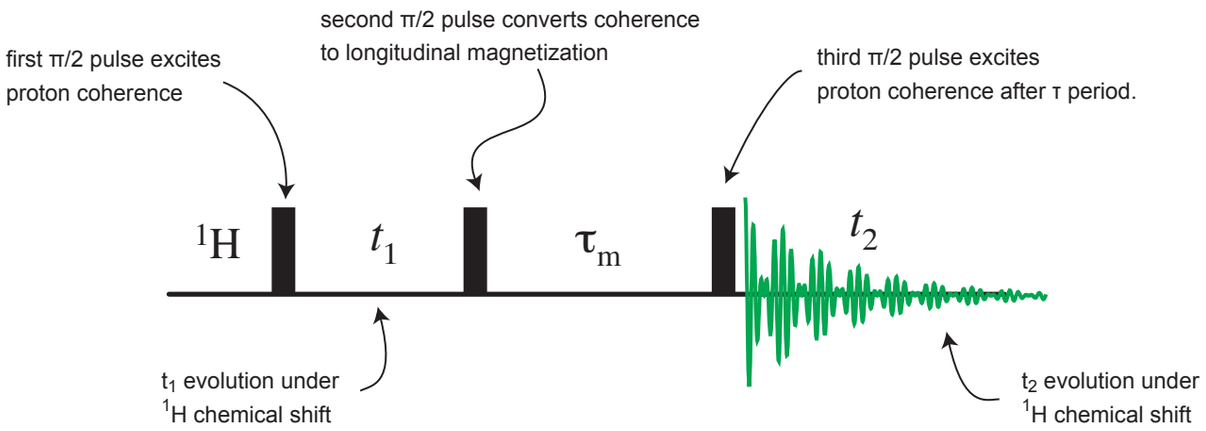

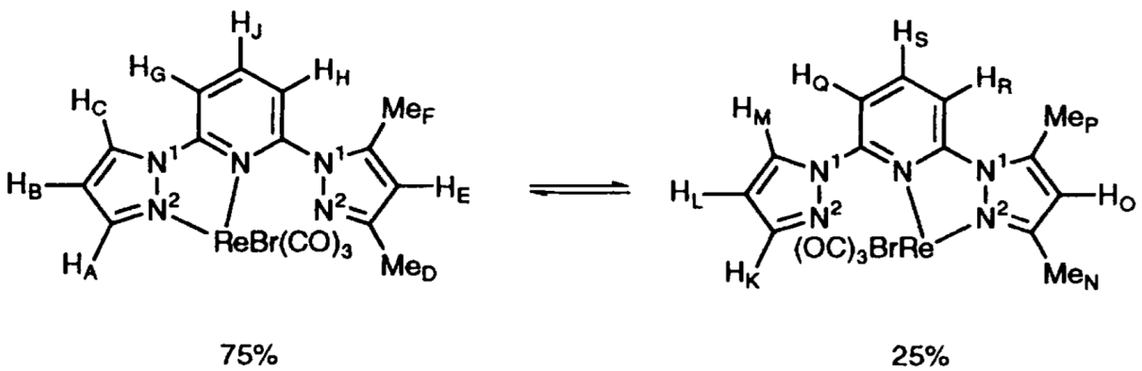

75% 25%

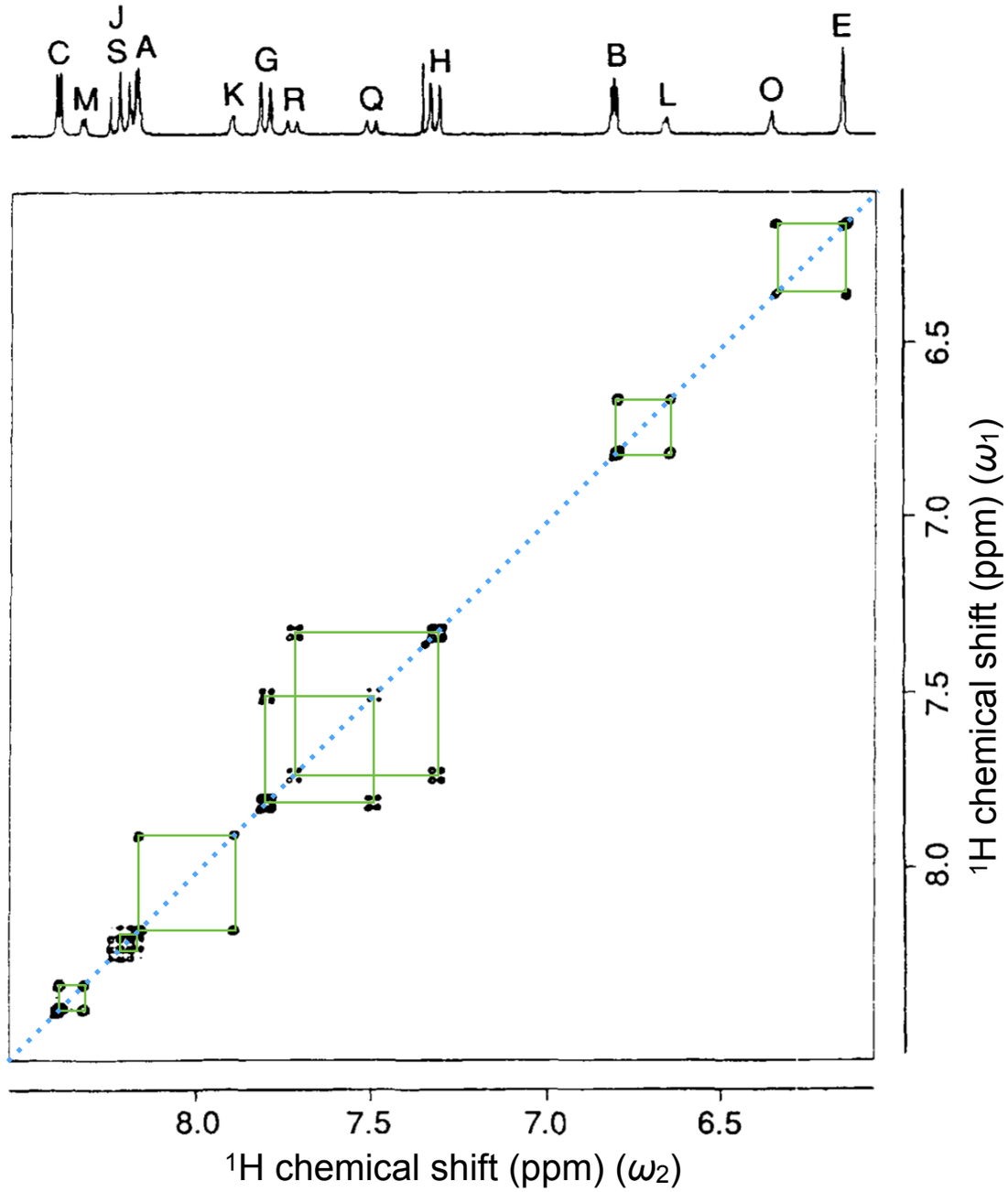

Proton two-dimensional exchange spectrum of the organometallic fluxional compound [ReBr(CO)3(Me2-bppy)], where bppy denotes 2,6-bis(pyrazol-1-yl)pyridine. The mixing interval was τ_m = 0.1 s. The off-diagonal peaks may be interpreted in terms of an exchange of the metal atom between two pairs of nitrogen binding sites.
Adapted from E. W. Abel, et al., J. Chem. Soc. Dalton Trans., 1079 (1994).

Cross Relaxation in a Nutshell

$$\frac{d}{dt}\begin{pmatrix} I_z \\ S_z \end{pmatrix} = \begin{pmatrix} \rho_I & \sigma \\ \sigma & \rho_S \end{pmatrix}\begin{pmatrix} \Delta I_z \\ \Delta S_z \end{pmatrix}$$

with

$$\rho_I = \frac{1}{10}\left(\frac{\gamma_I^2\gamma_S^2h^2}{r^6}\right)\tau_c\left\{\frac{3}{1+\omega_I^2\tau_c^2}+\frac{1}{1+(\omega_I-\omega_S)^2\tau_c^2}+\frac{6}{1+(\omega_I+\omega_S)^2\tau_c^2}\right\}$$

$$\sigma = \frac{1}{10}\left(\frac{\gamma_I^2\gamma_S^2h^2}{r^6}\right)\tau_c\left\{\frac{1}{1+(\omega_I-\omega_S)^2\tau_c^2}+\frac{6}{1+(\omega_I+\omega_S)^2\tau_c^2}\right\}$$

- We predict that dipolar relaxation between different spins will lead to ***magnetisation transfer with a rate that depends on internuclear distances and molecular dynamics***

- This is the nuclear Overhauser effect

Longitudinal Exchange in EXSY

For a 2 spin system, the 2x2 dynamic matrix leads to an analytical solution, and for a symmetrical case we obtain:

$$I_{AA}(\tau_m) = \tfrac{1}{2}\left[1+\exp\{-2k\tau_m\}\right]\exp\{-\tau_m/T_1\}M_{A0}$$

$$I_{BB}(\tau_m) = \tfrac{1}{2}\left[1+\exp\{-2k\tau_m\}\right]\exp\{-\tau_m/T_1\}M_{B0}$$

$$I_{AB}(\tau_m) = \tfrac{1}{2}\left[1-\exp\{-2k\tau_m\}\right]\exp\{-\tau_m/T_1\}M_{B0}$$

$$I_{BA}(\tau_m) = \tfrac{1}{2}\left[1-\exp\{-2k\tau_m\}\right]\exp\{-\tau_m/T_1\}M_{A0}$$

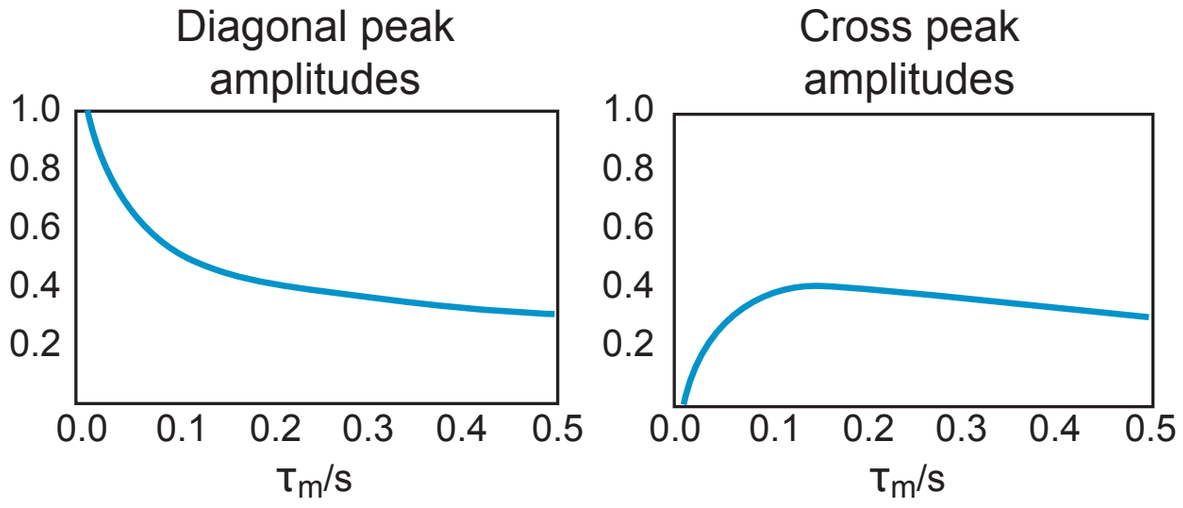

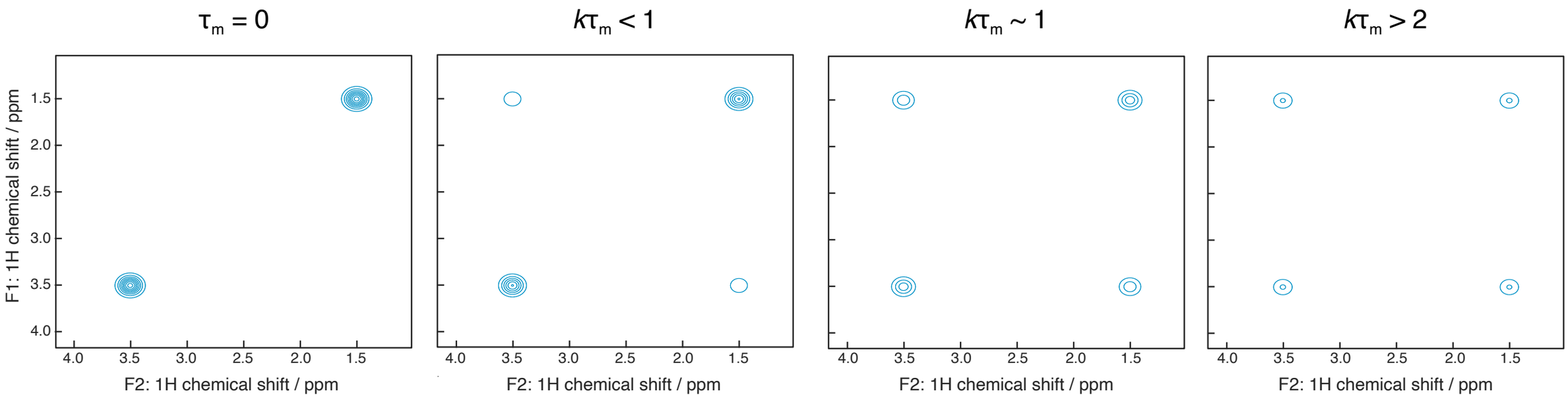

where for magnetization exchange induced by nOe, $k = \sigma$ and $T_1 = \rho$.

Cornerstone NMR Experiments: NOESY

(Determining Internuclear Distances)

NOESY Spectrum of Gramicidin
The intensity of the cross peaks is related to the inernuclear distance between the two nuclei that are correlated.

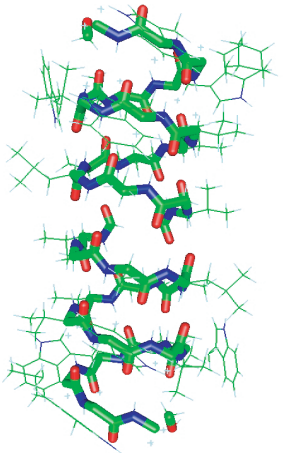

Gramicidin A

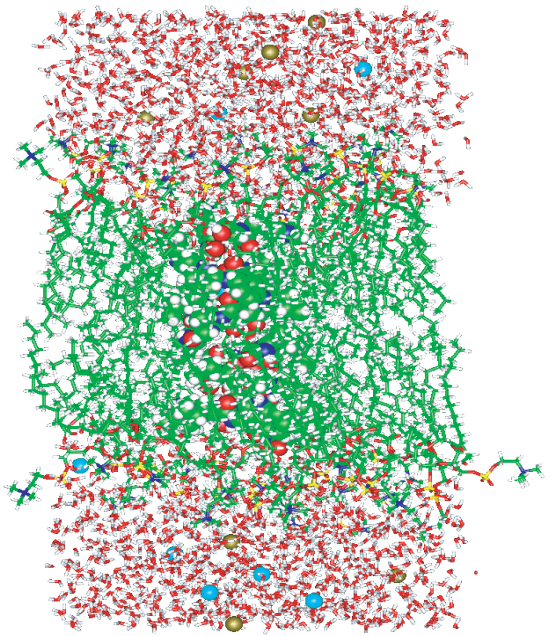

The whole system

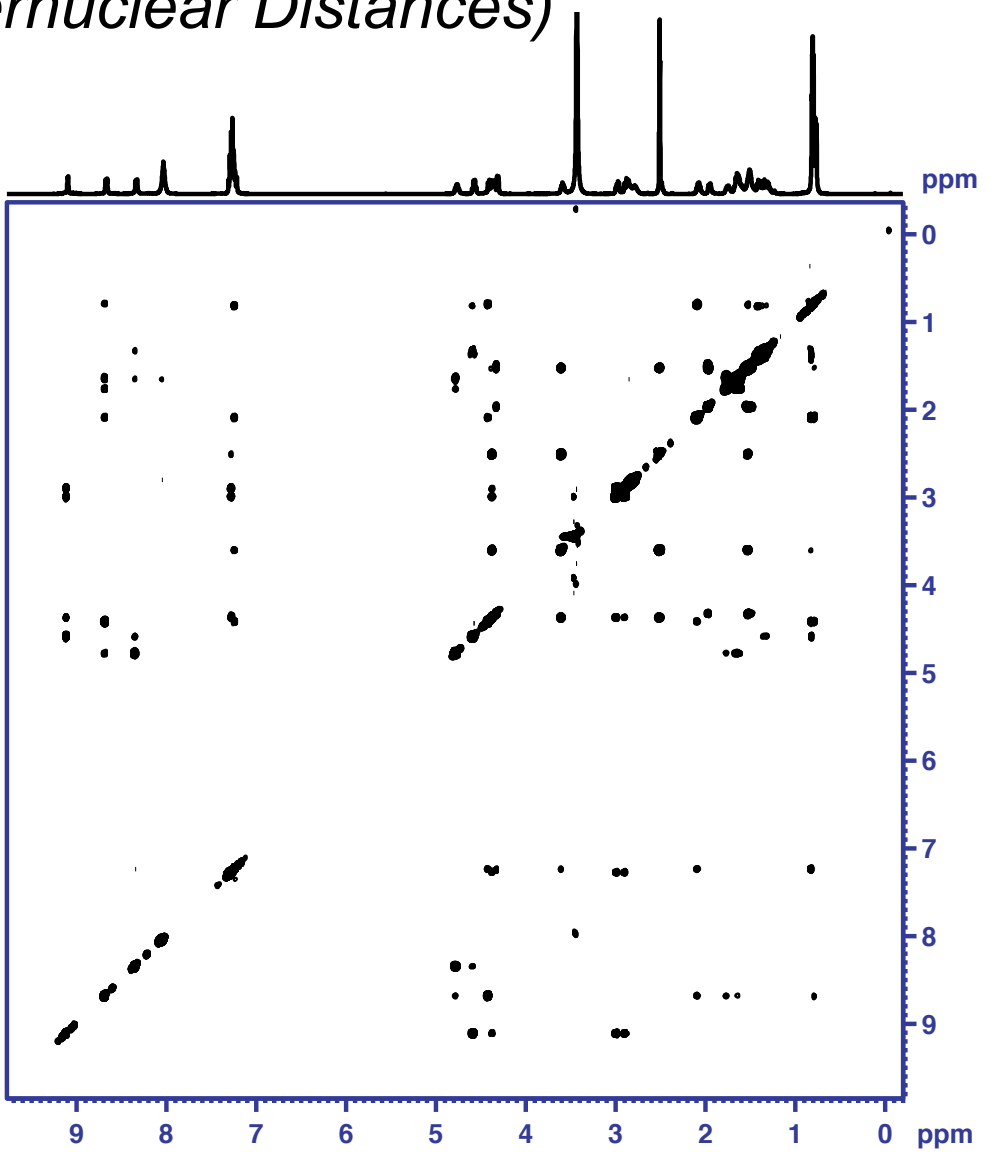

A Protocol for NMR 3D Structure Determination of Proteins

1. Sample Preparation: Overexpression, isotopic labelling (^{13}C, ^{15}N, ^{2}H), solubility, folding, stability.....

2. Resonance Assignment: COSY (TOCSY) - HSQC/HMQC - NOESY, higher dimensions.....

3. **Distance Measurement**: NOESY (+3D variations)

4. **Structure Determination Using Experimentally Constrained Modelling**

5. **Dynamic Information from Relaxation Times**

yields a full structural and dynamic model

A Protocol for NMR 3D Structure Determination of Proteins

2. Resonance Assignment: COSY (TOCSY) - HSQC/HMQC - NOESY, higher dimensions.....

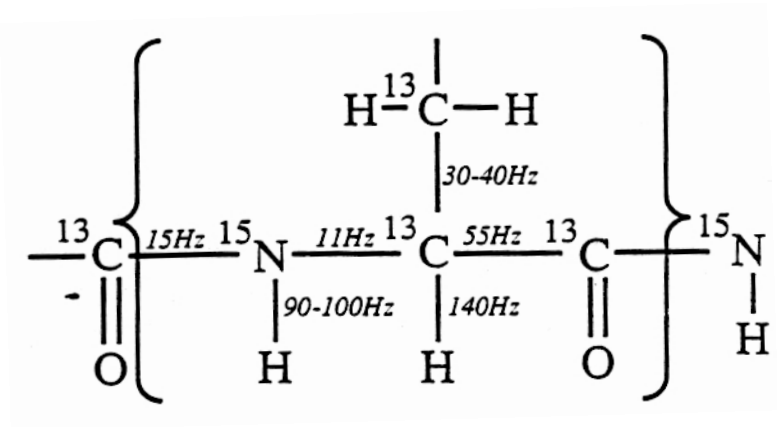

TABLE I

CORRELATIONS OBSERVED IN THREE-DIMENSIONAL DOUBLE- AND TRIPLE-RESONANCE EXPERIMENTS USED FOR SEQUENTIAL AND SIDE-CHAIN ASSIGNMENTS

Experiment	Correlation	*J* Coupling[a]
^{15}N-edited HOHAHA	$C^{\alpha}H(i)$–$^{15}N(i)$–$NH(i)$	$^{3}J_{HN^{\alpha}}$ (~3–11 Hz)
	$C^{\beta}H(i)$–$^{15}N(i)$–$NH(i)$	$^{3}J_{HN^{\alpha}}$ (~3–11 Hz), $^{3}J_{\alpha\beta}$ (~3–11 Hz)
H(CA)NH	$C^{\alpha}H(i)$–$^{15}N(i)$–$NH(i)$	$^{1}J_{NC^{\alpha}}$ (~9–13 Hz)
	$C^{\alpha}H(i-1)$–$^{15}N(i)$–$NH(i)$	$^{2}J_{NC^{\alpha}}$ (~5–10 Hz)
HN(CO)HB	$C^{\alpha}H(i-1)$–$^{15}N(i)$–$NH(i)$	$^{2}J_{COH^{\beta}}$ (~4–7 Hz)
	$C^{\beta}H(i-1)$–$^{15}N(i)$–$NH(i)$	$^{3}J_{COH^{\beta}}$ (~8 Hz for trans coupling)
HNHB	$C^{\beta}H(i)$–$^{15}N(i)$–$NH(i)$	$^{3}J_{NH^{\beta}}$ (~5 Hz for trans coupling)
HNCA	$^{13}C^{\alpha}(i)$–$^{15}N(i)$–$NH(i)$	$^{1}J_{NC^{\alpha}}$ (~9–13 Hz)
	$^{13}C^{\alpha}(i-1)$–$^{15}N(i)$–$NH(i)$	$^{2}J_{NC^{\alpha}}$ (~5–10 Hz)
CBCANH	$^{13}C^{\beta}/C^{\alpha}(i)$–$^{15}N(i)$–$NH(i)$	$^{1}J_{CC}$ (~30–40 Hz), $^{1}J_{NC^{\alpha}}$ (~9–13 Hz)
	$^{13}C^{\beta}/C^{\alpha}(i-1)$–$^{15}N(i)$–$NH(i)$	$^{1}J_{CC}$ (~30–40 Hz), $^{2}J_{NC^{\alpha}}$ (~5–10 Hz)
HN(CO)CA	$^{13}C^{\alpha}(i-1)$–$^{15}N(i)$–$NH(i)$	$^{1}J_{NCO}$ (~15 Hz), $^{1}J_{C^{\alpha}CO}$ (~55 Hz)
CBCA(CO)NH	$^{13}C^{\beta}/C^{\alpha}(i-1)$–$^{15}N(i)$–$NH(i)$	$^{1}J_{CC}$ (~30–40 Hz), $^{1}J_{NCO}$ (~15 Hz), $^{1}J_{C^{\alpha}CO}$ (~55 Hz)
HBHA(CBCACO)NH	$C^{\beta}H/C^{\alpha}H(i-1)$–$^{15}N(i)$–$NH(i)$	$^{1}J_{CC}$ (~30–40 Hz), $^{1}J_{NCO}$ (~15 Hz), $^{1}J_{C^{\alpha}CO}$ (~55 Hz)
C(CO)NH	$^{13}C^{\gamma}(i-1)$–$^{15}N(i)$–$NH(i)$	$^{1}J_{CC}$ (~30–40 Hz), $^{1}J_{NCO}$ (~15 Hz), $^{1}J_{C^{\alpha}CO}$ (~55 Hz)
H(CCO)NH	$C^{\gamma}H(i-1)$–$^{15}N(i)$–$NH(i)$	$^{1}J_{CC}$ (~30–40 Hz), $^{1}J_{NCO}$ (~15 Hz), $^{1}J_{C^{\alpha}CO}$ (~55 Hz)
HNCO	$^{13}CO(i-1)$–$^{15}N(i)$–$NH(i)$	$^{1}J_{NCO}$ (~15 Hz)
HCACO	$C^{\alpha}H(i)$–$^{13}C^{\alpha}(i)$–$^{13}CO(i)$	$^{1}J_{C^{\alpha}CO}$ (~55 Hz)
HCA(CO)N	$C^{\alpha}H(i)$–$^{13}C^{\alpha}(i)$–$^{15}N(i+1)$	$^{1}J_{C^{\alpha}CO}$ (~55 Hz), $^{1}J_{NCO}$ (~15 Hz)
HCCH-COSY	$H(j)$–$^{13}C(j)$–$^{13}C(j \pm 1)$–$H(j \pm 1)$	$^{1}J_{CC}$ (~30–40 Hz)
HCCH-TOCSY	$H(j)$–$^{13}C(j) \ldots {}^{13}C(j \pm n)$–$H(j \pm n)$	$^{1}J_{CC}$ (~30–40 Hz)

[a] In addition to the couplings indicated, all experiments make use of the $^{1}J_{CH}$ (~140 Hz) and/or $^{1}J_{NH}$ (~95 Hz) couplings.

A Protocol for NMR 3D Structure Determination of Proteins

2. Resonance Assignment:
COSY (TOCSY) - HSQC/HMQC
NOESY, higher dimensions.....

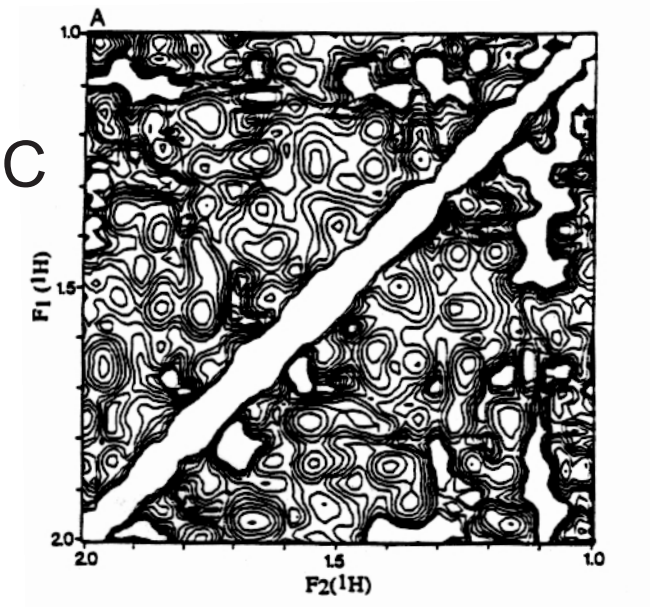

A Protocol for NMR 3D Structure Determination of Proteins

2. Resonance Assignment:
COSY (TOCSY) - HSQC/HMQC - NOESY, higher dimensions.....

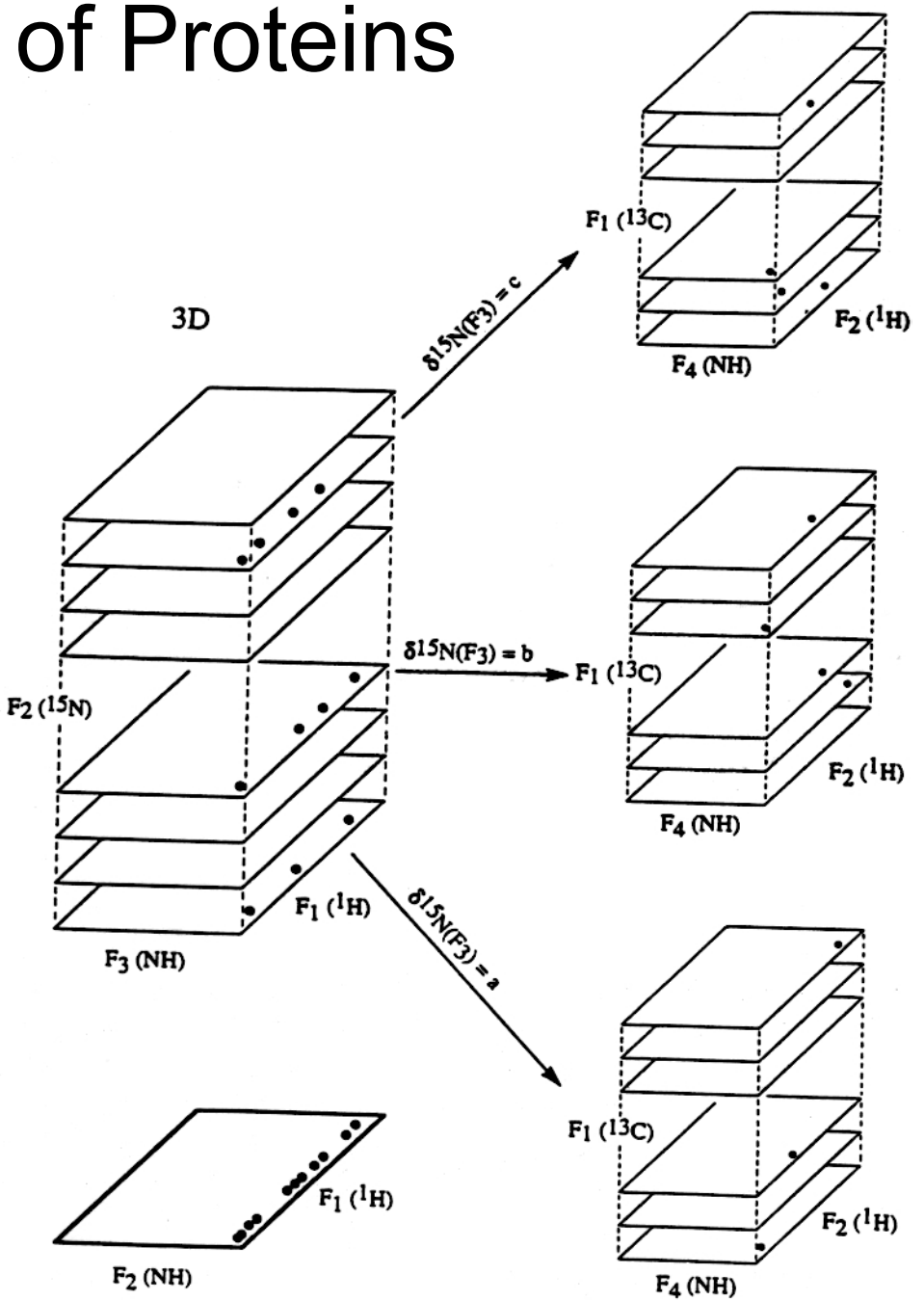

A Protocol for NMR 3D Structure Determination of Proteins

2. Resonance Assignment:
COSY (TOCSY) - HSQC/HMQC
NOESY, higher dimensions.....

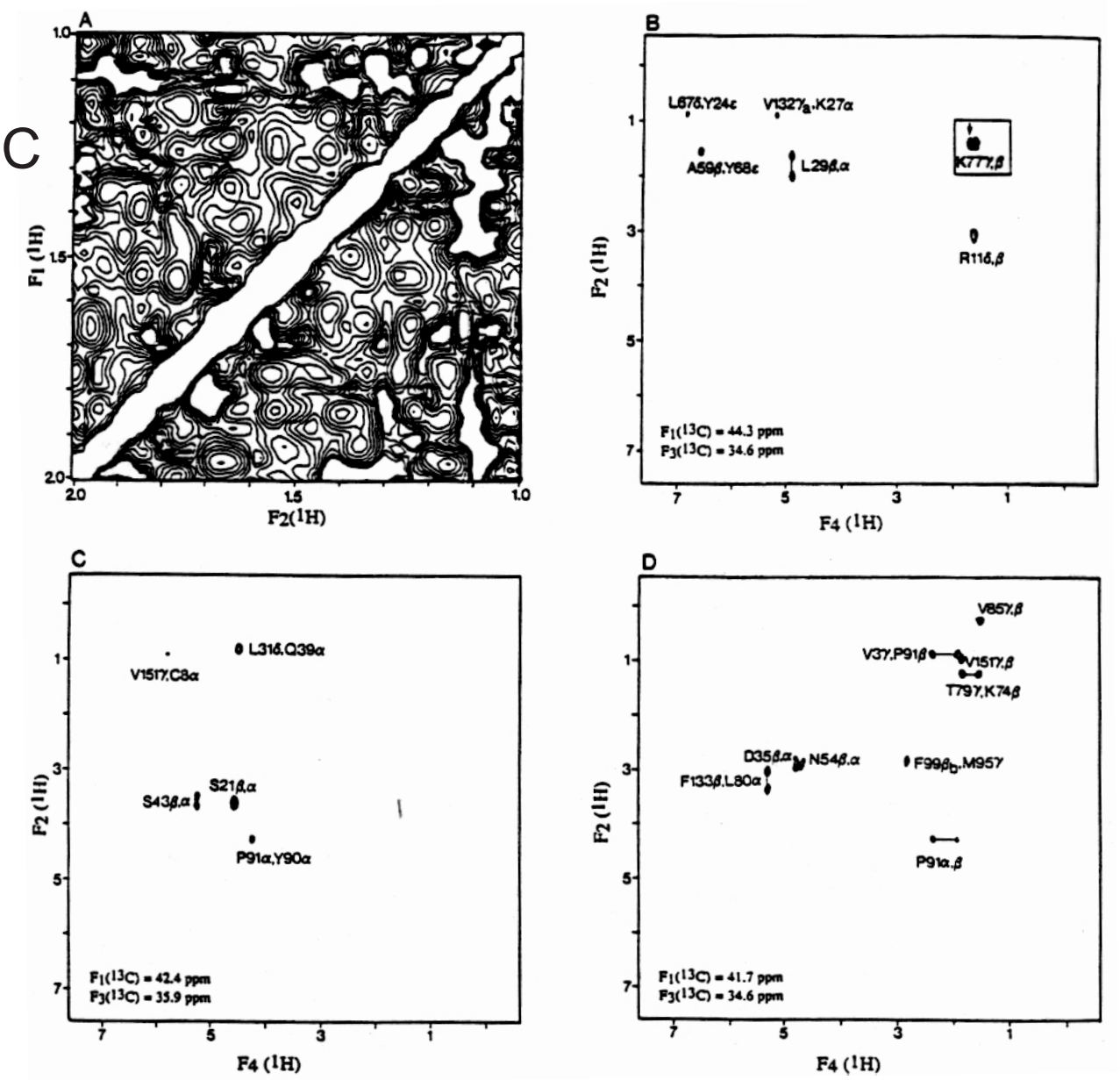

A Protocol for NMR 3D Structure Determination of Proteins

2. Resonance Assignment: COSY (TOCSY) - HSQC/HMQC - NOESY, higher dimensions.....

TABLE V
TWO-, THREE-, AND FOUR-DIMENSIONAL NMR EXPERIMENTS

Experiment class[a] (X = C or N)	Experiment[b]	Ref.[c]
(t_1, t_2) = (H, H)	COSY	(1)
	RELAY	(2)
	HOHAHA-TOCSY	(3)
	NOESY	(4)
	ROESY	(5)
	DEPT-HMQC	(23)
	DEPT-HMQC filtered TOCSY	(23)
(t_1, t_2, t_3) = (H, H, H)	HOHAHA-NOESY	(6)
(t_1, t_2) = (X, H)	HMQC	(7)
	HSQC	(8)
	CT-HSQC	(9)
	HSMQC	(10)
	HMBC	(11)
	HETERO-RELAY	(12)
	HETERO-NOE	(13)
	H-X EXCSY	(14)
(t_1, t_2) = (C, C)	CC-DQC	(15, 16)
	CC-COSY	(16)
	XX-EXCSY	(14)
(t_1, t_2) = (N, C)	CN-MBC	(17)
(t_1, t_2, t_3) = (H, X, H)/(X, H, H)	NOESY-HMQC	(18)
	HOHAHA-HMQC	(19)
	SE-TOCSY-HSQC	(20)
	SE-HSQC-TOCSY	(20)
	SE-NOESY-HMQC	(20)
	SE-NOESY-HSQC	(20)
	HMQC-TOCSY	(21)
	^{15}N-TOCSY-NOESY	(22)
	^{15}N-NOESY-TOCSY	(22)
	DEPT-TOCSY	(23)
	HMQC-COSY (gradient)	(24)
	NOESY-HMQC (gradient)	(25)
(t_1, t_2, t_3) = (H, C, H)	HCCH-COSY	(26)
	CT-HCCH-COSY	(27)
	HCCH-TOCSY	(26)
	HCCH-TOCSY (gradient)	(28)
	H(CA)CO-TOCSY	(29)
	H(CA)CO-COSY	(29)
	(HCA)CO-CBHB	(29)
	HA[CAN]HN	(30)

TABLE V (*continued*)

Experiment class[a] (X = C or N)	Experiment[b]	Ref.[c]
(t_1, t_2, t_3) = (C, C, H)	HCACO	(31)
	CT-HCACO	(32)
	C TOCSY-REVINEPT	(33)
	H(N)CACO	(34)
	^{13}C–^{13}C correlations	(35)
	CBCACOHA (gradient)	(36)
	CBCACOHA-TOCSY	(37)
(t_1, t_2, t_3) = (N, C, H)	HNCO	(31)
	CT-HNCO	(38)
	HNCA	(31, 39)
	CT-HNCA	(38)
	HN(CO)CA	(40, 41)
	CT-HN(CO)CA	(38)
	CT-HN(CA)CO	(42)
	HNCO (gradient)	(43)
(t_1, t_2, t_3) = (C, N, H)	HCA(CO)N	(31)
	CT-HCA(CO)N	(32, 44)
	CBCA(CO)NH	(45)
	HNCACB	(46)
	HC(CO)NH-TOCSY	(47)
	HC(C)NH-TOCSY	(48)
(t_1, t_2, t_3) = (H, N, H)	HA(CA)NNH	(49)
	HN(CA)HA-GLY	(50)
	HBHA(CO)NH	(51)
	H(CCO)NH-TOCSY	(47)
	HN(CA)NNH	(52)
	HA[CAN]HN	(30)
(t_1, t_2, t_3) = (N, N, H)	^{15}N/^{15}N edited ^{1}H–^{1}H NOESY	(53)
	HN(CA)NNH	(52)
(t_1, t_2, t_3) = (N, H, H)	HN(CA)HA	(54)
	HN(COCA)HA	(55)
(t_1, t_2, t_3, t_4) = (C, H, N, H)	^{13}C/^{15}N-edited ^{1}H–^{1}H NOESY	(56)
	HNCAHA	(57)
	HN(CO)CAHA	(57)
(t_1, t_2, t_3, t_4) = (H, C, N, H)	HCANNH	(58)
	HCC(CO)NNH	(59)
(t_1, t_2, t_3, t_4) = (C, H, C, H)	^{13}C/^{13}C-edited ^{1}H–^{1}H NOESY	(60)
	^{13}C/^{13}C ^{1}H–^{1}H NOESY (gradient)	(61)
(t_1, t_2, t_3, t_4) = (C, C, N, H)	HCACON	(62)
(t_1, t_2, t_3, t_4) = (H, C, C, H)	HCCH-TOCSY	(63)
(t_1, t_2, t_3, t_4) = (H, N, N, H)	HN(COCA)NH	(64)

[a] Pulse sequences are organized by the nuclei that are operative in the various acquisition periods. The number of time domains (t_i values) establishes the dimensionality of the

(*continued*)

A Protocol for NMR 3D Structure Determination of Proteins

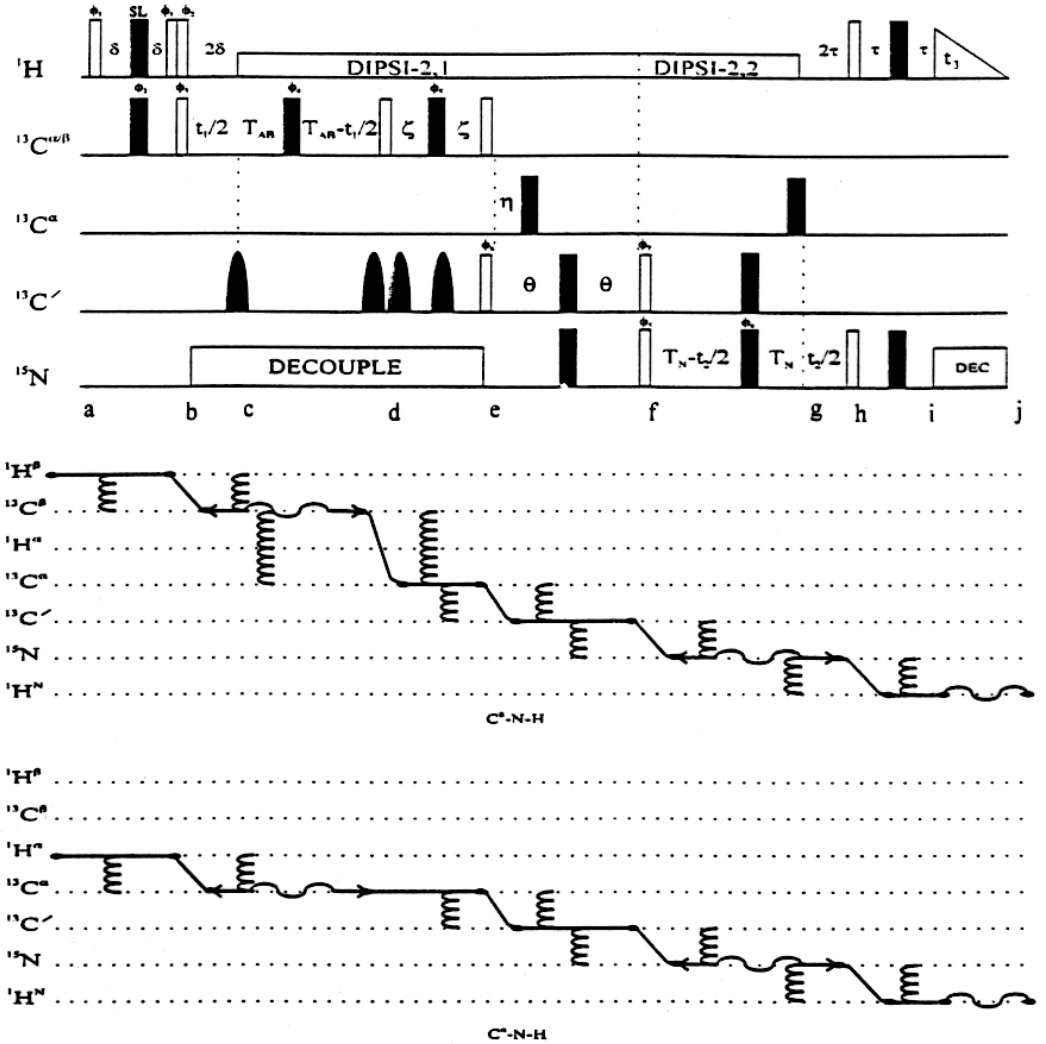

FIG. 14. Pulse sequence and CFN for 3D-CBCA(CO)NH.[11] The pulses and phases have the same convention described in Fig. 12. For values of the delays, consult the original work. The second and third selective (rounded) carbonyl pulses and the phase labeled ϕ_7 serve to remove nonresonant phase distortions (Section III,C). The CFN is best shown as two separate experiments, one originating from $^1H^\beta$ and the second originating from $^1H^\alpha$.

A Protocol for NMR 3D Structure Determination of Proteins

3. Distance Measurement: NOESY (+3D variations)

Biochemistry **1994,** *33,* 15036−15045

Solution Structure of Dimeric Mnt Repressor (1−76)[†,‡]

Maurits J. M. Burgering,[§] Rolf Boelens,[*,§] Dara E. Gilbert,[§,||] Jan N. Breg,[§] Kendall L. Knight,[⊥,#] Robert T. Sauer,[⊥] and Robert Kaptein[§]

Bijvoet Center for Biomolecular Research, Padualaan 8, Utrecht University, 3584 CH Utrecht, The Netherlands, and Department of Biology, Massachusetts Institute of Technology, Cambridge, Massachusetts 023139

Received May 20, 1994; Revised Manuscript Received August 30, 1994[®]

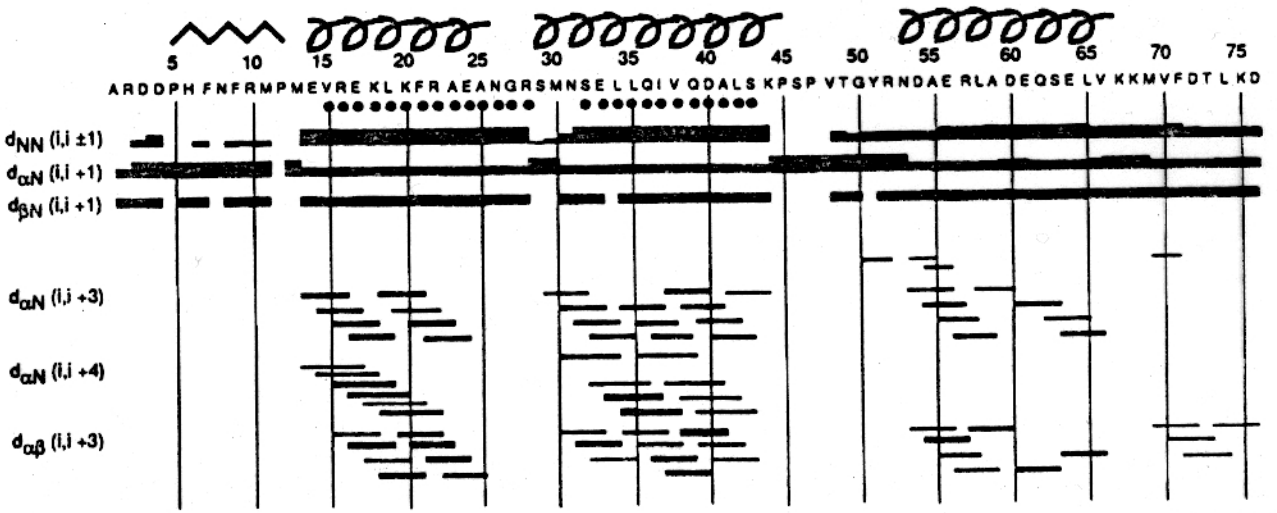

FIGURE 3: Amino acid sequence of Mnt (1−76) repressor together with a schematic summary of short- and medium-range NOEs observed indicating regions of secondary structure. The thickness of the connecting bars is a measure for the intensity of the NOEs. The filled circles under the amino acid sequence denote residues with slowly exchanging amide protons. Sequential $d_{\alpha\delta}(i,i+1)$ NOEs of prolines are indicated at $d_{\alpha N}(i,i+1)$.

A Protocol for NMR 3D Structure Determination of Proteins

4. Structure Determination Using Experimentally Constrained Modelling

Biochemistry **1994,** *33,* 15036−15045

Solution Structure of Dimeric Mnt Repressor (1−76)[†,‡]

Maurits J. M. Burgering,[§] Rolf Boelens,[*,§] Dara E. Gilbert,[§,||] Jan N. Breg,[§] Kendall L. Knight,[⊥,#] Robert T. Sauer,[⊥] and Robert Kaptein[§]

Bijvoet Center for Biomolecular Research, Padualaan 8, Utrecht University, 3584 CH Utrecht, The Netherlands, and Department of Biology, Massachusetts Institute of Technology, Cambridge, Massachusetts 023139

Received May 20, 1994; Revised Manuscript Received August 30, 1994[⊗]

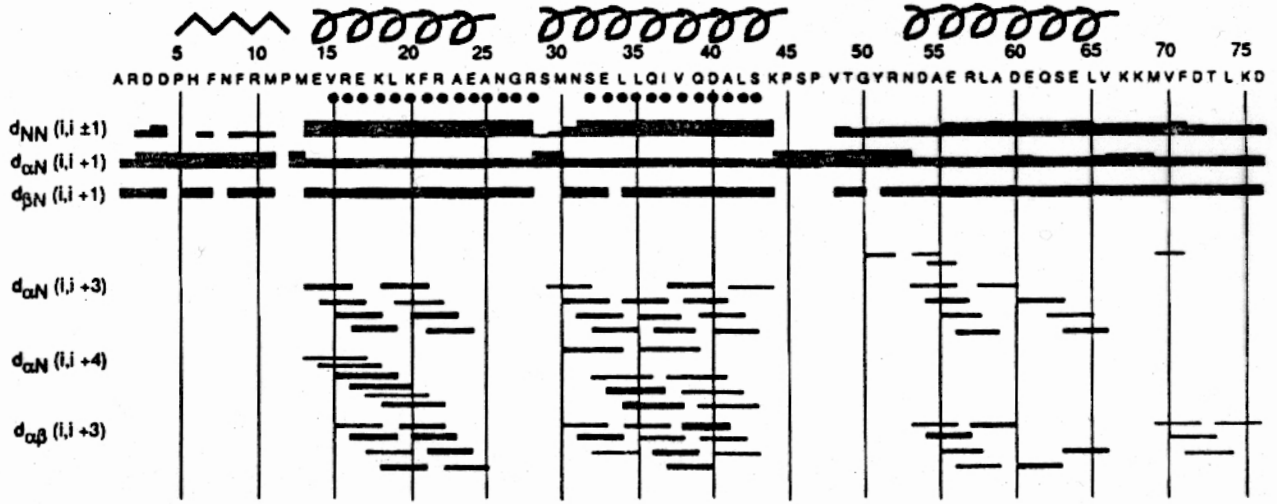

FIGURE 3: Amino acid sequence of Mnt (1−76) repressor together with a schematic summary of short- and medium-range NOEs observed indicating regions of secondary structure. The thickness of the connecting bars is a measure for the intensity of the NOEs. The filled circles under the amino acid sequence denote residues with slowly exchanging amide protons. Sequential $d_{\alpha\delta}(i,i+1)$ NOEs of prolines are indicated at $d_{\alpha N}(i,i+1)$.

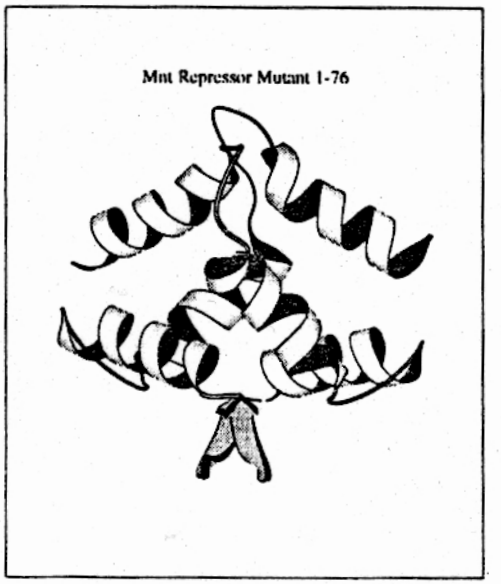

Restrained Molecular Dynamics

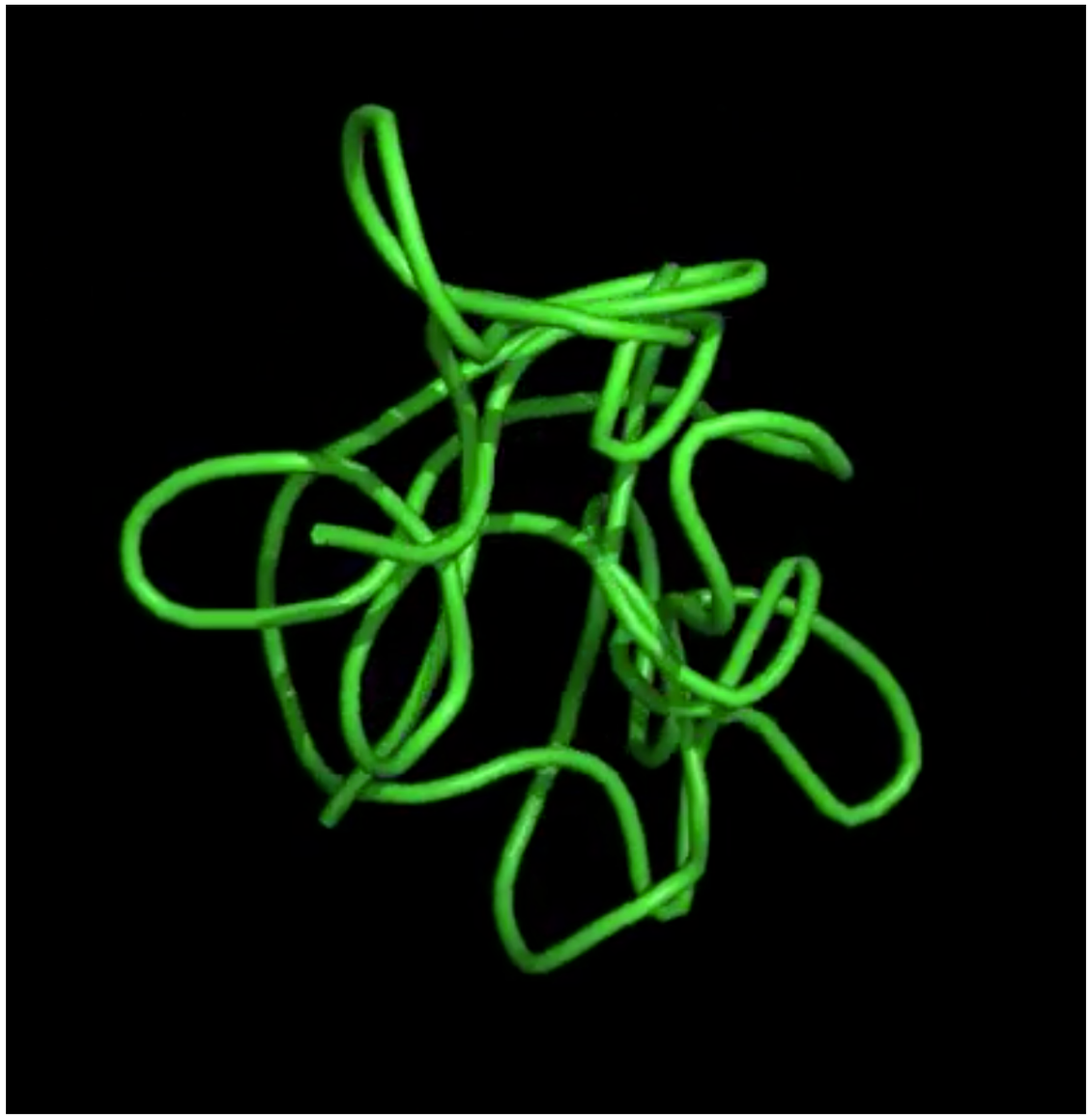

https://www.youtube.com/watch?v=KBiVkWlOxTs

A Protocol for NMR 3D Structure Determination of Proteins

5. Dynamic Information from Relaxation Times

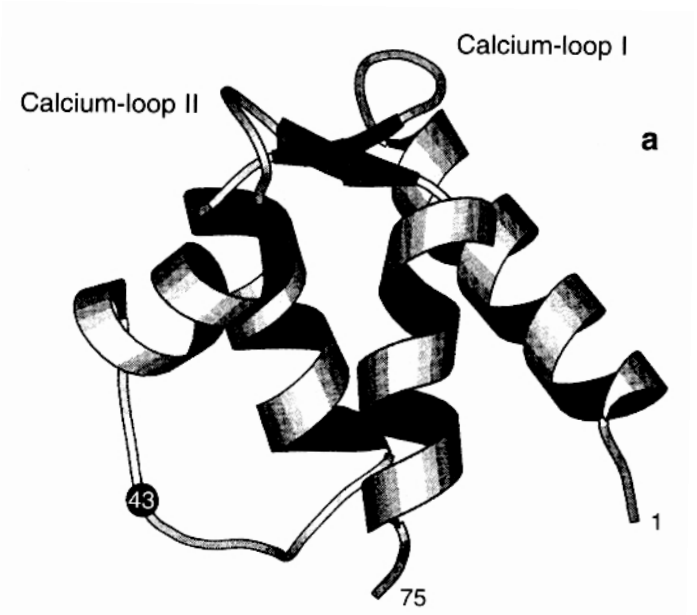

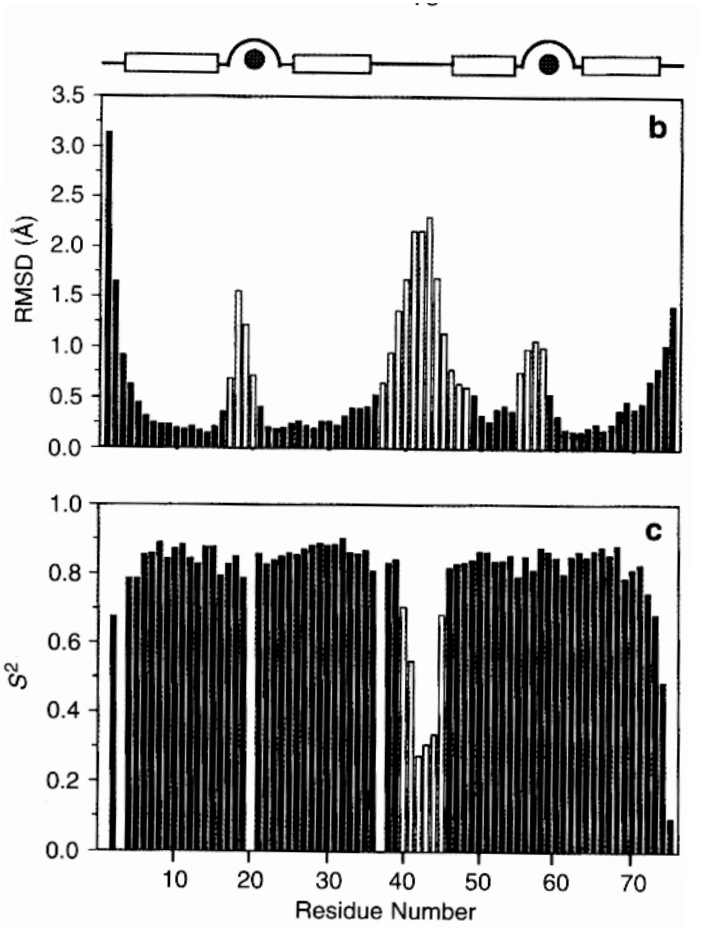

Conclusions I

- Transverse and longitudinal relaxation rates are directly related to the rotational correlation times and the timescale of motion. *Relaxation rates are direct probes of molecular structure & dynamics.*

- Dipolar relaxation between two inequivalent spins induces cross relaxation: spontaneous exchange of magnetisation between dipolar coupled spins. This is the Overhauser effect. (When the two spins are both nuclear spins, it is the *nuclear Overhauser effect* (nOe)).

- Cross relaxation rates are determined by the ***rate of motion and the internuclear distance*** ($\sigma_{ij} \propto r_{ij}^{-6}$).

Conclusions II

- The size and sign of the nOe effect depends on the motional correlation times.
- Steady-state nOe vary from extrema of +0.5 for fast motions to -1 for slow motions.
- Conformational analysis can be performed with steady-state or transient 1D nOe experiments involving selective saturation or inversion, respectively.
- Multiple nOe can be be measured simultaneously in the 2D EXSY experiment
- Pairwise distances can be obtained quantitatively from NOESY spectra using exactly the same analysis as for exchange.
- Full structural & dynamic pictures of proteins can be obtained from a 5 step protocol

Did You Understand?

Structure and Flexibility Adaptation in Nonspecific and Specific Protein-DNA Complexes

Charalampos G. Kalodimos,[1]* Nikolaos Biris,[1]*
Alexandre M. J. J. Bonvin,[1] Marc M. Levandoski,[2]
Marc Guennuegues,[1] Rolf Boelens,[1] Robert Kaptein[1]†

Interaction of regulatory DNA binding proteins with their target sites is usually preceded by binding to nonspecific DNA. This speeds up the search for the target site by several orders of magnitude. We report the solution structure and dynamics of the complex of a dimeric *lac* repressor DNA binding domain with nonspecific DNA. The same set of residues can switch roles from a purely electrostatic interaction with the DNA backbone in the nonspecific complex to a highly specific binding mode with the base pairs of the cognate operator sequence. The protein-DNA interface of the nonspecific complex is flexible on biologically relevant time scales that may assist in the rapid and efficient finding of the target site.

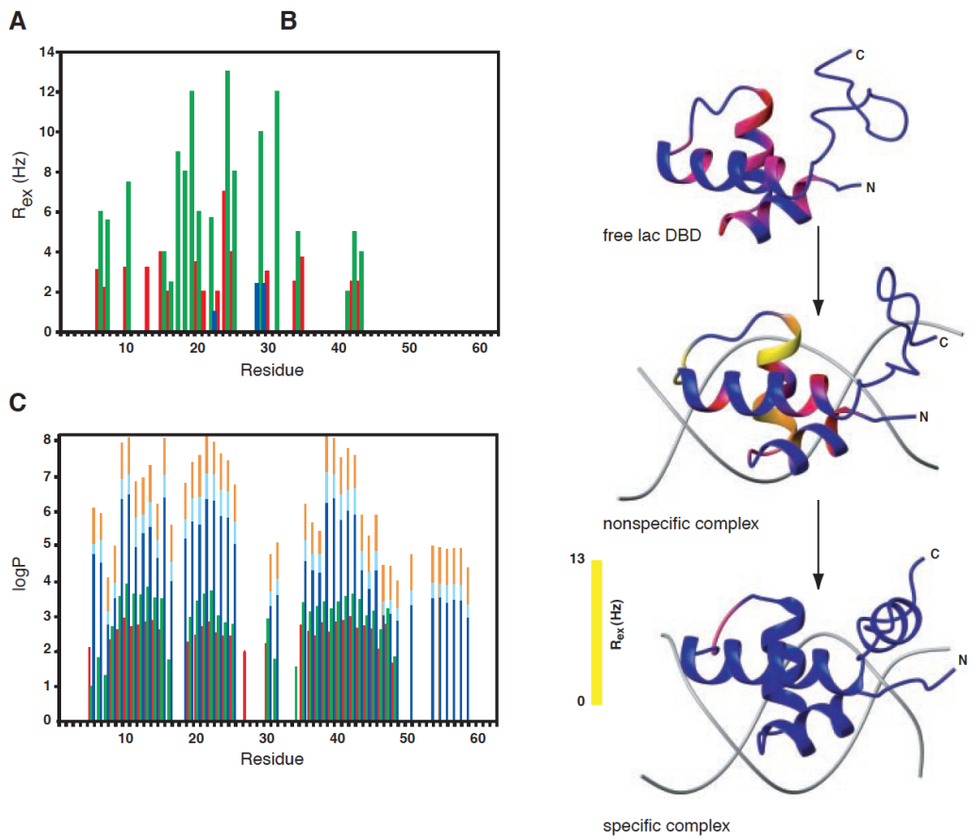

Fig. 4. Dynamic and H-D exchange rates analysis of the dimeric *lac* DBD-DNA interaction. (**A**) Exchange values, R_{ex}, indicating motions on the micro- to millisecond time regime plotted as a function of residue number of the *lac* DBD. Values for the free state, nonspecific, and specific *O1* complex are shown in red, green, and blue, respectively. Only residues with significant R_{ex} values (>1 Hz) are displayed. (**B**) Color-coded representation of the conformational exchange dynamics alteration along the protein-DNA recognition pathway. (**C**) Protection factors of the dimeric *lac* DBD plotted as a function of residue number. Values for the free state, nonspecific, natural operators *O3* and *O1*, and SymL complexes are shown in red, green, blue, cyan, and orange, respectively. Protection factors were calculated from the rate ratio k_{int}/k_{obs} and are displayed as a logarithmic scale.

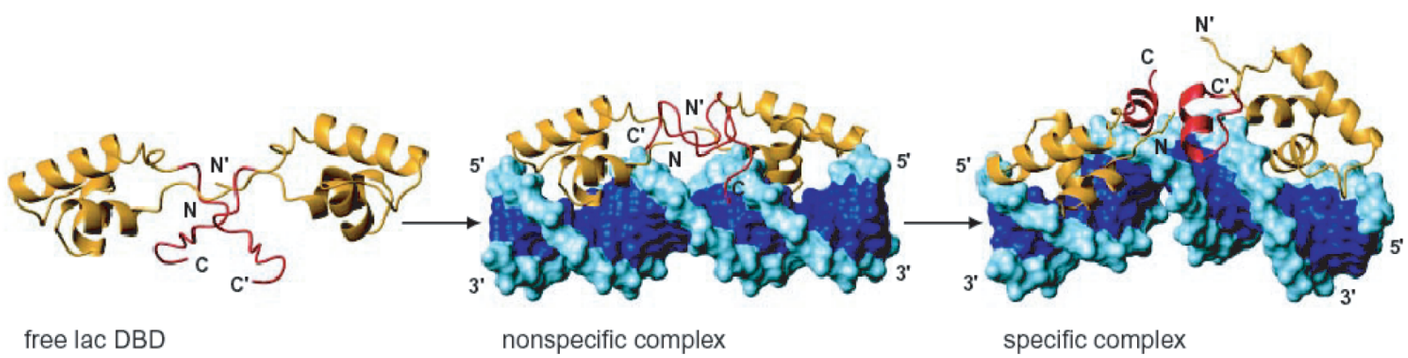

Fig. 3. Structural pathway of protein-DNA recognition. The hinge region (residues 50 to 62), which is colored red, remains unstructured in both the free state and the nonspecific complex, whereas it folds up to an α helix in the specific complex with the natural operator *O1*. In the nonspecific complex, the DNA adopts a canonical B-DNA conformation, whereas in the specific complex it is bent by ~36°.

Next Week:

Problem session: Friday 10th May?